Development of nanotherapeutics for the treatment of recalcitrant and antibiotic resistant infections

by

Nathan Peroutka-Bigus

A dissertation submitted to the graduate faculty

in partial fulfillment of the requirements for the degree of

DOCTOR OF PHILOSOPHY

Major: Microbiology

Program of Study Committee:
Bryan H. Bellaire, Major Professor
Balaji Narasimhan
Michael J. Wannemuehler
Mark Lyte
F. Chris Minion

The student author, whose presentation of the scholarship herein was approved by the program of study committee, is solely responsible for the content of this dissertation. The Graduate College will ensure this dissertation is globally accessible and will not permit alterations after a degree is conferred.

Iowa State University

Ames, Iowa

2020

TABLE OF CONTENTS

Page

LIST OF FIGURES

Page

NOMENCLATURE

ADME	Absorption, Distribution, Metabolism, and Excretion
AOT	Dioctyl Sulfosuccinate Sodium Salt
BBB	Blood Brain Barrier
CDC	Centers for Disease Control and Prevention
CFU	Colony Forming Unit
CNS	Central Nervous System
CPH	1,6-bis(p-Carboxyphenoxy)Hexane
CPTEG	1,8-bis(p-Carboxyphenoxy)-3,6-Dioxaoctane
CSF	Cerebrospinal Fluid
DMEM	Dulbecco's Modified Eagle Medium
EP	Epinephrine
FDA	Food and Drug Administration
GAE	Granulomatous Amebic Encephalitis
HOX-1	Hemeoxygenase 1
IC_{50}	Inhibitory Concentration 50
ICV	Intracellular Viability
LDAO	N,N-Dimethyldodecylamine N-Oxide
MIC	Minimum Inhibitory Concentration
MNGC	Multinucleated Giant Cell
MOI	Multiplicity of Infection
MWCO	Molecular Weight Cutoff
NE	Norepinephrine

PAM	Primary Amoebic Meningoencephalitis
SA	Sebacic Acid
SE	Serotonin
TrxR	Thioredoxin Reductase
WHO	World Health Organization

ACKNOWLEDGMENTS

To begin with I would like to thank Dr. Bryan Bellaire for his mentorship and providing me the opportunity to join his lab. I am also thankful for the support and guidance that my additional committee members provided; thank you Balaji Narasimhan, Michael Wannemuehler, Mark Lyte, and F. Chris Minion. None of this would be possible without my fellow graduate students and laboratory managers who provided friendship and research support; in no particular order, thank you Andy Petersen, Andrea Binnebose, Paul Leuth, Kristina Larsen, Kruttika Phadke, and Adam Mullis.

ABSTRACT

The main focus of this dissertation is on the use of polyanhydride nanoparticles as antimicrobial delivery vehicles to treat the diseases melioidosis caused by the bacterium *Burkholderia pseudomallei* and primary amoebic meningoencephalitis (PAM) caused by the free-living amoeba *Naegleria fowleri*.

Melioidosis represents a bacterial disease characterized by antimicrobial resistance, recrudesce, and high mortality. *B. pseudomallei* is classified as a category B bioterrorism agent as this agent has been studied as a potential bioweapon by various nations. This dissertation shows that these polyanhydride nanoparticles are effective at delivering the antibiotics meropenem, ceftazidime, and chloramphenicol against *B. pseudomallei* in *in vitro* broth assays and tissue culture cell models of intracellular pathogenesis.

PAM is a rare disease yet results in a fatal infection with close to 100% mortality with aggressive antimicrobial therapy. Antimicrobials recommended for the treatment of primary amoebic meningoencephalitis were loaded into nanoparticles and screened against *N. fowleri* in *in vitro* growth assays. When rifampicin and azithromycin were loaded into these nanoparticles, an improvement in anti-parasitic efficacy was noted. In summary, these results bolster the effectiveness of polyanhydride nanoparticles as effective drug delivery vehicles across prokaryotic and eukaryotic pathogens.

Additional research discussed is the anti-parasitic activity of the anti-rheumatoid drug auranofin on *N. fowleri*. *In vitro* assays found that auranofin has an IC_{50} of 0.788 µg/mL with the HB-1 strain of *N. fowleri*. When these amoeba were treated with 3.0 µg/mL auranofin, staining of the nucleus with the cell membrane impermeable dye

propidium iodide suggests that auranofin exerts amoebicidal activity. This data suggests that auranofin has potential as a therapy for primary amoebic meningoencephalitis.

Lastly, the impact that the catecholamine hormones norepinephrine and epinephrine have on the replication and antimicrobial susceptibility of *Bacillus anthracis* and *Yersinia pestis*. *Bacillus anthracis* is the causative agent behind the disease anthrax and *Y. pestis* is the cause of the many manifestation of plague. Norepinephrine was found to accelerate the replication of *B. anthracis* and render the bacteria less susceptible to the antibiotic rifampicin. While, norepinephrine and epinephrine had the inverse effect with *Y. pestis* and resulted in a decreased replication rate.

CHAPTER 1: INTRODUCTION

Infections caused by a variety of pathogenic organisms, whether they be caused by bacteria or protozoa, represent ongoing and evolving challenges in treating animal and human disease. Antimicrobial resistance within bacteria is a leading concern and represents one of the biggest threats to human wellbeing (1, 2). While rare, encephalitic infections caused by free-living amoeba are associated with high mortality and may become more common with global warming (3, 4). This dissertation describes the utilization of polyanhydride nanoparticles as a means to improve therapies against the bacterium *Burkholderia pseudomallei* which exhibit substantial antimicrobial resistance and *Naegleria fowleri*, a free-living fresh water, amoeba associated with high mortality.

Burkholderia pseudomallei

Burkholderia pseudomallei is a gram-negative saprophytic, soil bacterium known to cause the disease melioidosis in humans. This bacterium has a worldwide distribution, with *B. pseudomallei* being known to occur in Asia, Australia, Africa, Middle East, South America, and Central America (5, 6). The absence of *B. pseudomallei* in North America and Europe is suspected to be due to acidic soil conditions in these regions; there are some regions in the North American continent that are suitable for *B. pseudomallei* including Florida and other Southern States (7). The majority of documented cases of melioidosis occurs in South East Asia and Northern Australia. It is thought that incidences of melioidosis are underreported as melioidosis can present with a multitude of clinical manifestations and isolates can be difficult to positively identify using conventional identifications methods; it is estimated that as many as 165,000 cases of melioidosis occur annually with 89,000 deaths (7). Of positively identified melioidosis

cases mortality can range from 10% to 40% depending on antibiotics prescribed and supportive care given; individuals with diabetes, alcoholism, renal, and lung disease are known to be more susceptible to melioidosis (8). As *B. pseudomallei* is highly infectious via aerosol exposure and has high mortality, it is considered as a biowarfare/bioterrorism agent. It was explored as a bioweapon by the United States and Soviet Union (9, 10). Infection can also occur through contact with mucosal membranes and through broken skin.

Under the current treatment guidelines for melioidosis, the CDC recommends a two-part treatment regimen consisting of an intensive intravenous two week treatment phase of ceftazidime or meropenem followed by several months of oral antibiotics consisting of trimethoprim-sulfamethoxazole or amoxicillin with clavulanic acid (11). The WHO recommends the inclusion of doxycycline during the intensive phase of treatment (12). Resistance to antibiotics from the following classes, aminoglycosides, macrolides, chloramphenicol, fluoroquinolones, tetracyclines, and trimethoprim is associated with efflux pump activity (13). Resistance to ceftazidime and meropenem can occur following mutations to the *penA* gene and alterations in efflux activity; resistance to these antimicrobials can occur during the course of conventional treatment which can lead to recurrence and chronic infections (13-15). Antibiotic resistance is often attributed to mobile elements, such as plasmids, but documented resistance in *B. pseudomallei* is restricted to the bacteria's chromosomal DNA (16). Resistance to ceftazidime and meropenem is rare with less than 0.2% of isolates being resistant to ceftazidime and no reported incidences of meropenem resistance in primary clinical isolates. The incidence of clinical isolates attributed to trimethoprim-sulfamethoxazole resistance range from

2.5% to 16% depending on the geographical region. Resistance to doxycycline in primary clinical isolates is rare with an occurrence of less than 2 percent. The incidence of chloramphenicol resistance clinical isolates is 7 percent (17). In light of these restrictions in treating melioidosis there is an urgent need for improved therapeutics. Currently, there isn't a licensed vaccine against melioidosis.

Current advances in therapeutics to treat melioidosis are aimed at screening *B. pseudomallei* against a wider spectrum of available antibiotics, testing newly developed compounds, development of vaccines, and the use of nanoparticles. A promising newly developed monobactum antimicrobial is BAL30072, which has shown *in vitro* activity that is superior to ceftazidime and meropenem (18). The anti-rheumatic drug auranofin, while having a high MIC concentration is very effective at reducing the frequency of persister cells which is significant as theses cell populations are associated with recurrence of infection. The compounds MMV688271 and MMV688179 were also shown to be effective at reducing persister cell populations (19). Vaccines that have been evaluated include live attenuated versions including the non-virulent related *Burkholderia thailandensis* E555 and the attenuated *B. pseudomallei* strain Bp82, which both induced improved survival in the acute mouse model of melioidosis (20, 21). Vaccines derived from outer membrane vesicles (OMVs) from *B. pseudomallei* 1026b were shown to provide a significant increase in survival in the murine model of melioidosis; however, this vaccine didn't provide complete clearance of bacteria from the spleen and lungs (22). BALB/c mice vaccinated with polymer acetylated dextran microparticles encapsulating *B. pseudomallei* whole cell lysate and toll-like receptor (TLR) 7/8 agonist resulted in an extended time to death but failed to provide complete protection (23). Silver

nanoparticles have been screened *in vitro* against several *B. pseudomallei* strains with reported MICs of 32 to 48 μg/mL (24). As a comparison reported values of MIC for ceftazidime and meropenem in conventional broth assays are 32 and 4 μg/mL,respectively: these numbers representing the average values across 50 strains of *B. pseudomallei*. Here we report an MIC of 2.0 μg/mL meropenem for *B. pseudomallei* K96243, which is then reduced to 0.5 μg/mL when meropenem is loaded in polyanhydride nanoparticles.

One aspect of *B. pseudomallei* infection is that the facultative intracellular niche wherein these bacteria reside affords them a degree of protection from antibiotics, and also from elements of the immune system. Previous work has shown that polyanhydride nanoparticles succeed in the ability to reduce the intracellular burden of infected tissue culture cells with the facultative intracellular pathogens *Brucella melitensis* and *Mycobacterium* species to a degree vastly superior to conventional methods used to delivery antibiotics. Nanoparticle delivery of a cocktail of tuberculocidal antibiotics to THP-1 macrophages infected with *Mycobacterium marinum* was able to achieve a 6-log reduction in the intracellular burden, while the antibiotics used in the absence of nanoparticle encapsulation achieved a mere 1.7 log reduction in intracellular bacteria (25). With the encapsulation of the antibiotic rifampicin in polyanhydride nanoparticles a complete eradication of intracellular *Brucella melitensis* was achieved with infected RAW 264.7 macrophages, which wasn't achieved with the conventional use of rifampicin (26). Nanoparticles represent a new means of extending the usefulness of currently approved antibiotics through facilitating improved delivery of these antimicrobials to the

target pathogen and potentially reducing the development of antibiotic resistance, which is reported in this dissertation.

In addition to *B. pseudomallei*, other *Burkholderia* species that are known to cause disease are *Burkholderia mallei* and species belonging to the *Burkholderia* cepacia complex (27). *B. mallei* represents another *Burkholderia* species that is associated with both high infectivity and high mortality like *B. pseudomallei*; *B. mallei* is found within the *Burkholderia pseudomallei* complex of *Burkholderia* species and has similarities to *B. pseudomallei* in terms of pathogenesis. The disease caused by *B. mallei* is referred to Glanders and is an infliction of both humans and solipeds. Unlike *B. pseudomallei*, *B. mallei* is regarded as an obligate pathogen and is not saprophytic in nature (28). Like *B. pseudomallei*, *B. mallei* is classified as a category B bioterrorism agent and has been used and pursued as a biowarfare agent in the past (10). During the First World War allied pack animals were infected with *B. mallei* to disrupt the flow of wartime goods (29). Treatments for melioidosis are generally considered suitable to treat Glanders, and *B. mallei* is susceptible to a larger swath of antibiotics because it lacks a multidrug efflux pump found in *B. pseudomallei* (13). With both *B. pseudomallei* and *B. mallei* having potential for use as biowarfare and bioterrorism agents and their associated high mortality and invasive treatment regimens it stands that new therapeutic options are needed and chapter two of this dissertation addresses this concern through using polyanhydride nanoparticles as vehicles for the delivery of currently approved antibiotics used to treat these diseases.

Species belonging to the *Burkholderia* cepacia complex are opportunistic pathogens known to cause disease in immunocompromised individuals and those

suffering from cystic fibrosis. These species include *Burkholderia cepacia*, *Burkholderia cenocepacia*, and *Burkholderia multivorans* to name a few (30). Infections caused by these organisms are very recalcitrant to treatment as they possess high degrees of multidrug resistance (13). The scope of chapter two of this dissertation is focused on bacteria belonging to the *Burkholderia pseudomallei* complex, but there exists a need for better therapeutics to treat disease caused by bacteria of this complex as there is a high associated mortality within susceptible populations.

Naegleria fowleri

Free-living pathogenic amoeba represent rare but usually fatal infections in humans requiring extensive supportive care and intensive antimicrobial therapies. *Naegleria fowleri* is perhaps the best known of these amoeba as it is often referred to as the "brain eating" amoeba and cases are often reported by the media. *Acanthamoeba* species and *Balamuthia mandrillaris* are also free-living amoeba that cause significant morbidity and mortality (31). Disease caused by *N. fowleri* is referred to as primary amoebic meningoencephalitis (PAM) and is associated with mortality approaching 100%. In the United States as of 2013, of the 142 known incidences of PAM, 139 of these resulted in fatal infection (32). Treatment usually involves the intrathecal administration of the antifungal drug amphotericin B along with oral or intravenous administration of the antifungal fluconazole, and the antibiotics azithromycin and rifampicin (33). An experimental drug recently approved for treating PAM is miltefosine, which has its origin as a drug to treat breast cancer (34). Supportive care is needed to address the inflammation and intracranial pressure that develops during the course of infection and

has included dexamethasone and therapeutic hypothermia (35). Given the dire outcome of these infections there is a profound need for better therapeutics.

N. fowleri has a world-wide distribution and is commonly found in fresh water sources including ponds, lakes, ditches, and improperly chlorinated swimming pools and potable water (36, 37). The first characterized instance of PAM was in 1965 and was described by Fowler and Carter (38). Even with *N. fowleri* being ubiquitous in the environment, cases are rare with the United States reporting less than 5 cases a year, while Pakistan reports in excess of 10 cases a year. In the United States most instances of PAM are in teenagers and children that became infected while playing in bodies of freshwater In contrast, most cases of PAM in Pakistan are in adults; this is likely due to different cultural practices in Pakistan where ritual ablution of the nasal passages is a common practice (36, 39). Infection is the result of getting water contaminated with these amoebae deep into the nose were the amoeba gain access to the olfactory neural epithelium. From the olfactory neural epithelium, the amoeba can then transit through the cribriform plate via the olfactory nerves to the olfactory bulb and then brain (40). Symptoms of PAM include fever, headache, emesis, progressing to seizure, and coma. From onset of symptoms to death, the course of infection is typically three to seven days (41).

While there have been advances in treating PAM with the recent inclusion of miltefosine and the use of therapeutic hypothermia, these new measures do not ensure survival of the patient. Survival does not mean a return to normal life as permanent brain damage can occur (34). Along with prescribing the correct treatment, which may not be initiated upon admittance to a hospital as the symptoms of PAM resemble that of

bacterial meningoencephalitis, starting antimicrobial therapy in a prompt fashion is critical for treating this disease. Chapter 3 addresses the potential to use polyanhydride nanoparticles to improve therapeutic delivery of currently prescribed antimicrobials as a means to improve their efficacy. Chapter 4 details the *in vitro* amoebicidal activity of the anti-rheumatoid drug auranofin on *N. fowleri*.

Polyanhydride Nanoparticles

Polyanhydride nanoparticles have demonstrated marked improvements in drug delivery in both *in vitro* and *in vivo* systems, to include such arenas as vaccine, antibiotic, and antiparasitic delivery (26, 42, 43). The co-polymer nanoparticles utilized in chapters 2 and 3 are composed of the monomers 1,6-bis(p-carboxyphenoxy)hexane (CPH), 1,8-bis(p-carboxyphenoxy)-3,6-dioxaoctane (CPTEG), or sebacic acid (SA). These nanoparticles are capable of entrapping a diverse payload within their polymer matrix, to include proteins used in vaccine preparations to small molecule drugs such as antibiotics. Degradation occurs through hydrolysis of the anhydride bounds linking the monomers, with the resultant degradation products being biocompatible and non-toxic dicarboxylic acids (44). To illustrate the point that polyanhydride devices are safe delivery vehicles, the FDA has approved the use of implantable wafers composed of 1,3-bis(p-carboxyphenoxy)propane (CPP) and sebacic acid (SA) in the treatment of malignant glioma (45). Release of cargo entrapped with the polymer matrix is dependent on the polymer glass transition state (T_g), and drug hydrophobicity. Diffusion rates within the nanoparticle are decreased below the polymer T_g, when the polymer is in a glassy state, and increased when above the T_g, when the polymer is in a rubbery state. Hydrophobic drugs favor release driven through surface erosion, were as, hydrophilic drug release is

dependent on solute transportation (46). Depending upon polymer chemistry and cargo the release kinetics of polyanhydride nanoparticles can range from burst release profiles to sustained release. Previous research with these polyanhydride nanoparticles has shown improvements in antimicrobial delivery to *Mycobacterium* species, *Brucella* species, and pathogenic filarial nematodes (25, 26, 42). An aspect of these nanoparticles that is exploited in this research is the propensity of phagocytic cells to internalize these nanoparticles; this enables us to target antimicrobials into phagocytes infected with intracellular bacteria.

Advances in understanding host pathogen interactions: Effect of catecholamines on bacterial replication and antimicrobial susceptibility

Taking a step back from therapeutic discovery, the relevancy of treating these bacteria in the context that occurs *in vivo* is difficult to do *in vitro* as these approaches fail to take into account the low nutrient conditions found within a biological host and the effect that non-nutrients encountered *in vivo* may have on bacterial replication and susceptibility towards antibiotics. Most media developed for antimicrobial testing is highly enriched and supports the robust replication of bacteria, while this may be ideal for general cultivation, these nutrient rich conditions are not found/available in a host, and inhibitory concentrations of antimicrobials found using highly enriched media may not represent what would occur *in vivo*.

One key nutrient for bacterial growth would be iron, which is very limited *in vivo*; in serum, most iron is bound to host transferrin or sequestered in heme. Pathogenic bacteria have evolved means to circumvent host iron sequestration by means of producing siderophores which have a high affinity for iron and are able to liberate the

iron bound to transferrin (47). It has been shown that host derived catecholamines, such as norepinephrine, are able to aid bacteria in acquiring iron from host transferrin (48). The addition of norepinephrine in Serum-SAPI medium, which was developed to mimic the physiological conditions present in blood, facilitates the robust replication of several pathogen bacteria as it improved iron acquisition by these bacteria (49, 50). Serum-SAPI medium was designed so that most iron contained within the medium is bound to transferrin as it would occur *in vivo*. The addition of norepinephrine was shown to facilitate better acquisition of this transferrin bound iron and supported the robust replication of these bacteria; in the absence of norepinephrine these same bacteria showed limited replication. With staphylococcal species, it was shown that not only could norepinephrine aid in iron acquisition from transferrin, but that norepinephrine also altered the susceptibility of these bacteria to the antibiotic rifampicin (51). The presence of norepinephrine and dopamine promoted replication of these bacteria at rifampicin concentrations that inhibited the complete replication of bacteria in the absence of these catecholamines, and norepinephrine reduced the bactericidal activity of rifampicin. Of particular interest is that adrenergic receptor antagonist, such as the alpha-adrenergic receptor antagonist phentolamine, have been shown to block the effects of norepinephrine on these bacteria in Serum-SAPI medium (52). This would suggest that norepinephrine is signally through a cell surface receptor that is orthologous to adrenergic receptors found in eukaryotes. In *Mycoplasma hyopneumoniae* it was shown that norepinephrine exposure led to changes in the expression of 84 genes (53).

Given the proven altered susceptibility to antibiotics and alterations in replication, chapter 5 examines how catecholamines affect the replication and antimicrobial

susceptibility of *Bacillus anthracis* and *Bacillus cereus*. Inhalation anthrax has a high degree of mortality and has a history of use and development as a biowarfare and bioterrorism agent (10). The impact that circulating norepinephrine may have on the pathogenesis and susceptibility to antibiotics of *B. anthracis* represents new findings in the field of microbial endocrinology and provide meaningful data for the treatment of Anthrax. Nothing is known how *Yersinia pestis* will respond to catecholamines, and like *B. anthracis* represents a highly virulent bacterium with the potential to cause epidemics and use as a biowarfare or bioterrorism agent. Data obtained from *Yersinia enterocolitica* would suggest that norepinephrine should stimulate the replication of *Y. pestis*, if *Y. pestis* has a similar response to norepinephrine as *Y. enterocolitica* has (49). What was found is that *Y. pestis* has an inverse response to norepinephrine and that norepinephrine inhibits the replication of this bacteria.

References

1. Roca I, Akova M, Baquero F, Carlet J, Cavaleri M, Coenen S, Cohen J, Findlay D, Gyssens I, Heuer OE, Kahlmeter G, Kruse H, Laxminarayan R, Liebana E, Lopez-Cerero L, MacGowan A, Martins M, Rodriguez-Bano J, Rolain JM, Segovia C, Sigauque B, Tacconelli E, Wellington E, Vila J. 2015. The global threat of antimicrobial resistance: science for intervention. New Microbes New Infect 6:22-9.

2. Zhang R, Eggleston K, Rotimi V, Zeckhauser RJ. 2006. Antibiotic resistance as a global threat: evidence from China, Kuwait and the United States. Global Health 2:6.

3. De Jonckheere JF. 2011. The impact of man on the occurance of the pathogenic free-living amoeboflagellate *Naegleria fowleri*. Future Microbiol 7:3.

4. Kemble SK, Lynfield R, DeVries AS, Drehner DM, Pomputius WF, 3rd, Beach MJ, Visvesvara GS, da Silva AJ, Hill VR, Yoder JS, Xiao L, Smith KE, Danila R. 2012. Fatal *Naegleria fowleri* infection acquired in Minnesota: possible expanded range of a deadly thermophilic organism. Clin Infect Dis 54:805-9.

5. Chewapreecha C, Holden MT, Vehkala M, Valimaki N, Yang Z, Harris SR, Mather AE, Tuanyok A, De Smet B, Le Hello S, Bizet C, Mayo M, Wuthiekanun

V, Limmathurotsakul D, Phetsouvanh R, Spratt BG, Corander J, Keim P, Dougan G, Dance DA, Currie BJ, Parkhill J, Peacock SJ. 2017. Global and regional dissemination and evolution of *Burkholderia pseudomallei*. Nat Microbiol 2:16263.

6. Wiersinga WJ, Virk HS, Torres AG, Currie BJ, Peacock SJ, Dance DAB, Limmathurotsakul D. 2018. Melioidosis. Nat Rev Dis Primers 4:17107.

7. Limmathurotsakul D, Golding N, Dance DAB, Messina JP, Pigott DM, Moyes CL, Rolim DB, Bertherat E, Day NPJ, Peacock SJ, Hay SI. 2016. Predicted global distribution of *Burkholderia pseudomallei* and burden of melioidosis. Nature Microbiology 1.

8. Currie BJ, Ward L, Cheng AC. 2010. The epidemiology and clinical spectrum of melioidosis: 540 cases from the 20 year Darwin prospective study. PLoS Negl Trop Dis 4:e900.

9. Hilleman MR. 2002. Overview: cause and prevention in biowarfare and bioterrorism. Vaccine 20:13.

10. Withers MR. 2014. USAMRIID'S medical management of biological casualties handbook (8th ed.). Fort Detrick, MD: US Army Medical Research Institute of Infectious Diseases.

11. Rebecca L, Susan G, Rosemarie A, Prasith B, David DB, Allen CC, Bart JC, David D, Jay EG, Joseph L, Direk L, Meredith GM, Robert N, Elizabeth OM, Sharon JP, Nicki P, Rogers LP, Herbert PS, Ivo S, Gladys T, Patrick T, Wiersinga WJ, Vanaporn W, Theresa LS. 2012. Workshop on Treatment of and Postexposure Prophylaxis for *Burkholderia pseudomallei* and *B. mallei* Infection, 2010. Emerg Infec Dis 18(12): e2.

12. World Health Organization. 2001. WHO Model Prescribing Information: Drugs used in Bacterial Infections. Geneva, World Health Organization https://appswhoint/iris/handle/10665/42372

13. Rhodes KA, Schweizer HP. 2016. Antibiotic resistance in *Burkholderia* species. Drug Resist Updat 28:82-90.

14. Sam IC, See KH, Puthucheary SD. 2009. Variations in ceftazidime and amoxicillin-clavulanate susceptibilities within a clonal infection of *Burkholderia pseudomallei*. J Clin Microbiol 47:1556-8.

15. Sarovich DS, Webb JR, Pitman MC, Viberg LT, Mayo M, Baird RW, Robson JM, Currie BJ, Price EP. 2018. Raising the Stakes: Loss of Efflux Pump Regulation Decreases Meropenem Susceptibility in *Burkholderia pseudomallei*. Clin Infect Dis 67:243-250.

16. Schweizer HP. 2012. Mechanisms of antibiotic resistance in *Burkholderia pseudomallei*: implications for treatment of melioidosis. Future Microbiol 7:11.

17. Estes DM, Dow SW, Schweizer HP, Torres AG. 2010. Present and future therapeutic strategies for melioidosis and glanders. Expert Rev Anti Infect Ther 8:325-38.

18. Mima T, Kvitko BH, Rholl DA, Page MG, Desarbre E, Schweizer HP. 2011. In vitro activity of BAL30072 against *Burkholderia pseudomallei*. Int J Antimicrob Agents 38:157-9.

19. Ross BN, Myers JN, Muruato LA, Tapia D, Torres AG. 2018. Evaluating New Compounds to Treat *Burkholderia pseudomallei* Infections. Front Cell Infect Microbiol 8:210.

20. Scott AE, Laws TR, D'Elia RV, Stokes MG, Nandi T, Williamson ED, Tan P, Prior JL, Atkins TP. 2013. Protection against experimental melioidosis following immunization with live *Burkholderia thailandensis* expressing a manno-heptose capsule. Clin Vaccine Immunol 20:1041-7.

21. Silva EB, Goodyear A, Sutherland MD, Podnecky NL, Gonzalez-Juarrero M, Schweizer HP, Dow SW. 2013. Correlates of immune protection following cutaneous immunization with an attenuated *Burkholderia pseudomallei* vaccine. Infect Immun 81:4626-34.

22. Nieves W, Asakrah S, Qazi O, Brown KA, Kurtz J, Aucoin DP, McLachlan JB, Roy CJ, Morici LA. 2011. A naturally derived outer-membrane vesicle vaccine protects against lethal pulmonary *Burkholderia pseudomallei* infection. Vaccine 29:8381-9.

23. Schully KL, Bell MG, Prouty AM, Gallovic MD, Gautam S, Peine KJ, Sharma S, Bachelder EM, Pesce JT, Elberson MA, Ainslie KM, Keane-Myers A. 2015. Evaluation of a biodegradable microparticulate polymer as a carrier for *Burkholderia pseudomallei* subunit vaccines in a mouse model of melioidosis. Int J Pharm 495:849-61.

24. Siritongsuk P, Hongsing N, Thammawithan S, Daduang S, Klaynongsruang S, Tuanyok A, Patramanon R. 2016. Two-Phase Bactericidal Mechanism of Silver Nanoparticles against *Burkholderia pseudomallei*. PLoS One 11:e0168098.

25. Binnebose AM. 2018. Development of a novel anti-infectivity platform for the treatment of neglected tropical and infectious diseases. Graduate Theses and Dissertations doi:https://doi.org/10.31274/etd-180810-5948.

26. Lueth P, Haughney SL, Binnebose AM, Mullis AS, Peroutka-Bigus N, Narasimhan B, Bellaire BH. 2019. Nanotherapeutic provides dose sparing and improved antimicrobial activity against *Brucella melitensis* infections. J Control Release 294:288-297.

27. Sawana A, Adeolu M, Gupta RS. 2014. Molecular signatures and phylogenomic analysis of the genus *Burkholderia*: proposal for division of this genus into the emended genus *Burkholderia* containing pathogenic organisms and a new genus *Paraburkholderia* gen. nov. harboring environmental species. Front Genet 5:429.

28. Galyov EE, Brett PJ, DeShazer D. 2010. Molecular insights into *Burkholderia pseudomallei* and *Burkholderia mallei* pathogenesis. Annu Rev Microbiol 64:495-517.

29. Wheelis M. 1998. First shots fired in biological warfare. Nature 395:1.

30. Mahenthiralingam E, Urban TA, Goldberg JB. 2005. The multifarious, multireplicon *Burkholderia cepacia* complex. Nat Rev Microbiol 3:144-56.

31. Visvesvara GS, Moura H, Schuster FL. 2007. Pathogenic and opportunistic free-living amoebae: *Acanthamoeba* spp., *Balamuthia mandrillaris*, *Naegleria fowleri*, and *Sappinia diploidea*. FEMS Immunol Med Microbiol 50:1-26.

32. Capewell LG, Harris AM, Yoder JS, Cope JR, Eddy BA, Roy SL, Visvesvara GS, Fox LM, Beach MJ. 2015. Diagnosis, Clinical Course, and Treatment of Primary Amoebic Meningoencephalitis in the United States, 1937-2013. J Pediatric Infect Dis Soc 4:e68-75.

33. Grace E, Asbill S, Virga K. 2015. *Naegleria fowleri*: pathogenesis, diagnosis, and treatment options. Antimicrob Agents Chemother 59:6677-81.

34. Cope JR, Conrad DA, Cohen N, Cotilla M, DaSilva A, Jackson J, Visvesvara GS. 2016. Use of the Novel Therapeutic Agent Miltefosine for the Treatment of Primary Amebic Meningoencephalitis: Report of 1 Fatal and 1 Surviving Case. Clin Infect Dis 62:774-6.

35. Linam WM, Ahmed M, Cope JR, Chu C, Visvesvara GS, da Silva AJ, Qvarnstrom Y, Green J. 2015. Successful treatment of an adolescent with *Naegleria fowleri* primary amebic meningoencephalitis. Pediatrics 135:e744-8.

36. Yoder JS, Eddy BA, Visvesvara GS, Capewell L, Beach MJ. 2010. The epidemiology of primary amoebic meningoencephalitis in the USA, 1962-2008. Epidemiol Infect 138:968-75.

37. Visvesvara GS, Stehr-Green JK. 1990. Epidemiology of Free-Living Ameba Infections. J Protozool 37:9.

38. Carter RF. 1970. Description of a Naegleria sp. isolated from two cases of primary amoebic meningo-encephalitis, and of the experimental pathological changes induced by it. J Pathol 100:217-44.

39. Naqvi A, Yazdani N, Ahmad R, Zehra F, Ahmad N. 2016. Epidemiology of primary amoebic meningoencephalitis-related deaths due to *Naegleria fowleri*

infections from freshwater in Pakistan: An analysis of 8-year dataset. Archives of Pharmacy Practice 7.

40. Jarolim KL, McCosh JK, Howard MJ, John DT. 2000. A light microscopy study of the migration of *Naegleria fowleri* from the nasal submucosa to the central nervous system during the early stage of primary amebic meningoencephalitis in mice. J Parasitol 86:50-5.

41. Barnett ND, Kaplan AM, Hopkin RJ, Saubolle MA, Rudinsky MF. 1996. Primary amoebic meningoencephalitis with *Naegleria fowleri*: clinical review. Pediatr Neurol 15:230-4.

42. Binnebose AM, Haughney SL, Martin R, Imerman PM, Narasimhan B, Bellaire BH. 2015. Polyanhydride Nanoparticle Delivery Platform Dramatically Enhances Killing of Filarial Worms. PLoS Negl Trop Dis 9:e0004173.

43. Wagner DA, Kelly SM, Petersen AC, Peroutka-Bigus N, Darling RJ, Bellaire BH, Wannemuehler MJ, Narasimhan B. 2019. Single-dose combination nanovaccine induces both rapid and long-lived protection against pneumonic plague. Acta Biomater 100:326-337.

44. Huntimer L, Ramer-Tait AE, Petersen LK, Ross KA, Walz KA, Wang C, Hostetter J, Narasimhan B, Wannemuehler MJ. 2013. Evaluation of biocompatibility and administration site reactogenicity of polyanhydride-particle-based platform for vaccine delivery. Adv Healthc Mater 2:369-78.

45. Dang W, Daviau T, Ying P, Zhoa Y, Nowotnik D, Clow CS, Tyler B, Brem H. 1996. Effects of GLIADEL wafer initial molecular weight on the erosion of wafer and release of BCNU. Journal of Controlled Release 42:10.

46. Kamaly N, Yameen B, Wu J, Farokhzad OC. 2016. Degradable Controlled-Release Polymers and Polymeric Nanoparticles: Mechanisms of Controlling Drug Release. Chem Rev 116:2602-63.

47. Payne SM. 1993. Iron acquisition in microbial pathogenesis. Trends in Microbiology 1:4.

48. Freestone PPE, Lyte M, Neal CP, Maggs AF, Haigh RD, Williams PH. 2000. The Mammalian Neuroendocrine Hormone Norepinephrine Supplies Iron for Bacterial Growth in the Presence of Transferrin or Lactoferrin. Journal of Bacteriology 182:8.

49. Freestone PP, Haigh RD, Lyte M. 2007. Specificity of catecholamine-induced growth in *Escherichia coli* O157:H7, *Salmonella enterica* and *Yersinia enterocolitica*. FEMS Microbiol Lett 269:221-8.

50. Anderson MT, Armstrong SK. 2008. Norepinephrine mediates acquisition of transferrin-iron in *Bordetella bronchiseptica*. J Bacteriol 190:3940-7.

51. Freestone PP, Haigh RD, Lyte M. 2008. Catecholamine inotrope resuscitation of antibiotic-damaged staphylococci and its blockade by specific receptor antagonists. J Infect Dis 197:1044-52.

52. Freestone PP, Haigh RD, Lyte M. 2007. Blockade of catecholamine-induced growth by adrenergic and dopaminergic receptor antagonists in *Escherichia coli* O157:H7, *Salmonella enterica* and *Yersinia enterocolitica*. BMC Microbiol 7:8.

53. Oneal MJ, Schafer ER, Madsen ML, Minion FC. 2008. Global transcriptional analysis of *Mycoplasma hyopneumoniae* following exposure to norepinephrine. Microbiology 154:2581-2588.

CHAPTER 2: POLYANHYDRIDE NANOPARTICLES IMPROVE THE BACTERIOSTATIC AND BACTERICIDAL PROPERTIES OF CONVENTIONAL ANTIBIOTICS AGAINST THE POTENTIAL BIOWARFARE AGENT *BURKHOLDERIA PSEUDOMALLEI*

Modified from a manuscript to be submitted to Antimicrobial Agents and Chemotherapy

Nathan Peroutka-Bigus,[a,b] Adam Mullis,[c] Kruttika Phadke,[a,b] Kristina Larsen,[a,b] Balaji Narasimhan,[c,d] Bryan H Bellaire[a,b,d]

[a]Department of Veterinary Microbiology and Preventive Medicine, Iowa State University, Ames, IA, USA, [b]Interdepartmental Microbiology Program, Iowa State University, Ames, IA, USA, [c]Department of Chemical and Biological Engineering, Iowa State University, Ames, IA, USA, [d]Nanovaccine Institute, Iowa State University, Ames, IA, USA

Abstract

Therapies to treat melioidosis are in a constant state of evolution as the bacterium responsible, *Burkholderia pseudomallei*, is recalcitrant to many antibiotics and as a category B bioterrorism agent effective therapies are desired in the event of the use of this organism as a bioweapon. Depending on antibiotics prescribed and supportive care, mortality from melioidosis is as high as 40%; this represents an unacceptable burden given that this bacterium has been explored as a biowarfare agent and is endemic in many parts of the world. No licensed vaccines to prevent melioidosis currently exist, so antimicrobial therapy is the cornerstone of treatment. Resistance to aminoglycosides, macrolides, chloramphenicol, fluoroquinolones, tetracyclines, and trimethoprim antibiotics is well documented. Polyanhydride nanoparticles present a means to improve antimicrobial delivery, thereby improving the efficacy of currently prescribes antibiotics; these nanoparticles were loaded with antibiotics used to treat melioidosis and tested against *B. pseudomallei* in *in vitro* broth assays and against macrophages infected with *B.*

pseudomallei. The loading of meropenem, ceftazidime, and chloramphenicol into polyanhydride nanoparticles resulted in improved bacteriostatic and bactericidal activity in *in vitro* assays. Meropenem loaded nanoparticles were able to clear infected macrophages of *B. pseudomallei*. These improvements in antimicrobial efficacy through nanoparticle delivery represent a means to evolve melioidosis therapy without the need to identify new antimicrobial drugs.

Introduction

The genus *Burkholderia* is comprised of greater than 70 species; many of which exist as environmental saprophytes (1). Of these many species, several are regarded as potential pathogens. Within the *Burkholderia pseudomallei* complex, there are the known pathogens *Burkholderia pseudomallei* and *Burkholderia mallei*. Of these, *B. mallei* is considered an obligate pathogen causing the disease Glanders, while *B. pseudomallei* is saprophytic in nature with the ability to cause varying disease states in humans and animals termed melioidosis; both these diseases are associated with high mortality (2). In northern Thailand, *B. pseudomallei* is responsible for 20% of community acquired sepsis (3).

Both *B. pseudomallei* and *B. mallei* are classified as category B bioterrorism agents (4). These *Burkholderia* species were both used and developed as biological warfare agents by numerous countries. During the First World War *B. mallei* was used by German sympathizers to infect allied pack animals in an attempt to disrupt the flow of wartime goods. During World War II, the Japanese biological weapons program was believed to have infected prisoners with various biological agents, including *B. mallei*, in efforts to study and develop these agents as weapons. Both the Soviet Union and the

United States considered *B. pseudomallei* for use as a biological weapon (5-7). The potential use of these agents in a bioterrorism or biowarfare act is not unfounded, and the development of improved therapeutics would save lives in a mass casualty situation.

Melioidosis can result from exposure to these bacteria through inhalation, contact with mucosal membranes, and introduction into broken skin (8). Exposure to *B. pseudomallei* following inhalation can result in symptoms developing within days or in some cases decades. Respiratory infection is characterized by fever, headache, sweats, and pleuritic chest pain. The disease can progress rapidly with dissemination of the bacteria resulting in sepsis that is usually fatal without treatment (4).

The current guidelines for the treatment of melioidosis recommended by the CDC consist of two weeks of intravenously administered ceftazidime or meropenem, followed by 3 to 6 months of oral trimethoprim-sulfamethoxazole or amoxicillin with clavulanic acid (9). The WHO adds to the initial intravenous treatment phase by recommending the addition of doxycycline or trimethoprim-sulfamethoxazol (10). Chloramphenicol is useful in the treatment of melioidosis with neurological involvement, as this drug attains high concentrations in the CNS (11).

Much of the mortality associated with melioidosis can be attributed to the bacterium's innate antimicrobial resistance which has hindered effective treatment. Depending on the antimicrobials prescribed and supportive care, mortality can range from 10 to 40%; this represents a significant milestone to overcome (8). It is estimated that melioidosis is severally underreported and that there could be as many as 165,000 cases per year with 89,000 deaths (12). Reduced influx of antimicrobials into the bacteria cell and highly efficient efflux mechanisms to remove antimicrobials from the

intracellular environment are responsible for much of this resistance (13). It should be noted that Glanders is easier to treat, as *B. mallei* is more sensitive to antimicrobials than *B. pseudomallei*; this is thought to be due to the absence of a multidrug efflux pump that is found in *B. pseudomallei*, but is lacking in *B. mallei* (14). Efflux pump activity is responsible for resistance to aminoglycosides, macrolides, chloramphenicol, fluoroquinolones, tetracyclines, and trimethoprim (15). While rare, mutations in the *penA* gene, which encodes a Class A β-lactamase, can result in resistance to ceftazidime and clavulanate; these resistant isolates are still susceptible to carbapenems (15).

With the invasive and lengthy duration of treatment needed to treat melioidosis, high associated mortality, community risk in endemic areas, and potential for use as a bioweapon, there is an urgent need for improved therapeutic options (7, 16). These include tigecycline, which is a derived from the antibiotic tetracycline, which has shown both *in vitro* activity against *B. pseudomallei* and protection in the acute murine model of melioidosis when administered along with ceftazidime (17). A new monocyclic β-lactam antibiotic BAL30072 has shown *in vitro* efficacy that surpasses that of many of the prescribed antibiotics (18). However, it was found that 40% of tested *B. pseudomallei* isolates are resistant to the new 5th generation cephalosporin ceftobiprole (19). Through the use of a polyanhydride nanoparticle antimicrobial delivery system we can take existing antibiotics and improve upon their antimicrobial activity and extend their usefulness in combating melioidosis and Glanders.

Polyanhydride nanoparticles represent a polymeric drug delivery system with surface erosion and drug hydrophobicity largely dictating release parameters. Surface erosion is more important for the release of hydrophobic drugs and leads to more

sustained release profiles. Were as, hydrophilic drugs diffuse out of the nanoparticles via concentration gradient dependent solute transportation, which results in a more rapid release profile (20). These nanoparticles are comprised of the monomers of 1,6-bis(p-carboxyphenoxy)hexane (CPH), 1,8-bis(p-carboxyphenoxy)-3,6-dioxaoctane (CPTEG), or sebacic acid (SA), and degrade into biocompatible and nontoxic dicarboxylic acids (21). These nanoparticles are readily internalized by phagocytic cells which enables the targeting of antimicrobials into the intracellular environment favored by intracellular pathogens, such as *Burkholderia* species. Previous work has already shown that these nanoparticles improve the antimicrobial efficacy of doxycycline and rifampicin against the facultative intracellular bacterial pathogen *Brucella melitensis* (22)

Herein, we demonstrate that the encapsulation of meropenem, ceftazidime, and chloramphenicol into polyanhydride nanoparticles composed of CPTEG, CPH, or SA polymers leads to improved *in vitro* efficacy when compared to these antibiotics used conventionally, as seen in improvements in bacteriostatic and bactericidal activity. With the encapsulation of meropenem into nanoparticles, we have shown a 5-fold reduction in IC_{50} value against *Burkholderia pseudomallei*. The encapsulation of ceftazidime resulted in a 2-fold reduction in IC_{50} value. Aside from lowering the inhibitory concentration, these nanoparticles also resulted in greater bactericidal activity than that of conventionally applied antibiotics. We have visualized these nanoparticles in giant multi-nucleated cells derived from RAW 264.7 macrophages, which is significant as *Burkholderia* species induce these cell formations and demonstrates that we can target nanomedicines to these infected cells. We also see that these same nanoparticles show increased efficacy against *B. mallei*. With these improvements over conventionally

formulated antibiotics, we expect that the use of these nanoparticle will lead to improved patient outcomes in the case of melioidosis.

Materials and Methods

Cell culture

Burkholderia psuedomallei strain K96243, NR-4073, *Burkholderia mallei* strain China, NR-4071, and *Burkholderia thailandensis* strain E264, NR-10275 were obtained through BEI Resources, NIAID, NIH. Cultivation was on trypticase soy agar supplemented with 1% bovine hemoglobin or Columbia agar supplemented with 1% bovine hemoglobin at 37°C and 5% CO_2; *B. pseudomallei* and *B. mallei* grow equally well on both of these media. Murine macrophage RAW 264.7 and human monocyte THP-1 cells were obtained from ATCC, Manassas VA. Mammalian tissue culture cells were maintained in 75 cm^2 tissue culture flasks with either DMEM supplemented with 10% FBS for RAW 264.7 cells or RPMI supplemented with 10% FBS for THP-1 cells and cultivated at 37°C and 5% CO_2.

Antibiotics and nanoparticle preparation

Antibiotics were suspended in PBS and filtered through a sterile 0.2 μm syringe filter and stored at -80°C; with the exception of rifampicin which was suspended in DMSO. Nanoparticle CPTEG and CPH monomers were synthesized in house as previously described, and SA monomers were purchased from Sigma (23, 24). Nanoparticle synthesis was as previously described (25). Nanoparticle suspensions were made in PBS at 10 mg/mL concentration with sonication for 15 to 30 seconds at 14 amplitude (Misonix S-4000, Newton, CT). Once suspended the suspensions were stored at -80°C until used in an experiment. Actual loading of antibiotics into nanoparticles was

determined by suspending 9-11 mg of nanoparticles in PBS. Over the course of a week supernatants containing the released antibiotics were routinely removed; at the end of the week 40 mM sodium hydroxide was added to the nanoparticle suspension to rapidly degrade the remaining nanoparticle mass releasing any remaining antibiotic. Antibiotics released from meropenem and ceftazidime loaded nanoparticles were quantified by RP-HPLC-UV (1200 series, Agilent Technologies, Santa Clara, CA). UV spectrophotometry was used to quantify the release of rifampicin and doxycycline using absorbance at 333 and 350 nm, respectively (SpectraMax M3, Molecular Devices, San Jose, CA). Antibiotic loading was then determined from the sum of antibiotics released in the PBS supernatants and sodium hydroxide samples.

Broth culture inhibition assays

Nanoparticle inhibition assays followed CLSI guidelines for antimicrobial susceptibility testing. Briefly, an 0.5 OD_{600} suspension of bacteria was made in PBS from a colony scraped off an overnight grown culture. This suspension was then diluted 1:100 in Mueller Hinton both II and 50 µL was pipetted into the wells of a 96 well tissue culture plate. Nanoparticle and soluble antimicrobials were prepared at 2x concentration in Mueller Hinton broth II and 50 µL of these were added to the bacteria already in the tissue culture plates; an untreated control was included. The antibiotics ceftazidime, meropenem, chloramphenicol, doxycycline, and rifampicin were screened either individually or in cocktails. Following 20 hours of growth at 37°C at 5% CO_2 the antimicrobial concentration that inhibited 50% of the metabolic activity of the bacteria (IC_{50}) was determined through the addition of the viability reagent resazurin. After a 30-minute incubation for *B. pseudomallei* or 60-minute incubation for *B. mallei* with

resazurin the reduction of resazurin to resorufin was quantified with a Fluostar Omega plate reader (BMG LABTECH, Cary, NC) using 544 excitation and 590 emission filters. Using the fluorescent data, IC_{50} values were calculated using nonlinear regression analysis in Graphpad Prism software. In separate experiments, in place of resazurin reduction, the endpoint analysis was done through CFU enumeration following serial dilution and plating onto agar plates with overnight cultivation at 37°C and 5% CO_2, which enabled us to determine bactericidal action. Bactericidal activity is qualified if the resultant CFU/mL count was less than the starting CFU/mL concentration at the start of the experiment. Statistical comparison of CFU numbers between nanoparticle and soluble treated broth cultures was done using a One-way ANOVA with Bonferroni's comparison of means test using GraphPad Prism.

Broth culture antibiotic resistance assays

Generation of resistance to meropenem was accomplished by exposing *B. pseudomallei* to 2 µg/mL meropenem in either soluble form or nanoparticle delivered meropenem in broth assays in 100 µL volume of Mueller Hinton broth II for 20 hours. Following 20 hours of exposure to meropenem, the entire contents of the broth cultures were plated onto agar plates supplemented with 16 µg/mL meropenem and the agar plates were held at 37°C and 5% CO_2 for 3 days. The presence of growth on these meropenem supplemented agar plates indicated the development of resistance to meropenem; each culture was treated as a separate event and were scored either positive or negative for a resistant phenotype. Two micrograms per mL meropenem was chosen as the meropenem concentration to drive selection for resistance as this concentration represents the MIC for *B. pseudomallei* and is also pharmacologically relevant. Growth on 16 µg/mL

meropenem is the demarcation threshold for classifying meropenem resistance. It needs to be noted that all meropenem resistant isolates were promptly destroyed.

Nanoparticle interaction with tissue culture cells

Tissue culture interaction studies with nanoparticles utilized the murine macrophage cell line RAW 246.7 and were conducted by seeding the tissue culture cells at a cell density of 1.0 x 10^6 cells/mL in either a 100 µL volume in 96 well tissue culture plates or a 500 µL volume in 24 well tissue culture plates. The 24 well tissue culture plates were used for fixed cell microscopy and the cells were seeded onto glass coverslips that had been placed into the wells. After allowing sufficient time for the cells to attach, nanoparticles were added and then the cells were centrifuged at 250 rcf for 10 minutes at 4°C to pellet the nanoparticles onto the cell layer. Following centrifugation, the cells were placed at 37°C and 5% CO2 for various lengths of time to assess macrophage internalization of the nanoparticles, intracellular localization of the nanoparticles, and cell viability and health. Cell viability was measured through the addition of the viability reagent resazurin. General cellular markers of stress and cellular function used during live cell imaging were annexin V and Mitotracker red (ThermoFisher Scientific, Waltham, MA) using an IX71 DSU microscope (Olympus, Center Valley, PA) with Metamorph Advanced acquisition software. Antibodies and stains used for fixed cell imaging were the anti-LAMP antibody 1D4B (August, J.T. (DSHB Hybridoma Product 1D4B) and stains used were wheat germ agglutin 488 and DAPI (Invitrogen) imaged on an inverted fluorescence microscope (Olympus BX71, Olympus, Center Valley, PA) using Olympus Fluoview acquisition software. To assess the intracellular localization of our nanoparticles in giant multi-nuclear cells, cells were first infected with *B.*

thailandensis at a multiplicity of infection (MOI) of 10:1 before the addition of nanoparticles that had been loaded with the red fluorescent molecule rhodamine. *B. thailandensis* is found within the *Burkholderia pseudomallei* complex and causes the formation of giant multi-nucleated cells through a similar type 6 secretion system mechanism as *B. pseudomallei* and allows experiments to be carried out in a BSL2 setting (26). Post-acquisition processing was performed with imageJ (https://fiji.sc/)

Nanoparticle targeted drug delivery to infected macrophages

Intracellular viability (ICV) experiments were conducted using the human monocyte cell line THP-1. In 96 well tissue culture plates the macrophages were seeded at a cell density of 200,000 cells per well for THP-1 cells in 100µL of tissue culture media. The THP-1 monocytes were activated through the addition of 50 nM phorbol 12-myristate 13-acetate (PMA) for 24 hours, followed by removal of the PMA for an additional 24 hours prior to infection. Bacteria were added at a series of MOIs encompassing MOIs of 0.1:1, 2:1, and 15:1 bacterium to macrophages in a 10 µL volume of PBS. Immediately following the addition of the bacteria, the tissue culture plates were centrifuged at 250 rcf at 4°C for 10 minutes to pellet the bacteria among the macrophages. Once removed from the centrifuge the tissue culture plates were placed in an incubator set at 37°C and 5% CO_2. After one hour the cells were washed with PBS to remove extracellular bacteria and media containing 400 µg/mL kanamycin was added to the tissue culture plates to eliminate any remaining extracellular bacteria. An hour following the addition of the kanamycin the infected macrophages were treated with either nanoparticles loaded with antimicrobials, nanoparticles devoid of cargo, soluble antimicrobials, or left untreated. Fifty micrograms per mL kanamycin was maintained

throughout the experiment to inhibit extracellular growth of the bacteria. A subset of macrophages at this time were lysed with 0.1% deoxycholate in serum free DMEM to enumerate the bacterial burden at this time. At various time points post-treatment the bacterial burden in the macrophages was assessed through CFU enumeration. To accomplish this the media was removed from the macrophages and the cells were washed with PBS, then the PBS was removed, and the macrophages were lysed by the addition of 0.1% deoxycholate in serum free DMEM. The lysate was serially diluted and plated onto agar plates. Following overnight incubation at 37°C and 5% CO_2 the colonies were counted. Statistical comparison between nanoparticle and soluble treated macrophages was done using a One-way ANOVA with Bonferroni's comparison of means test using GraphPad Prism.

Results

Individual drug screening utilizing the viability reagent resazurin showed that the antibiotics meropenem, ceftazidime, and chloramphenicol benefited the most from nanoparticle encapsulation when tested against *B. pseudomallei*, while rifampicin was hindered by nanoparticle encapsulation (Fig. 1). Improvement in the efficacy provided by nanoparticle encapsulation compared to the use of soluble antibiotics was chemistry and loading percentage dependent, with the 10:90 CPTEG:SA formulae yielding the greatest benefit. The greatest improvement over soluble meropenem came from 10:90 CPTEG:SA nanoparticles with a 0.8% drug loading (Fig. 2A). This nanoparticle batch resulted in an IC_{50} value of 0.1073 µg/mL meropenem, whereas the corresponding IC_{50} for soluble meropenem in this experiment was 0.646 µg/mL; nanoparticle treatment resulted in a 5-fold decrease in antibiotic concentration needed to achieve an IC_{50}.

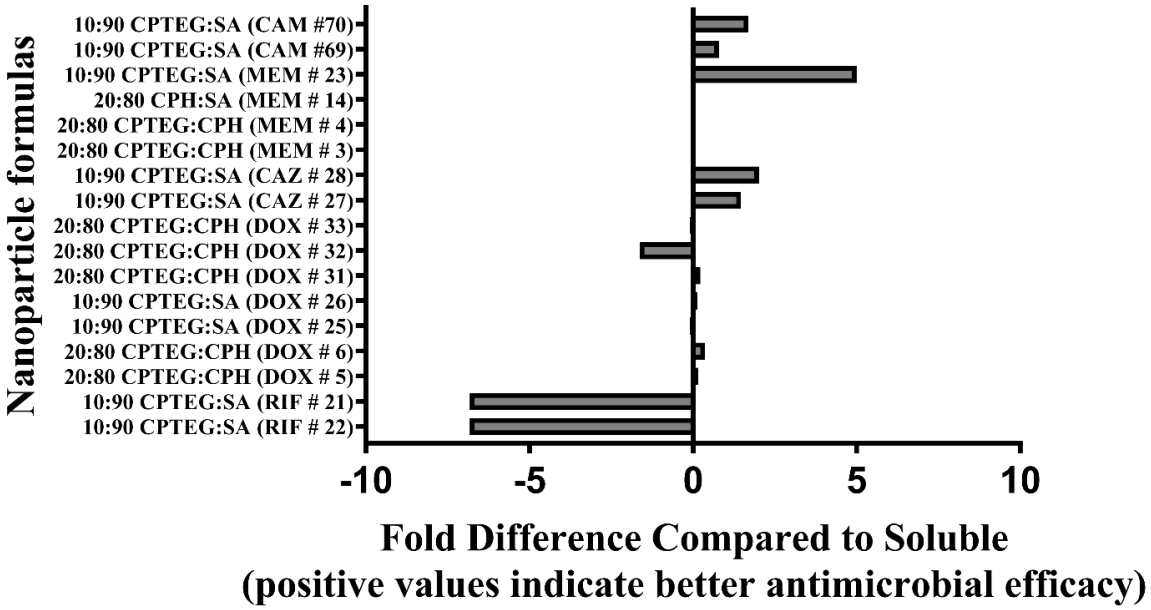

FIG 2-1. Fold change in IC_{50} values of nanoparticle treatments compared to conventional soluble treatments with *Burkholderia pseudomallei*. IC_{50} values determined through the reduction of the viability reagent resazurin following conventional antimicrobial susceptibility broth assay experimental design. Fold changes are represented in an additive fashion; i.e. a 1-fold change would be a 2x change by multiplication. Positive values indicate an improvement in antimicrobial activity and a negative value indicates a decrease in antimicrobial activity with nanoparticle delivery. Antibiotics: chloramphenicol (CAM), meropenem (MEM), ceftazidime (CAZ), doxycycline (DOX), and rifampicin (RIF). The number following the antibiotic is a reference to the nanoparticle formulation and batch number.

With ceftazidime a 2-fold decrease in IC_{50} was achieved with 10:90 CPTEG:SA nanoparticles with 8.7% drug loading which resulted in an IC_{50} of 1.05 µg/mL ceftazidime (Fig. 2B). Soluble ceftazidime in this experiment has an IC_{50} of 3.157 µg/mL. When the ceftazidime loading in these 10:90 CPTEG:SA nanoparticles was reduced to 4.7% the resulting IC_{50} was 1.276 µg/mL. The inclusion of chloramphenicol into 10:90 CPTEG:SA nanoparticles led to an IC_{50} of 2.721 µg/mL and 1.804 µg/mL with nanoparticles loaded at 5.4% and 10% chloramphenicol. In contrast, soluble antibiotic resulted in an IC_{50} 4.858 µg/mL chloramphenicol; nanoparticles deliver

resulted in a 0.8 and a 1.7-fold improvement in IC_{50} depending on nanoparticle formulation. The meropenem, ceftazidime, and chloramphenicol nanoparticles had burst release profiles with near 100% of the cargo released within the first 2 hours, while the poorer performing rifampicin nanoparticles had a more sustained release profile with approximately 50% coming out within the first 2 hours with the majority of the remaining cargo coming out over a 24-hour period.

Using doxycycline, there appears to be no benefit from nanoparticle encapsulation. When encapsulated in 10:90 CPTEG:SA nanoparticles at 3.3% and 8.1% loading percentage their IC_{50} values are grouped around soluble doxycycline. The 3.3% loading gave an IC_{50} 0.5395 µg/mL doxycycline and the 8.1% gave an IC_{50} of 0.5798 µg/mL, which is similar to the soluble IC_{50} of 0.5669 µg/mL (Fig. 2C). When 20:80 CPTEG:CPH co-polymer nanoparticles were employed with doxycycline a similar story unfolded. Loading percentages of 4.6% and 8.3% gave IC_{50} values of 0.5362 µg/mL and 0.4409 µg/mL, with soluble for these experiments giving an IC_{50} of 0.6034 µg/mL. A final approach with doxycycline was the incorporation of surfactants to alter release profiles. Surfactants employed were Span 80 (0.01% loading), AOT (11% loading), and LDAO (8% loading) with 10MAG (16% loading), with respective doxycycline loading percentages of doxycycline 2.3%, 1.4%, and 3.3%. The inclusion of Span 80 resulted in an IC_{50} of 0.7222 µg/mL doxycycline, AOT resulted in an IC_{50} 0.9522 µg/mL doxycycline, and the LDAO with 10MAG had an IC_{50} of 2.317 µg/mL doxycycline. The soluble doxycycline for these experiments had an IC_{50} of 0.8809 µg/mL. The incorporation of the LDAO with 10MAG surfactants resulted in a more pronounced

delayed release with 64% of cargo released within 24 hours, while the other formulations showed near complete release within 24 hours.

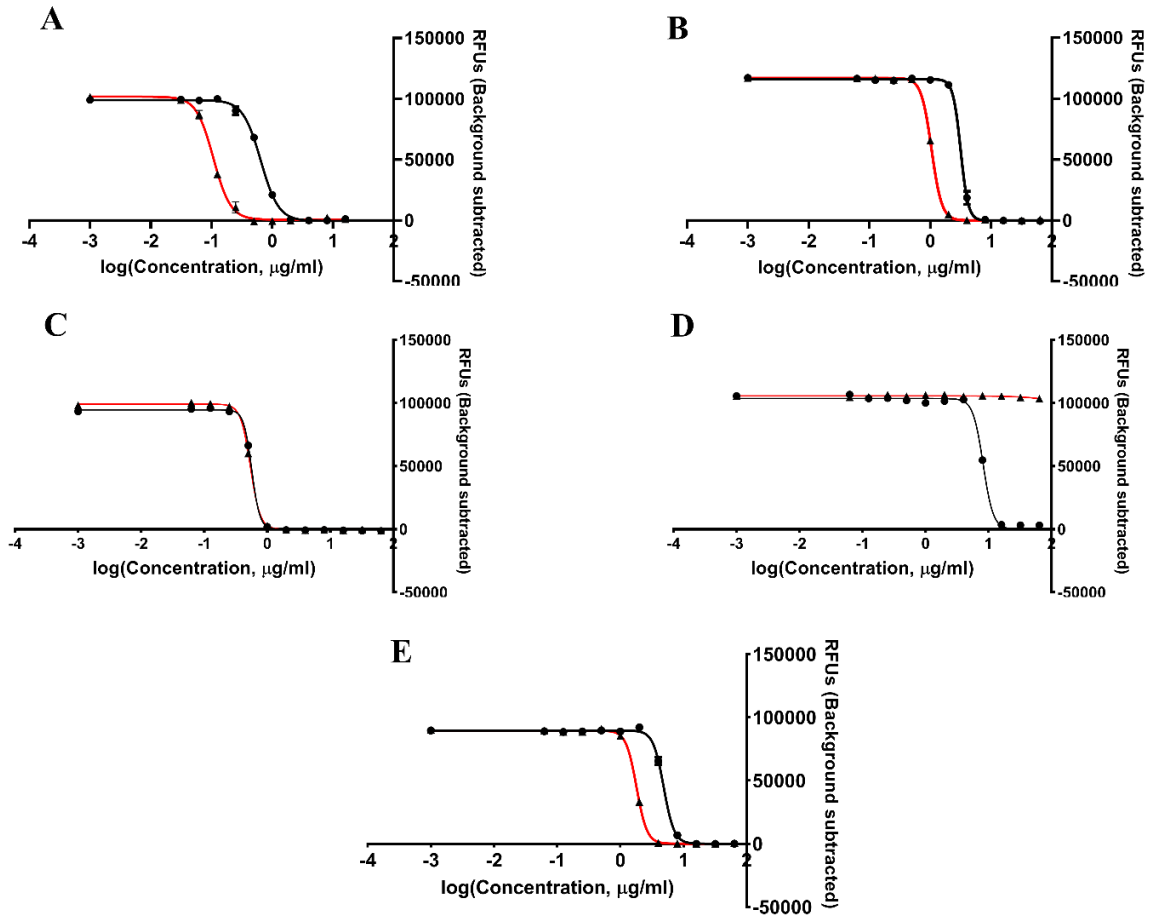

FIG 2-2. Nonlinear regression of *in vitro* antibiotic dose titration of *Burkholderia pseudomallei* viability to nanoparticle treatments compared to conventional soluble drug therapy. Viability of treated bacteria was determined through the reduction of resazurin. ● conventional soluble drug. ▲ nanoparticle treatment. (A) Meropenem (MEM). (B) Ceftazidime (CAZ). (C) Doxycycline (DOX). (D) Rifampicin (RIF). (E) Chloramphenicol (CAM). Nanoparticle formulation is 10:90 CPTEG:SA with 0.8% MEM (A), 8.7% CAZ (B), 3.3% DOX (C), 4.3% RIF (D), 10.0% CAM (E) percent loading.

The encapsulation of rifampicin in 10:90 CPTEG:SA nanoparticles resulted in poorer *in vitro* efficacy than soluble antibiotic in these broth assays (Fig. 2D). Soluble rifampicin resulted in an IC_{50} of 8.186 µg/mL, whereas nanoparticles loaded at 4.3% and 8.1% rifampicin showed no inhibition out to the maximum tested concentration of 64

µg/mL rifampicin. In the case of both of these nanoparticle batches release profiles showed a moderate delayed release profile with 42% and 50% of cargo released within 2 hours and a total of 85% and 86% released by 24 hours. Additional rifampicin formulations were not tested, as screening of these other chemistries in *Burkholderia cepacia* showed similar results as was seen with the 10:90 CPTEG:SA with *B. pseudomallei.*

When *B. pseudomallei* CFU enumeration of treated broth cultures was used to assess the bactericidal properties of these nanoparticles, again we see that nanoparticle delivery of meropenem is superior to soluble. With 10:90 CPTEG:SA nanoparticles loaded at 0.8% meropenem we see bactericidal activity down to 0.5 µg/mL meropenem, which provided the near equivalent level of bactericidal activity as 2.0 µg/mL soluble meropenem. When a higher loading percent of meropenem was used, 4.4%, bactericidal activity was noted down to 1.0 µg/mL meropenem (Fig. 3A). Meropenem was also screened in 20:80 CPH:SA nanoparticles and a slight yet significant improvement in bactericidal activity was noted (Fig. 3B). Soluble antibiotic produced a modest reduction in bacterial numbers with 2.0 µg/mL meropenem, both nanoparticles with loading percentages of 1.7% and 6.2% resulted in a 3 and 4 log reduction in bacterial CFUs compared to soluble at 2.0 µg/mL meropenem. No data is currently available on the bactericidal activity of the other nanoparticle formulations.

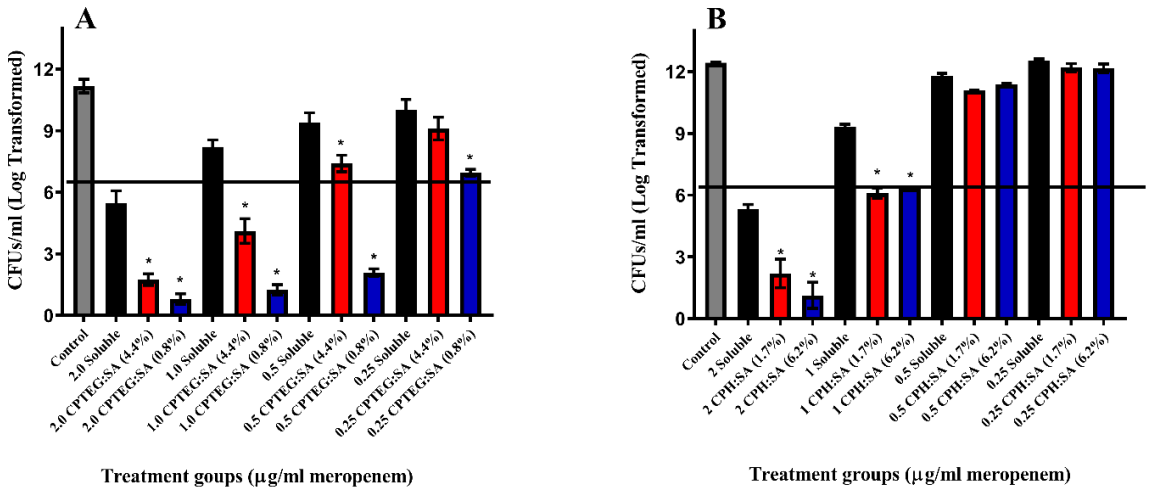

FIG 2-3. CFU determination of bactericidal activity of *in vitro* nanoparticle treatments using (A) 10:90 CPTEG:SA and (B) 20:80 CPH:SA nanoparticles loaded with meropenem against *Burkholderia pseudomallei*. Conventional soluble meropenem therapy is shown to highlight the increased efficacy of nanoparticle treatment. Black horizontal bar represents the staring CFU concentration at the beginning of the treatment; bars below indicate bactericidal activity. Percentage numbers in the x-axis labels indicate percent loading of meropenem into the nanoparticles. (A) Values represent the means ± the SEM of three experiments performed in triplicate. (B) Values represent the means ± the SEM of an experiment performed in triplicate. Statistical analysis by one-way ANOVA with a Bonferroni's comparison of means (*$p \leq 0.05$). *indicates significance between nanoparticle treatment and equivalent soluble treatments.

This is the first use of polyanhydride nanoparticles with a 10:90 ratio of CPTEG:SA; little is known how this particular chemistry will interact with phagocytic cells or the bacteria themselves. When *B. pseudomallei* was treated with unloaded 10:90 CPTEG:SA nanoparticles no inhibition of viability was witnessed with nanoparticle concentrations up to 1.250 mg/mL (Fig. 4A). To see if encapsulation of antibiotics is even needed or if the nanoparticle and antibiotic can be applied separately, *B. pseudomallei* was treated with unloaded 10:90 CPTEG:SA particles in the presence of soluble ceftazidime and the viability was compared to cultures treated with soluble ceftazidime alone or ceftazidime loaded into 10:90 CPTEG:SA nanoparticles (Fig. 4B).

The IC_{50} of the nanoparticles mixed with soluble drug was 3.313 µg/mL ceftazidime, which is similar to the IC_{50} of soluble ceftazidime of 3.079 µg/mL. In contrast, the IC_{50} of ceftazidime loaded in 10:90 CPTEG:SA nanoparticles was 1.228 µg/mL.

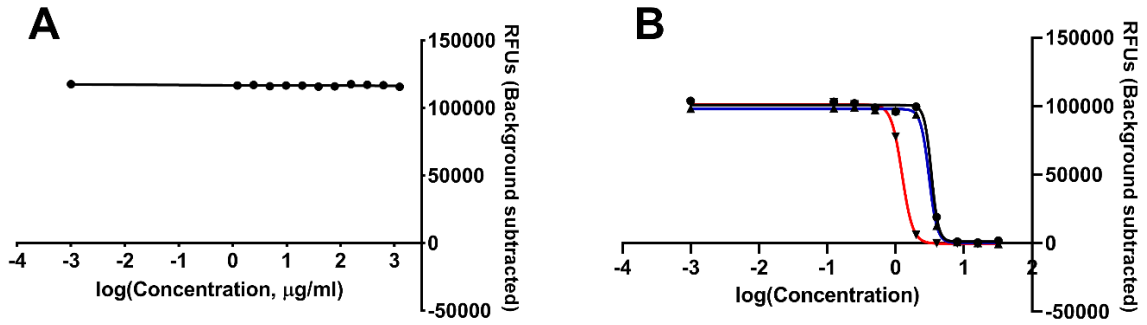

FIG 2-4. Evaluation of 10:90 CPTEG:SA nanoparticles devoid of cargo on the viability of *Burkholderia pseudomallei*. Viability of treated bacteria was determined through the reduction of resazurin. (A) Dose titration of 10:90 CPTEG:SA nanoparticles in a broth assay; x-axis shows nanoparticle concentration. (B) Dose titration of 10:90 CPTEG:SA nanoparticles combined with soluble ceftazidime (●) compared to soluble ceftazidime (▲) and 10:90 CPTEG:SA nanoparticles loaded with ceftazidime (▼); x-axis shows ceftazidime concentration.

To see the effect that 10:90 CPTEG:SA nanoparticles have on phagocytic cells, the murine cell line RAW 246.7 was treated with varying concentrations of nanoparticles and the impact on viability was measured through the reduction of resazurin (Fig. 5A). There was no loss in viability when cells were treated with 125 µg/mL nanoparticle concentration or less over a 24-hour period. At 250 µg/mL nanoparticle concentration a 31% loss in viability was noted, and at 500 µg/mL nanoparticle concentration a 75% loss in cell viability was noted. Live cell imaging was done on nanoparticle treated RAW 246.7 cells utilizing the cellular fluorescent probe annexin V conjugated to alexafluor 488 along with mitotracker red (Fig. 5B-5D).

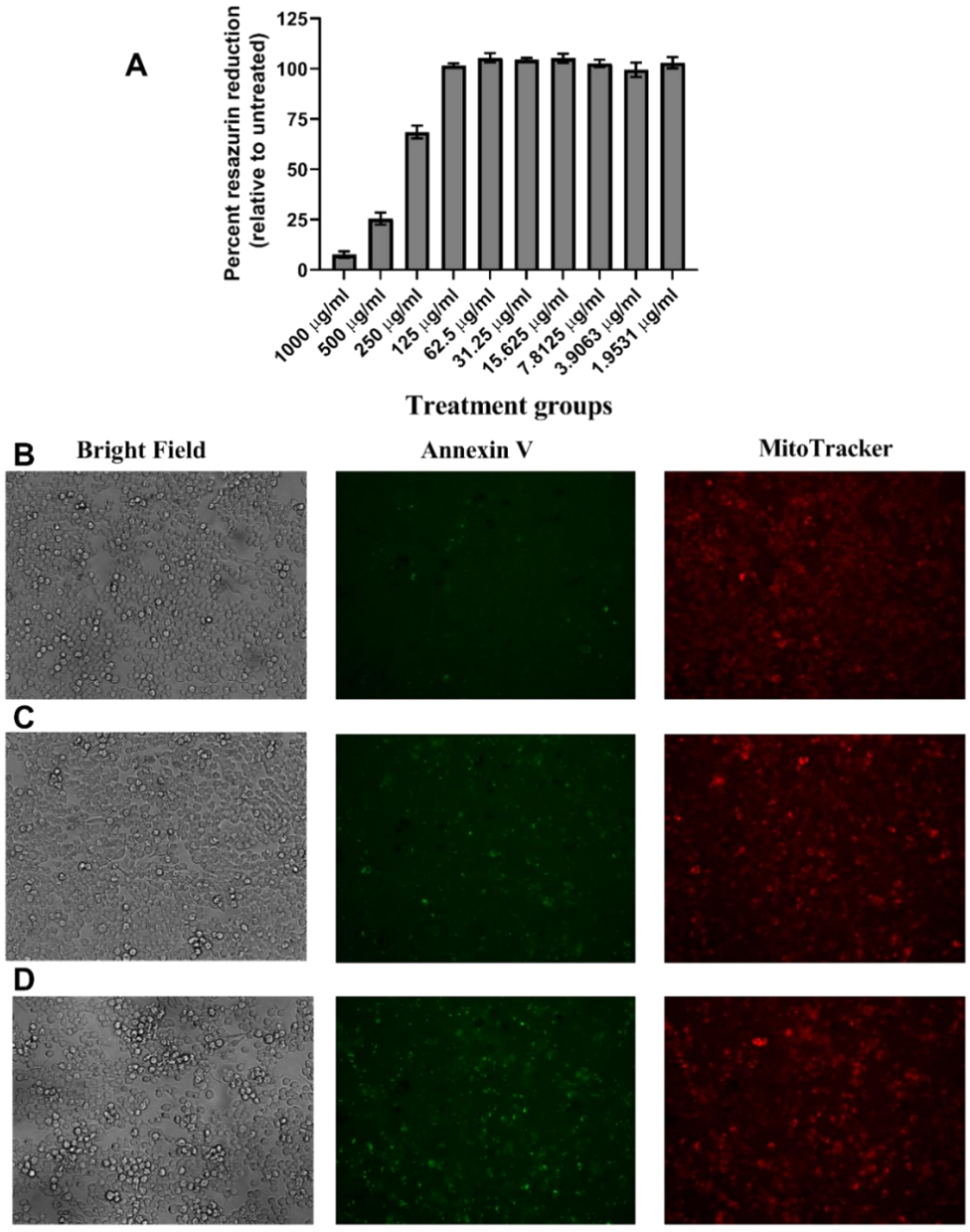

FIG 2-5. Viability of RAW 246.7 macrophages treated with 10:90 CPTEG:SA polyanhydride nanoparticles. Macrophages were treated with a dose titration of nanoparticles for 24 hours. (A) Viability of macrophages as determined through the reduction of the viability indicator resazurin. (B, C, and D) Confocal fluorescence microscope images of control and nanoparticle treated macrophages with annexin V and MitoTracker. (B) Control macrophages not treated with nanoparticles. (C) Macrophages treated with 62.5 µg/mL 10:90 CPTEG:SA nanoparticles. (D) Macrophages treated with 125 µg/mL 10:90 CPTEG:SA nanoparticles. Representative images.

Annexin V binds to phosphatidylserine that has flipped to the outer leaflet of the plasma membrane and is an apoptotic signal. MitoTracker red binding to mitochondria is dependent on membrane potential. Qualitative imaging indicates that at nanoparticle concentrations that had no impact on cell viability, increased annexin V staining was observed; this was at 125 and 62.5 µg/mL 10:90 CPTEG:SA nanoparticle concentrations. There was no apparent difference in MitoTracker staining.

Screening of the lead nanoparticle formulations identified with *B. pseudomallei* against the related *Burkholderia mallei* yielded similar results (Fig. 6). 10:90 CPTEG:SA nanoparticles loaded with 8.7% ceftazidime resulted in a 1.1-fold increase in efficacy producing an IC_{50} of 0.6934 µg/mL ceftazidime, when soluble drug gave an IC_{50} of 1.48 µg/mL ceftazidime. When the loading of ceftazidime was reduced to 4.7% a 1.4-fold increase in efficacy over soluble ceftazidime was noted. When chloramphenicol was loaded into these 10:90 CPTEG:SA nanoparticles loaded at 5.4% chloramphenicol yielded a 0.92-fold increase in efficacy over soluble, while particles loaded at 10% chloramphenicol gave a 2.7-fold increase in efficacy over soluble chloramphenicol. Soluble chloramphenicol gave an IC_{50} of 5.374 µg/mL, and the particles loaded at 5.4% and 10.0% gave IC_{50} values of 2.804 µg/mL and 1.451 µg/mL chloramphenicol. In the case of meropenem, 10:90 CPTEG:SA nanoparticles loaded at 0.8% gave an IC_{50} of 0.02036 µg/mL meropenem, which was a 4.4-fold increase in efficacy over soluble IC_{50} of 0.1094 µg/mL meropenem. Meropenem at a higher loading percentage of 4.4% gave an IC_{50} 0.04644 µg/mL, which is a 1.4-fold increase in efficacy over soluble meropenem.

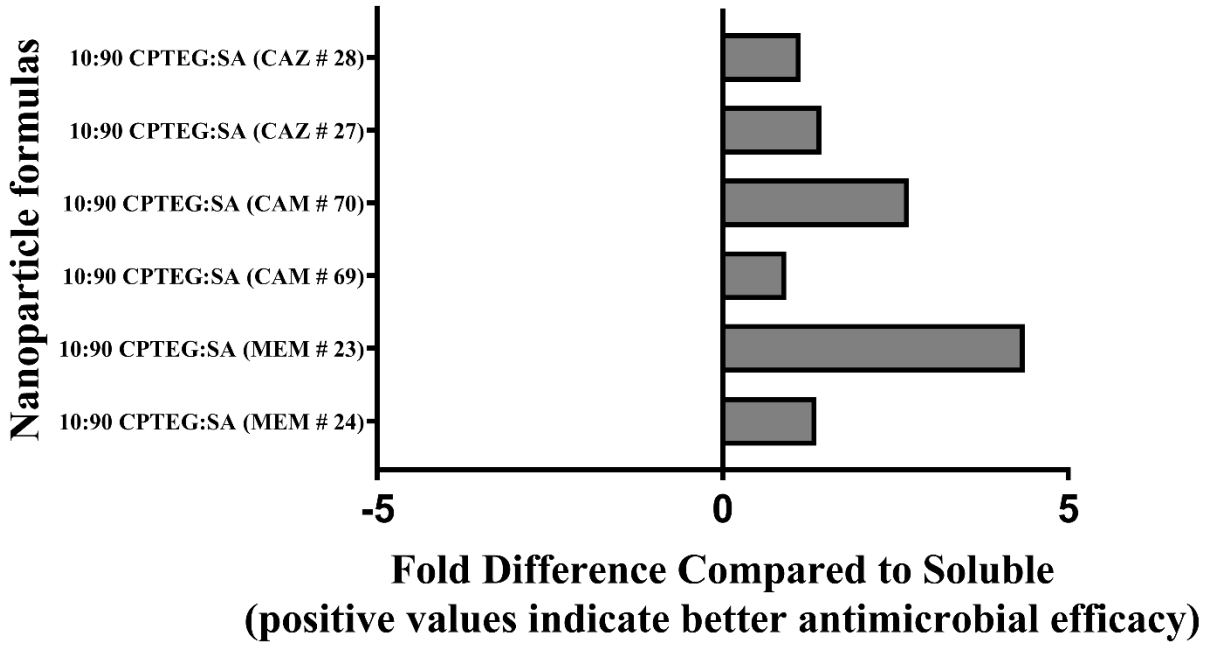

FIG 2-6. Fold change in IC_{50} values of nanoparticle treatments compared to conventional soluble treatments with *Burkholderia mallei*. IC_{50} values determined through the reduction of the viability reagent resazurin following conventional antimicrobial susceptibility broth assay experimental design. Fold changes are represented in an additive fashion; i.e. a 1-fold change would be a 2x change by multiplication. Positive values indicate an improvement in antimicrobial activity and a negative value indicates a decrease in antimicrobial activity with nanoparticle delivery. Antibiotics: chloramphenicol (CAM), meropenem (MEM), and ceftazidime (CAZ). The number following the antibiotic is a reference to the nanoparticle formulation and batch number.

CFU data showed that in the case of both ceftazidime and chloramphenicol that when these two drugs were loaded into 10:90 CPTEG:SA nanoparticles that an increase in bactericidal activity was found when screened against *B. mallei* (Fig. 7). In the case of ceftazidime, we show a MIC of 8.0 µg/mL ceftazidime, while with nanoparticle treatment we show an MIC of 2.0 µg/mL ceftazidime (Fig. 7A). While both soluble ceftazidime and nanoparticle delivered ceftazidime show similar levels of bactericidal activity at 8.0 µg/mL with approximately a 2-log reduction in bacteria. At 4.0 µg/mL ceftazidime nanoparticle delivered ceftazidime continues to show bactericidal activity with again an

approximate 2-log reduction in bacteria, which was not seen with soluble ceftazidime at this concentration. A significant reduction in bacterial numbers between soluble and nanoparticle treatments is seen down to 1.0 µg/mL, with an approximate 2-log reduction in CFUs with nanoparticle treatment. When chloramphenicol was loaded into these 10:90 CPTEG:SA nanoparticles we did not detect an MIC with soluble treatment at the dose range chosen (8.0 µg/mL to 1.0 µg/mL), however we do show an MIC of 4.0 µg/mL chloramphenicol with nanoparticle treatment (Fig 7B). Bactericidal activity also was not noted with soluble ceftazidime, but we did see an approximate 1-log reduction in bacteria with nanoparticle treatment at 8.0 µg/mL ceftazidime.

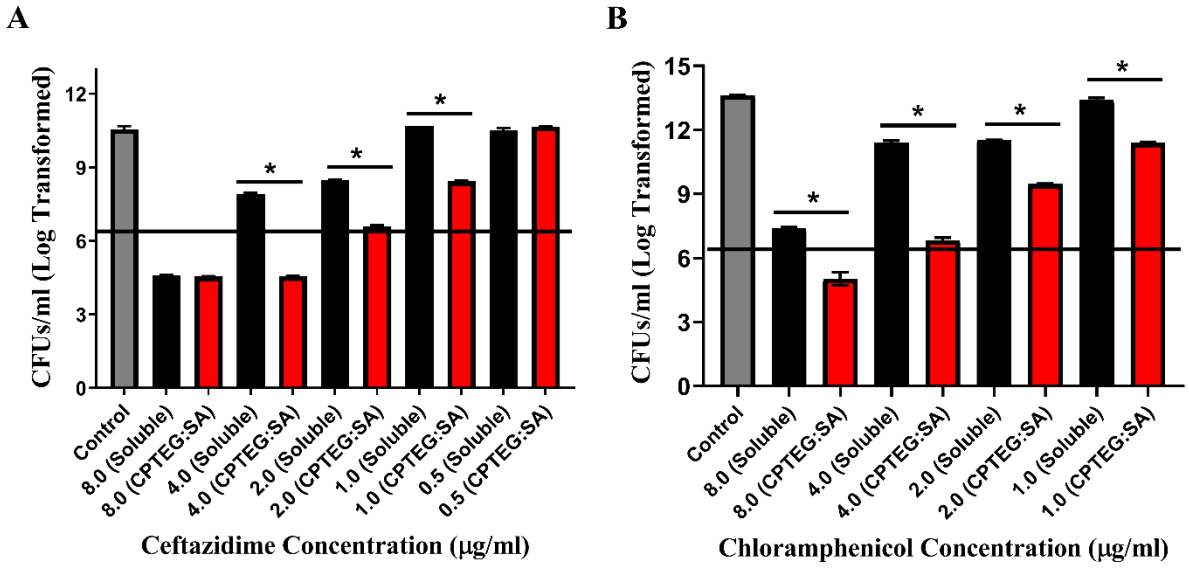

FIG 2-7. CFU determination of bactericidal activity of *in vitro* nanoparticle treatments using 10:90 CPTEG:SA nanoparticles against *Burkholderia mallei*. (A) Ceftazidime loaded nanoparticles; 10:90 CPTEG:SA nanoparticles loaded at 4.7% ceftazidime by mass. (B) Chloramphenicol loaded nanoparticles; 10:90 CPTEG:SA nanoparticles loaded at 10% chloramphenicol by mass. Black horizontal bars represent the staring CFU concentration at the beginning of the treatment; bars below indicate bactericidal activity. Values represent the means ± the SEM of an experiment performed in triplicate. Statistical analysis by one-way ANOVA with a Bonferroni's comparison of means (*$p \leq 0.05$). *indicates significance between nanoparticle treatment and equivalent soluble treatments.

The development of resistance by *B. pseudomallei* to meropenem was investigated to see if the use of nanoparticle delivered meropenem would reduce the incidence of resistance (Fig. 8). When these bacteria were exposed to 2.0 μg/mL meropenem in either soluble form or through nanoparticle delivery there were twice as many resistant events found with soluble treatment vs the nanoparticle treatment. With soluble treatment 68% of treated bacteria cultures developed resistance to meropenem. When meropenem was delivered by 10:90 CPTEG:SA nanoparticles a substantial decrease in the number of resistant events was noted, with 32% of cultures developing resistance to meropenem.

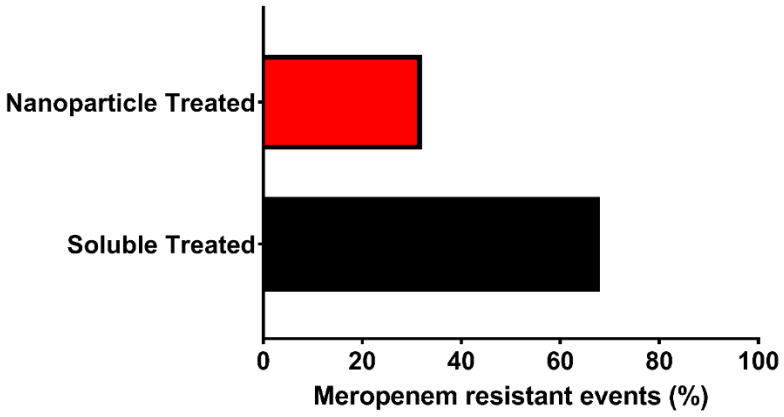

FIG 2-8. Comparison of meropenem resistance of *Burkholderia pseudomallei* between soluble treatment and nanoparticle treatment. In broth culture *B. pseudomallei* was treated with 2 μg/mL meropenem in either soluble form or nanoparticle form (10:90 CPTEG:SA) loaded at 4.4% meropenem for 20 hours. Following broth treatment, the contents were plated onto agar plates with 16 μg/mL meropenem and cultivated for 3 days; growth indicated the generation of resistant isolates. Data is shown as percent positive cultures for meropenem resistance. 28 culture replicates per broth culture treatments.

Effectively targeting of antimicrobials against intracellular *Burkholderia* is requisite for the successful treatment of disease. A hallmark of *B. pseudomallei* infection is the formation of multinucleated giant cells (MNGC). A microscopic experiment using

the surrogate bacterium *B. thailandensis* was used to generate MNGCs in the murine macrophage cell line RAW 246.7 to see if these nanoparticles would be present within MNGCs (Fig. 9).

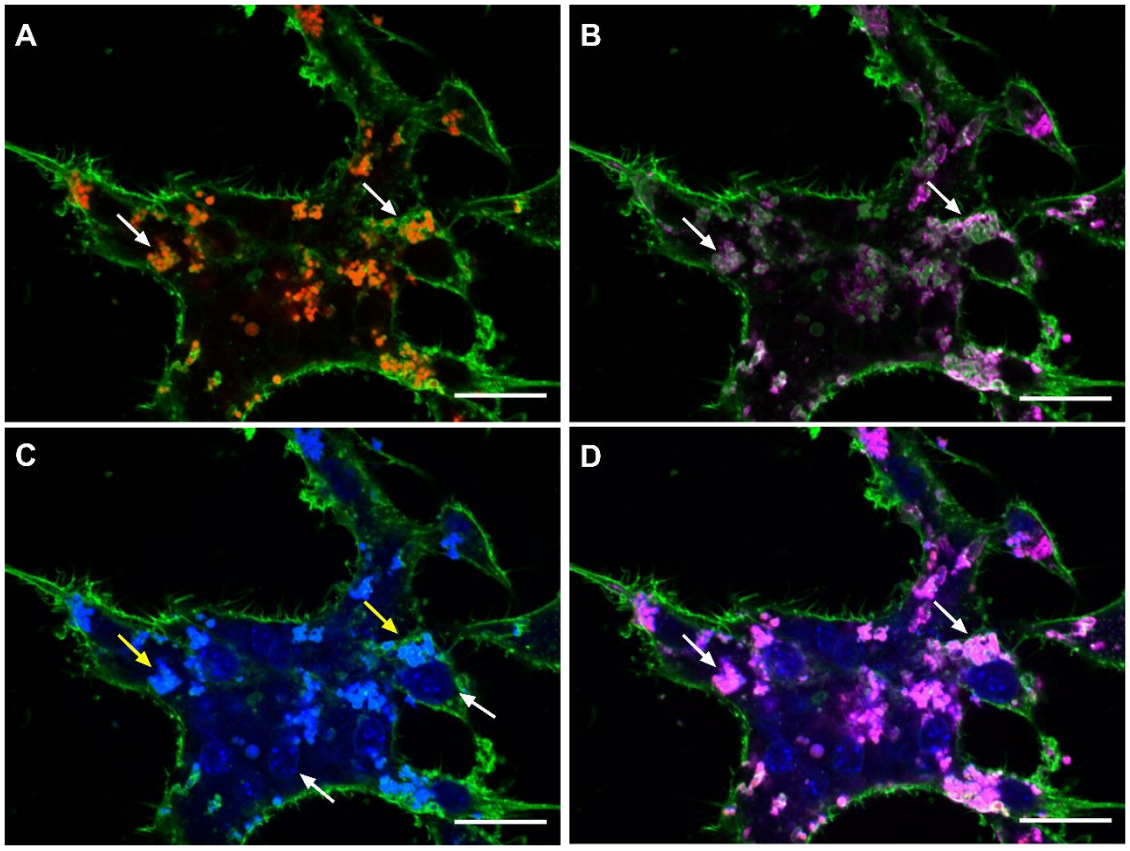

Figure 2-9. Laser scanning confocal image of 10:90 CPTEG:SA nanoparticles within a multinucleated giant cell (MNGC). Murine macrophages were infected with *Burkholderia thailandensis* to generate the formation of these giant multi-nucleated cells. The cell membrane is stained with Wheat Germ Agglutinin 488 (Green) shown in all panels. (A) Rhodamine (Red) loaded nanoparticles (white arrows). (B) Immunofluorescent (magenta) staining of Lysosome Associated Membrane Protein (LAMP-1) (white arrows). (C) DAPI staining showing numerous nuclei (white arrows) in the MNGC. Important note: these nanoparticles absorbed the DAPI stain (yellow arrows). (D) Composite image of panels A, B, and C. Scale bar represents 20 μM.

Nanoparticles were loaded with the red fluorescent dye rhodamine to visualize them within the MNGCs. Imaging by laser scanning confocal microscopy showed that these 10:90 CPTEG:SA nanoparticles did indeed reside within MNGCs, and that they co-

localized with the intracellular marker lysosome associated protein 1 (LAMP). DAPI staining showed numerous nuclei within these cells, indicating the presence of MNGCs induced by the surrogate bacterium *B. thailandensis*. The cell membrane surrounding these numerous nuclei was stained with wheat germ agglutin 488. It does appear that these 10:90 CPTEG:SA nanoparticles absorb DAPI stain as this stain does co-localize with the rhodamine loaded nanoparticles. The bacteria were not stained with a selective marker, but the bacteria within these MNGCs did lightly stain with DAPI and are present in the cytosol.

When activated human monocyte THP-1 cells were infected with *B. pseudomallei* across a series of MOIs and then treated with either nanoparticle delivered meropenem or soluble meropenem we see a profound increase in bactericidal activity with 10:90 CPTEG:SA nanoparticle delivered meropenem (Fig. 10). At 9 hours post-treatment there is a decline in the number of intracellular bacteria with soluble treatment, however, with nanoparticle treatment the bactericidal activity is far more pronounced and led to a significant reduction in bacteria compared to soluble meropenem. This same significant reduction in bacteria was seen across all MOI's tested. When taking the experiment out to 24 hours post-treatment, we see a further reduction in bacteria counts with nanoparticle treatment, with no viable bacteria recovered at the lower two MOIs tested. In contrast, with soluble delivered meropenem there is no meaningful reduction in viable bacteria from the earlier 9-hour time point. The treatment of these infected macrophages with 10:90 CPTEG:SA devoid of meropenem resulted in no appreciable reduction in viable intracellular bacterial burden, however, at the highest MOI tested there was a significant increase in the viable bacterial burden.

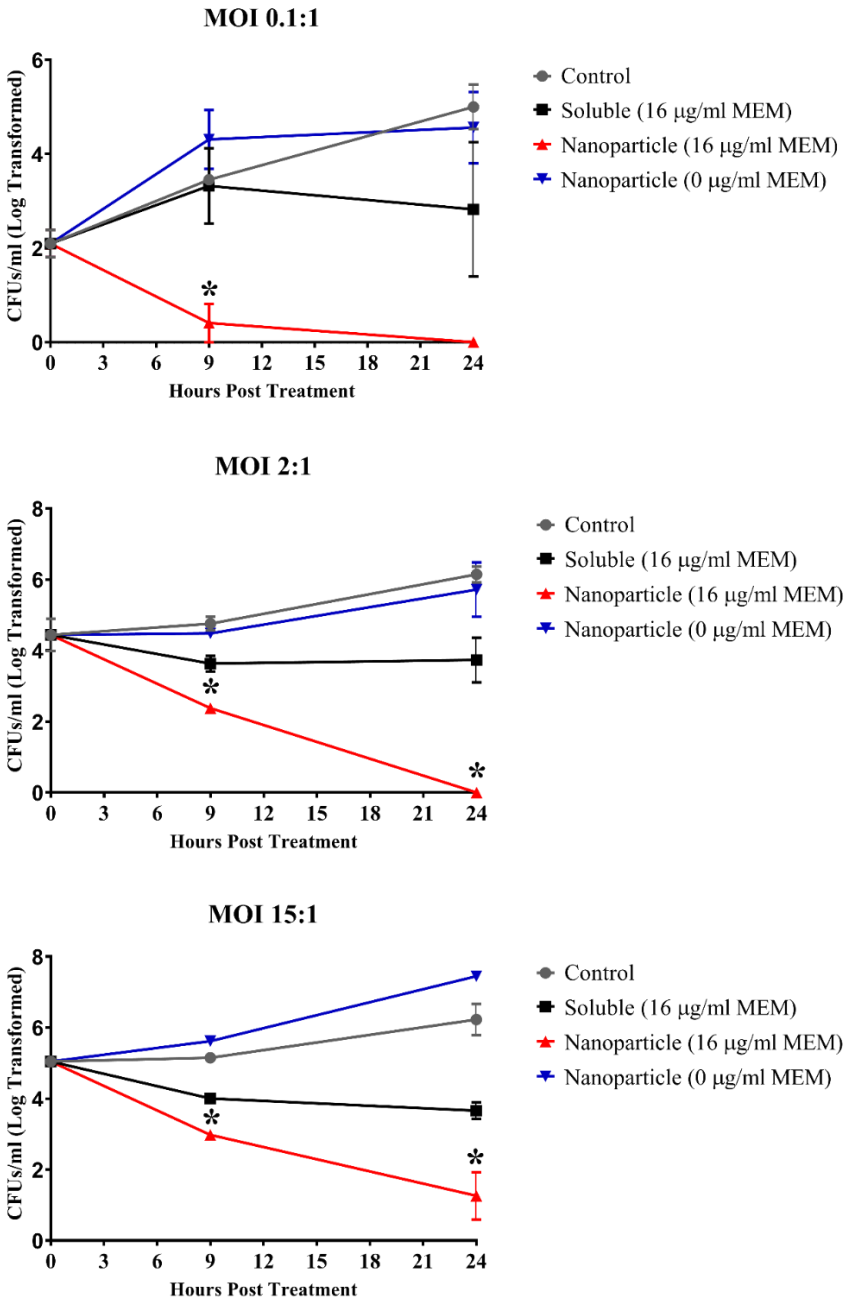

FIG 2-10. Intracellular viability of *Burkholderia pseudomallei* within activated human THP-1 macrophages following antimicrobial treatment. Treatment with either meropenem delivered via 10:90 CPTEG:SA nanoparticles or conventional soluble meropenem. Graphs show the results across a multiplicity of infection titration (MOI) of 0.1:1, 2:1, and 15:1 ratios of bacteria to macrophage. Values represent the means ± the SEM of an experiment performed in triplicate. Statistical analysis by one-way ANOVA with a Bonferroni's comparison of means (*$p \leq 0.05$). *indicates significance between nanoparticle treatment and equivalent soluble treatments.

When testing the antimicrobial efficacy of combined antimicrobials against *B. pseudomallei* there is improved efficacy with nanoparticle delivery. When meropenem was combined with doxycycline, an IC_{50} value of 0.1073 µg/mL meropenem/0.0536 µg/mL doxycycline was observed when the 10:90 CPTEG:SA 0.8% loaded meropenem nanoparticles were combined with 20:80 CPTEG:SA 2.3% loaded doxycycline nanoparticles (Fig. 11A). This IC_{50} value represents a 7.9-fold reduction in IC_{50} value over the soluble combination which had an IC_{50} of 0.9513 µg/mL meropenem/0.4756 µg/mL doxycycline. For this experiment the ratio of meropenem to doxycycline was 2:1; this ratio was chosen based off the individual IC_{50} values of the soluble drugs obtained in previous experiments where doxycycline's IC_{50} value had a concentration roughly half that of meropenem. In a separate experiment where meropenem in 20:80 CPH:SA nanoparticles were combined with doxycycline in 20:80 CPTEG:CPH nanoparticles, no significant difference was seen in its IC_{50} value vs the soluble combination of meropenem and doxycycline (Fig 11B).

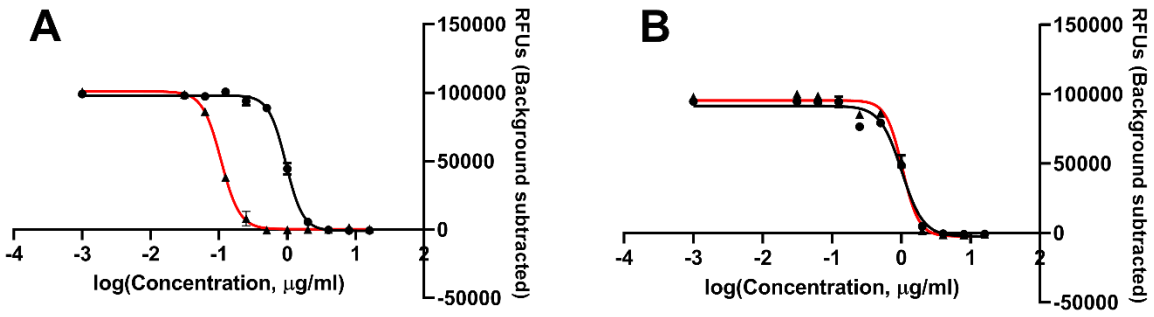

Figure 2-11. Nonlinear regression of *in vitro* dose titration response of *Burkholderia pseudomallei* to dual meropenem and doxycycline nanoparticle therapies compared to conventional soluble dual drug therapies. Viability of treated bacteria was determined through the reduction of resazurin. ● conventional soluble drug. ▲ nanoparticle therapy. (A) Meropenem loaded into 10:90 CPTEG:SA and doxycycline loaded into 20:80 CPTEG:CPH. (B) Meropenem loaded into 20:80 CPH:SA and doxycycline loaded into 20:80 CPTEG:CPH.

It should be noted that when meropenem was combined with doxycycline in these experiments, there was no benefit in the resulting IC_{50} values when compared to meropenem used alone; this was seen with both soluble and nanoparticle treatments (Fig. 12). Soluble meropenem resulted in an IC_{50} of 0.646 µg/ml, while the combination of meropenem with doxycycline resulted in a combined IC_{50} of 0.9513 µg/ml meropenem and 0.4756 µg/ml doxycycline (Fig. 12A). In the event of nanoparticle delivered combination of meropenem and doxycycline; meropenem alone resulted in an IC_{50} of 0.1073 µg/ml and the combination resulted in a combined IC_{50} of 0.1073 µg/mL meropenem and 0.0536 µg/mL doxycycline (Fig. 12B).

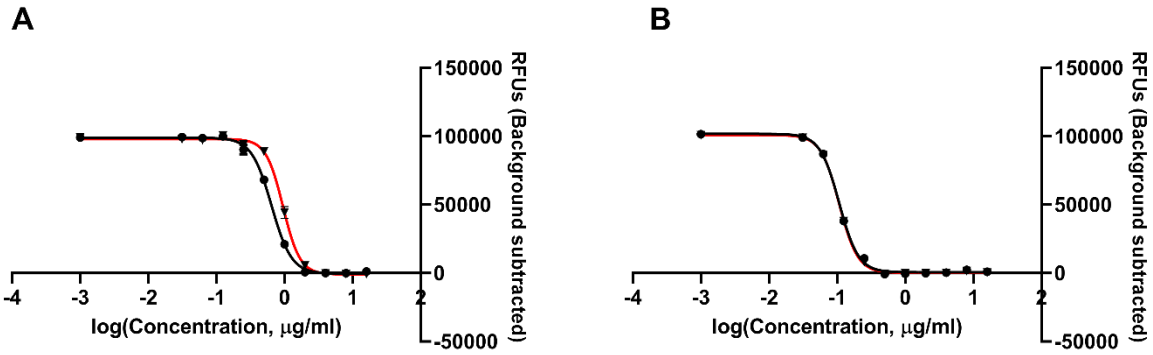

FIG 2-12. Nonlinear regression of *in vitro* dose titration response of *Burkholderia pseudomallei* comparing single meropenem treatment with the combination meropenem and doxycycline treatment with both soluble and nanoparticle formulations. Viability of treated bacteria was determined through the reduction of resazurin. ● single meropenem treatment. ▼ combination meropenem with doxycycline treatment (2:1 ratio). (A) Soluble treatment. (B) 10:90 CPTEG:SA nanoparticles loaded with meropenem combined with 20:80 CPTEG:CPH nanoparticles loaded with doxycycline; dose response curves are overlapping. X-axis represents the concentration of meropenem.

When ceftazidime was combined with doxycycline in nanoparticles, results favored nanoparticle incorporation (Fig. 13). When 10:90 CPTEG:SA 4.7% loaded ceftazidime nanoparticles were combined with 20:80 CPTEG:CPH 4.6% loaded doxycycline nanoparticles, a 1.3-fold reduction in IC_{50} value was achieved, with the nanoparticle combination giving an IC_{50} of 1.254 µg/mL ceftazidime/0.209 µg/mL

doxycycline and the soluble combination giving an IC_{50} value of 2.884 µg/mL ceftazidime/0.481 µg/mL doxycycline (Fig. 13A). The ratio of ceftazidime to doxycycline used was 6:1, which was based off the IC_{50} values of the individual soluble antibiotics. Again, the inclusion of doxycycline in these experiments leads to no additive or synergistic properties regardless of delivery method (Figs. 13B & 13C).

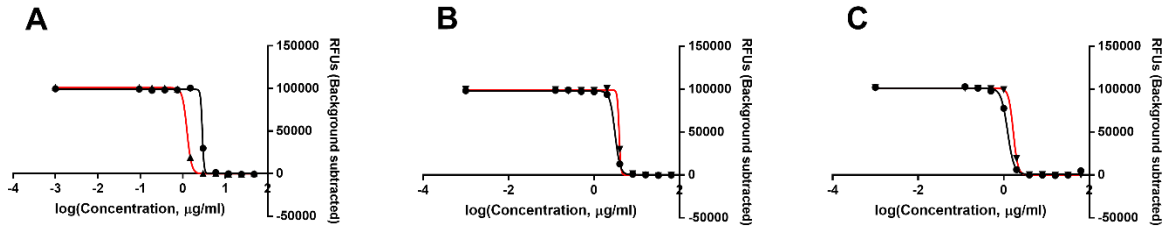

FIG 2-13. Nonlinear regression of *in vitro* dose titration response of *Burkholderia. pseudomallei* to dual ceftazidime and doxycycline nanoparticle therapies compared to conventional soluble dual drug therapies. Viability of treated bacteria was determined through the reduction of resazurin. (A) Ceftazidime loaded into 10:90 CPTEG:SA and doxycycline loaded into 20:80 CPTEG:CPH (6:1 ratio); ● conventional soluble drug, ▲ nanoparticle therapy. (B) Comparison of single soluble ceftazidime treatment with that of dual ceftazidime and doxycycline treatment (6:1 ratio); ● single ceftazidime treatment, ▼ combination ceftazidime with doxycycline treatment (6:1 ratio). (C) Comparison of single nanoparticle ceftazidime treatment with that of dual ceftazidime and doxycycline nanoparticle treatment (6:1 ratio); ● single ceftazidime treatment, ▼ combination ceftazidime with doxycycline treatment (6:1 ratio).

Discussion

The benefit to loading currently approved antibiotics for the treatment of melioidosis and Glanders into 10:90 CPTEG:SA polyanhydride nanoparticles is shown by a decrease in the IC_{50} concentration of the antibiotics, by decreasing the concentration of antibiotic needed for bactericidal activity, and an improvement of the targeting of these antibiotics to intracellular bacteria. Reductions in IC_{50} and bactericidal activity seems dependent on the antibiotic and the nanoparticle chemistry chosen. Of the antibiotics screened we have two, meropenem and ceftazidime, that target penicillin binding proteins and inhibit cell-wall synthesis. In the case of both these antibiotics, a significant

improvement in antimicrobial activity was observed through the reduction in IC_{50} value with encapsulation into 10:90 CPTEG:SA nanoparticles; to a lesser degree we saw improvement with 20:80 CPH:SA nanoparticles and no improvement with 20:80 CPTEG:CPH nanoparticles. The *B. pseudomallei* strain chosen in these experiments (K96243) is susceptible to both of these antibiotics; resistance to ceftazidime typically involves alteration of the penicillin binding protein gene *penA* and resistance to meropenem has been implicated through efflux pump dysregulation (15, 27). It is currently unknown as to why the 10:90 CPTEG:SA formulation is superior at improving the efficacy of these two drugs over the other nanoparticle chemistries used. Delivery of these two drugs into the periplasmic space would be crucial to their antimicrobial activity and it may be that the 10:90 CPTEG:SA formulation has unique interactions with the outer membrane of the bacteria and is better able at delivering antibiotics across this membrane into the periplasmic space; this will require further testing as it is currently speculation derived from observation. As these nanoparticles were observed to have no deleterious effect on *B. pseudomallei* when used in the absence of antimicrobial load any interactions of these nanoparticles with these bacteria cannot have profound impacts on their physiology. It could be possible that when these nanoparticles interact with the outer membrane of these bacteria, they are able to occlude efflux pumps thus enabling higher intracellular concentrations of these antibiotics to occur; as no benefit in antimicrobial activity was observed when these bacteria were treated with soluble meropenem in the presence of unloaded nanoparticles this hypothesis seems unlikely. As nanoparticles with burst release kinetics showed improved efficacy, it could simply be

that the high antibiotic concentration in the microenvironment around the nanoparticle and bacteria overwhelmed the bacteria.

The other antibiotic whose antimicrobial activity was enhanced through nanoparticle incorporation was chloramphenicol. The mechanism of action of chloramphenicol requires access to the cytosol where it binds to the 50s subunit thereby inhibiting protein synthesis. In the event of chloramphenicol, the only nanoparticle chemistry tried was the 10:90 CPTEG:SA formulation that worked so well with meropenem and ceftazidime, so it is unknown if the other nanoparticles chemistries would follow the trend shown with meropenem. Oddly enough with the antibiotic doxycycline, which inhibits protein synthesis through binding to the 30s ribosome, antimicrobial activity was not enhanced through nanoparticle incorporation; this was tested using several nanoparticle formulations and polyanhydride chemistries.

The last antibiotic tested, which is not currently recommended for the treatment of melioidosis or Glanders, rifampicin performed considerably worse in its antimicrobial activity when loaded into these nanoparticles. This antibiotic was chosen as it represents an antibiotic that has a cytosolic target that differs from those already screened; rifampicin inhibits the activity of RNA polymerase, thereby impeding transcription of DNA to RNA. The decrease in activity seen with the loading of rifampicin into these nanoparticles could be due in part to the slower release kinetics with rifampicin vs the faster release profiles with meropenem, ceftazidime, and chloramphenicol. When doxycycline was loaded into a nanoparticle formulation that resulted in a slower release profile, we saw a similar decline in activity, which indicates that in order for these nanoparticle formulations to successfully outperform soluble antibiotics there needs to be

a rapid release of loaded antibiotics. Even though a rapid release of the antibiotic was necessary to outperform soluble drugs, there is a unique interaction that is occurring between these antimicrobially loaded nanoparticles and the bacteria. Treating *B. pseudomallei* with 10:90 CPTEG:SA nanoparticles that are devoid of antimicrobials showed no positive or negative alteration on the viability of the bacteria; adding soluble antibiotic to cultures treated with unloaded 10:90 CPTEG:SA nanoparticles yielded viability inhibition similar to that of cultures treated with soluble antibiotics alone. Future studies will be needed to examine the mechanism behind these nanoparticles; possibilities are that the rapid release of antibiotics within the local environment of these bacteria result in very high focal concentrations of antibiotics that overcome normal permeability and efflux activity of the bacteria, or there is a unique interaction with the outer membrane of the bacteria that facilitates a more direct release of the antibiotic into the periplasmic space. The explanation on why there is improved efficacy with loading chloramphenicol into these nanoparticles and not doxycycline is vexing as they have similar intracellular targets and the release kinetics can be tailored to have similar profiles.

Screening of the three lead candidates, meropenem, ceftazidime, and chloramphenicol, against *B. mallei* in the 10:90 CPTEG:SA formulation yielded similar results to that of *B. pseudomallei* and indicates that these nanoparticle therapies would function in the treatment of diseases caused by both these organisms. The incidence of *B. pseudomallei* developing resistance to antimicrobial therapy during the course of treatment is concerning given that so few antibiotics are available to effectively treat this disease, and meropenem is typically used as an antibiotic of last resort; here we showed

that the incidence of meropenem resistance developed during exposure to these nanoparticles is approximately half of that when these bacteria were exposed to soluble meropenem.

In infections caused by both *B. pseudomallei* and *B. mallei* in the intracellular niche presents a barrier for the effective delivery of antimicrobials; in the activated human macrophage cell line THP-1, we demonstrate that 10:90 CPTEG:SA nanoparticles loaded with meropenem show vastly improved intracellular drug delivery and bactericidal activity compared to the conventional use of meropenem. Soluble meropenem was used at 16 µg/mL, which is 8x the broth MIC. While there was a complete inhibition of replication, there was limited bactericidal activity with approximately a log reduction in intracellular bacterial burden. When meropenem was loaded into 10:90 CPTEG:SA nanoparticles, a complete clearance of intracellular bacteria was observed when the macrophages were infected with low or moderate amounts of *B. pseudomallei*; at a higher MOI there was a 4-log reduction in intracellular bacteria. In the murine macrophage cell line RAW 267.4, these 10:90 CPTEG:SA nanoparticles are found within MNGCs, which are a hallmark of *B. pseudomallei* infection, showing that these nanomedicines can target into the intracellular niches established by this bacterium. Interactions of these 10:90 CPTEG:SA nanoparticles led to an interesting observation; concentrations of nanoparticles that led to no alteration in viability did cause an apparent increase in annexin V staining, which suggests that these nanoparticles cause the flipping of phosphatidylserine to the outer membrane, which is a marker of apoptosis. Future studies will be needed to further describe this cellular interaction.

As the WHO recommends the inclusion of doxycycline during the initial intravenous phase of melioidosis treatment, this antibiotic was tested in combination with meropenem. Doxycycline was tested with our 10:90 CPTEG:SA nanoparticle formulation and with the 20:80 CPH:SA nanoparticle formulation which showed no improvement in IC_{50} concentrations vs soluble meropenem. It should be noted that none of our doxycycline nanoparticle formulations using 20:80 CPTEG:CPH nanoparticles led to a significant improvement in IC_{50} value. While loading these antibiotics into 10:90 CPTEG:SA nanoparticles resulted in a 7.9-fold increase in antimicrobial efficacy compared to the combined use of these two antimicrobials in soluble form, there was no synergistic or additive qualities of combining these two antibiotics whether they were delivered via nanoparticle or in soluble form. In the case of these two antimicrobials used together in conventional soluble form the combined IC_{50} was 0.9513 µg/mL meropenem and 0.4756 µg/mL doxycycline; the individual IC_{50} concentrations for these two drugs used alone is 0.6460 µg/mL meropenem and 0.5365 µg/mL doxycycline. It appears that, at least when these two antibiotics are used at a 1:2 ratio of meropenem to doxycycline, that there is perhaps a degree of antagonism between the two and that the inclusion of doxycycline offers no benefit and could in fact be contraindicated. Other ratios of meropenem to doxycycline have not currently been tested but may provide different results. When meropenem was loaded into 10:90 CPTEG:SA nanoparticles the combined IC_{50} was 0.1073 µg/mL meropenem and 0.0536 µg/mL doxycycline, while the individual IC_{50} values were oddly enough 0.1073 µg/mL meropenem and 0.4730 µg/mL doxycycline. In the use of these nanoparticles the inclusion of doxycycline added no synergistic, additive or antagonistic effects; this is likely due to the fact that when used at

a 1:2 ratio of meropenem to doxycycline that the concentration of doxycycline falls below a biologically relevant concentration.

The combination of ceftazidime with doxycycline also favored nanoparticle encapsulation into our 10:90 CPTEG:SA formulation, but again we saw no benefit to the inclusion of doxycycline. The soluble combination resulted in a combined IC_{50} of 2.884 µg/mL ceftazidime and 0.481 µg/mL doxycycline, which is relatively similar to the individual IC_{50} values of 3.079 µg/mL ceftazidime and 0.5698 µg/mL doxycycline. A 1:6 ratio of ceftazidime to doxycycline yielded no synergistic, additive, or antagonistic effects. In the case of the combined delivery via nanoparticle we see a 1.3-fold increase in efficacy when ceftazidime was delivered in 10:90 CPTEG:SA nanoparticles and doxycycline was delivered in 20:80 CPTEG:CPH nanoparticles. The combined IC_{50} was 1.254 µg/mL ceftazidime and 0.209 µg/mL doxycycline, which were somewhat similar to the individual IC_{50} values of 1.228 µg/mL ceftazidime and 0.209 µg/mL doxycycline. Different ratios of ceftazidime to doxycyline might yield different results.

While providing *in vivo* data would further illuminate the benefit that these nanoparticles would have in combating infections caused by *Burkholderia* species, the *in vitro* data presented thus far provides a compelling argument in favor of their potential benefit in treating these diseases. Future work will include animal models of melioidosis and glanders, along with a more complete workup on toxicology and absorption, distribution, metabolism, and excretion (ADME). Previous work utilizing 20:80 CPTEG:CPH nanoparticles in the *in vivo* treatment of brucellosis in mice showed decreased bacterial burden compared to those mice treated with antibiotics through

conventional means, so it would be expected that we could see similar results with *Burkholderia* species (22).

References

1. Sawana A, Adeolu M, Gupta RS. 2014. Molecular signatures and phylogenomic analysis of the genus *Burkholderia*: proposal for division of this genus into the emended genus *Burkholderia* containing pathogenic organisms and a new genus *Paraburkholderia* gen. nov. harboring environmental species. Front Genet 5:429.

2. Galyov EE, Brett PJ, DeShazer D. 2010. Molecular insights into *Burkholderia pseudomallei* and *Burkholderia mallei* pathogenesis. Annu Rev Microbiol 64:495-517.

3. Cheng AC, Currie BJ. 2005. Melioidosis: epidemiology, pathophysiology, and management. Clin Microbiol Rev 18:383-416.

4. Withers MR. 2014. USAMRIID'S medical management of biological casualties handbook (8th ed.). Fort Detrick, MD: US Army Medical Research Institute of Infectious Diseases.

5. Riedel S. 2004. Biological warfare and bioterrorism: a historical review. BUMC Proceedings 17:7.

6. Wheelis M. 1998. First shots fired in biological warfare. Nature 395:1.

7. Hilleman MR. 2002. Overview: cause and prevention in biowarfare and bioterrorism. Vaccine 20:13.

8. Currie BJ, Ward L, Cheng AC. 2010. The epidemiology and clinical spectrum of melioidosis: 540 cases from the 20 year Darwin prospective study. PLoS Negl Trop Dis 4:e900.

9. Rebecca L, Susan G, Rosemarie A, Prasith B, David DB, Allen CC, Bart JC, David D, Jay EG, Joseph L, Direk L, Meredith GM, Robert N, Elizabeth OM, Sharon JP, Nicki P, Rogers LP, Herbert PS, Ivo S, Gladys T, Patrick T, Wiersinga WJ, Vanaporn W, Theresa LS. 2012. Workshop on Treatment of and Postexposure Prophylaxis for *Burkholderia pseudomallei* and *B. mallei* Infection, 2010. Emerg Infec Dis 18(12): e2.

10. World Health Organization. 2001. WHO Model Prescribing Information: Drugs used in Bacterial Infections. Geneva, World Health Organization https://appswhoint/iris/handle/10665/42372.

11. Estes DM, Dow SW, Schweizer HP, Torres AG. 2010. Present and future therapeutic strategies for melioidosis and glanders. Expert Rev Anti Infect Ther 8:325-38.

12. Limmathurotsakul D, Golding N, Dance DAB, Messina JP, Pigott DM, Moyes CL, Rolim DB, Bertherat E, Day NPJ, Peacock SJ, Hay SI. 2016. Predicted global distribution of *Burkholderia pseudomallei* and burden of melioidosis. Nature Microbiology 1.

13. Schweizer HP. 2012. Mechanisms of antibiotic resistance in *Burkholderia pseudomallei*: implications for treatment of melioidosis. Future Microbiol 7:1389-99.

14. Nierman WC, DeShazer D, Kim HS, Tettelin H, Nelson KE, Feldblyum T, Ulrich RL, Ronning CM, Brinkac LM, Daugherty SC, Davidsen TD, Deboy RT, Dimitrov G, Dodson RJ, Durkin AS, Gwinn ML, Haft DH, Khouri H, Kolonay JF, Madupu R, Mohammoud Y, Nelson WC, Radune D, Romero CM, Sarria S, Selengut J, Shamblin C, Sullivan SA, White O, Yu Y, Zafar N, Zhou L, Fraser CM. 2004. Structural flexibility in the *Burkholderia mallei* genome. Proceedings of the National Academy of Sciences of the United States of America 101:14246-14251.

15. Rhodes KA, Schweizer HP. 2016. Antibiotic resistance in *Burkholderia* species. Drug Resist Updat 28:82-90.

16. Wiersinga WJ, Virk HS, Torres AG, Currie BJ, Peacock SJ, Dance DAB, Limmathurotsakul D. 2018. Melioidosis. Nat Rev Dis Primers 4:17107.

17. Thamlikitkul V, Trakulsomboon S. 2006. In vitro activity of tigecycline against *Burkholderia pseudomallei* and *Burkholderia thailandensis*. Antimicrob Agents Chemother 50:1555-7.

18. Mima T, Kvitko BH, Rholl DA, Page MG, Desarbre E, Schweizer HP. 2011. In vitro activity of BAL30072 against *Burkholderia pseudomallei*. Int J Antimicrob Agents 38:157-9.

19. Thamlikitkul V, Trakulsomboon S. 2008. In vitro activity of ceftobiprole against *Burkholderia pseudomallei*. J Antimicrob Chemother 61:460-1.

20. Kamaly N, Yameen B, Wu J, Farokhzad OC. 2016. Degradable Controlled-Release Polymers and Polymeric Nanoparticles: Mechanisms of Controlling Drug Release. Chem Rev 116:2602-63.

21. Huntimer L, Ramer-Tait AE, Petersen LK, Ross KA, Walz KA, Wang C, Hostetter J, Narasimhan B, Wannemuehler MJ. 2013. Evaluation of biocompatibility and administration site reactogenicity of polyanhydride-particle-based platform for vaccine delivery. Adv Healthc Mater 2:369-78.

22. Lueth P, Haughney SL, Binnebose AM, Mullis AS, Peroutka-Bigus N, Narasimhan B, Bellaire BH. 2019. Nanotherapeutic provides dose sparing and improved antimicrobial activity against *Brucella melitensis* infections. J Control Release 294:288-297.

23. Torres MP, Vogel BM, Narasimhan B, Mallapragada SK. 2006. Synthesis and characterization of novel polyanhydrides with tailored erosion mechanisms. Journal of Biomedical Materials Research Part A 76A:102-110.

24. Shen E, Pizsczek R, Dziadul B, Narasimhan B. 2001. Microphase separation in bioerodible copolymers for drug delivery. Biomaterials 22:10.

25. Ulery BD, Petersen LK, Phanse Y, Kong CS, Broderick SR, Kumar D, Ramer-Tait AE, Carrillo-Conde B, Rajan K, Wannemuehler MJ, Bellaire BH, Metzger DW, Narasimhan B. 2011. Rational design of pathogen-mimicking amphiphilic materials as nanoadjuvants. Sci Rep 1:198.

26. Schwarz S, Singh P, Robertson JD, LeRoux M, Skerrett SJ, Goodlett DR, West TE, Mougous JD. 2014. VgrG-5 is a *Burkholderia* type VI secretion system-exported protein required for multinucleated giant cell formation and virulence. Infect Immun 82:1445-52.

27. Sarovich DS, Webb JR, Pitman MC, Viberg LT, Mayo M, Baird RW, Robson JM, Currie BJ, Price EP. 2018. Raising the Stakes: Loss of Efflux Pump Regulation Decreases Meropenem Susceptibility in *Burkholderia pseudomallei*. Clin Infect Dis 67:243-250.

CHAPTER 3: NANOPARTICLE BASED THERAPY AGAINST *NAEGLERIA FOWLERI*

Modified from a manuscript to be submitted to Antimicrobial Agents and Chemotherapy

Nathan Peroutka-Bigus,[a,b] Adam Mullis,[c] Shannon Haughney,[c] Balaji Narasimhan,[c,d] Bryan H. Bellaire[a,b,d]

[a]Department of Veterinary Microbiology and Preventive Medicine, Iowa State University, Ames, IA, USA, [b]Interdepartmental Microbiology Program, Iowa State University, Ames, IA, USA, [c]Department of Chemical and Biological Engineering, Iowa State University, Ames, IA, USA, [d]Nanovaccine Institute, Iowa State University, Ames, IA, USA

Abstract

The pathogenic free-living amoeba *Naegleria fowleri* is the cause of the fatal disease primary amoebic meningoencephalitis. While this amoeba is ubiquitous in the environment being found in warm freshwater bodies, primary amoebic meningoencephalitis is a rare disease. While rare this disease results in mortality exceeding 95 percent with aggressive antimicrobial therapy. Surviving this infection can leave the patient with permanent disabling brain damage. Given the apparent need to improve therapeutic outcome, we utilized polyanhydride nanoparticles to improve antimicrobial delivery to this amoeba *in vitro*. Laser scanning microscopy showed that these nanoparticles are readily internalized by these amoeba and come to reside in endosomal compartments. By loading currently approved antimicrobials for the treatment of primary amoebic meningoencephalitis that target intracellular processes we demonstrate that both the antimicrobials rifampicin and azithromycin show improved anti-parasitic activity when loaded into these nanoparticles. An improvement in anti-parasitic activity was not seen with the nanoparticle delivery of amphotericin B, which

targets ergosterol on the cell surface of the amoeba. These nanoparticles present a tool to facilitate the improved delivery and antimicrobial efficacy of drugs that target intracellular processes of *N. fowleri*.

Introduction

The pathogenic free-living amoeba *Naegleria fowleri* is the cause of the fatal disease primary amoebic meningoencephalitis (PAM). PAM was first characterized in 1965 in Australia by Fowler and Carter, PAM has now been documented throughout the world, with *N. fowleri* being routinely isolated from environmental sources (1, 2). Most cases of PAM are closely associated with exposure to water, in which the organisms gain access to the olfactory neural epithelium through contaminated water being introduced into the nasal cavity (3). These amoebae are then capable of penetrating the olfactory neural epithelium and subsequently gaining access to the olfactory nerve, which acts as a conduit for the migration of the amoeba through the cribriform plate to the olfactory bulb. From the olfactory bulb the amoeba are then able to access the brain, where in combination with the tissue disruption caused by the trogocytic activities and lytic enzymes of the amoeba and the inflammatory actions brought on by the influx of neutrophils and other immune cells, hemorrhaging and intracranial pressure ultimately leads to death of the individual 4 to 7 days following the appearance of symptoms (4-6). Symptoms initially present as fever, headache, and emesis and then progresses to seizure, and coma (5). Incidence of PAM is rare with on average fewer than 5 documented cases occurring in the U.S. (3). The Centers for Disease Control and Prevention (CDC) recommends a multidrug treatment when PAM is diagnosed and includes the intrathecal administration of amphotericin B, and the oral or intravenous (IV) administration of

azithromycin, fluconazole, rifampicin, and miltefosine (7). Even with this aggressive treatment, survival of PAM is still rare, with a historic mortality greater than 95% indicating the need for new therapeutics to treat this aggressive disease.

Identifying new therapies to treat PAM has constantly been evolving since the discovery of this disease. Much of the initial work was in accessing what currently available antimicrobials, whether they be antibiotics or antifungals, could inhibit the replication of this amoeba or improve survival in animal models of PAM (8, 9). Current drug discovery tends to revolve more around screening non-antimicrobials against this amoeba or utilizing new delivery platforms like nanoparticles to more effectively target the amoeba. The anti-rheumatoid arthritis drug auranofin has been found to have antimicrobial activity against numerous protozoa to include *N. fowleri* (10). Other interesting finds have been the neuroleptic drugs chlorpromazine and trifluoperazine are effective in inhibiting the replication of pathogenic *Acanthamoeba polyphaga* and *N. fowleri in vitro* (11). The use of nanoparticles is a more recent evolution in treatment of protozoan disease. Silver nanoparticles have been reported to improve the efficacy of anti-amoebic drugs against both *N. fowleri* and *Acanthamoeba castellani* when conventional antimicrobials were conjugated to them (12, 13). The use of gold nanoparticles has also shown promising anti-parasitic action against *N. fowleri* (14)

We examine the potential of nanoparticles composed of 1,6-bis(p-carboxyphenoxy)hexane (CPH), 1,8-bis(p-carboxyphenoxy)-3,6-dioxaoctane (CPTEG), and sebacic acid (SA) to be effective drug delivery vehicles against *N. fowleri* through the loading of conventionally used antimicrobials into these nanoparticles and testing them in *in vitro* assays. These nanoparticles degrade through surface erosion via hydrolysis of the

anhydride bounds linking the monomers, with the release of non-toxic and biocompatible dicarboxylic acids (15). Drug release from these nanoparticles is dependent upon surface erosion when the entrapped drug is hydrophobic; this can provide a more sustained release profile. Solute transport through the hydrated portion of the nanoparticle is import in the release of hydrophilic drugs and will provide a more rapid release profile (16). With the encapsulation of the hydrophobic antibiotic rifampicin in these polyanhydride nanoparticles, we have been able to take a drug with poor *in vitro* efficacy against *N. fowleri* and significantly improve upon its ability to inhibit the replication of this amoeba. Along with rifampicin we have seen an improvement in efficacy with the nanoparticle encapsulation of azithromycin. The encapsulation of amphotericin B did not yield improvement. In the case of rifampicin, we saw differences in efficacy depending on co-polymer ratios and nanoparticles polymer chemistries employed. This demonstrates the potential for polyanhydride nanoparticles as a means to improve upon the therapeutic potential of already prescribed antimicrobials in the treatment of PAM.

Materials & Methods

Antimicrobials and nanoparticle preparation

Antimicrobial agents were prepared in suitable solvents and maintained at ideal temperatures for each antimicrobial. Nanoparticle CPTEG and CPH monomers were synthesized in house as previously described, and SA monomers were purchased from Sigma (17, 18). Nanoparticles were fabricated by flash nanoprecipitation as previously described (19). Prior to an experiment, nanoparticle stock suspensions were made to 10 mg/mL nanoparticle concentration in PBS and were sonicated on ice at 14 amps to suspend the nanoparticles (Misonix S-4000, Newton, CT).

Cell culture

The virulent *Naegleria fowleri* HB-1 strain (ATCC 30174) was obtained from the American Type Culture Collection and were maintained under axenic conditions in Nelson's media (ATCC medium 710) supplemented with 10% FBS at 37°C and 5% CO_2 in 75 cm^2 tissue culture flasks in 12 mL of media.

Microscopy and nanoparticle interactions with amoeba

Amoeba grown in T75 flasks were suspended and centrifuged at 500 rcf for 5 minutes. The supernatant was removed and replaced with Nelson's media with 5% FBS; the cultures were then adjusted to a cell density of 5.0×10^5. Five hundred microliters of these cell suspensions were added to 24 well plates containing coverslips. The amoeba were allowed to grow overnight on the coverslips in an incubator set at 37°C and 5% CO_2, and prior to nanoparticle treatment cultures were washed and replaced with fresh media. Amoeba in the 24 well plates were treated with 50 µg of rhodamine loaded nanoparticles in 500 µL of media. Contact of nanoparticle to amoeba were synchronized by centrifuging treated cultures at 4°C for 10 minutes at 250 rcf. Cultures were immediately placed in 37°C incubator; internalization was assessed beginning at 2 hours with 24-hour intervals as indicated.

Imaging of nanoparticles within amoeba was performed on fixed cells using laser scanning microscopy. Prior to fixation amoeba were treated for 30 minutes with 10 µM Cell Tracker Green (ThermoFisher Scientific, Waltham, MA). The amoeba were then fixed with 4% PFA for 20 minutes, followed by 2 washes with PBS and the coverslips were mounted onto slides with Prolong Gold Antifade Mountant with DAPI (ThermoFisher Scientific, Waltham, MA). Internalized nanoparticles were visualized and

quantified using inverted fluorescence microscope (Olympus BX71, Olympus, Center Valley, PA) on fixed samples. For each experiment a minimum of 200 amoeba were scored for the presence or absence of nanoparticles. Post-acquisition processing was performed with imageJ (https://fiji.sc/)

LysoSensor (ThermoFisher Scientific, Waltham, MA) was utilized following the specifications found with the product manual. In brief, 100,000 *N. fowleri* trophozoites were added to 96 well tissue culture plates in a volume of 50 µL. Ten micrograms of 20:80 CPH:SA nanoparticles loaded with rhodamine were added to the cultures with amoeba in a volume of 50 µL and were allowed to interact with the amoeba; as a control amoeba without nanoparticle treatment was included. Anticipating that the nanoparticles would increase the lysosomal pH an additional treatment group included nanoparticles with the addition of 10 mM ammonium chloride. LysoSensor Green DND-189 was used at 1 µM and imaged with an IX71 DSU microscope (Olympus, Center Valley, PA) with Metamorph Advanced acquisition software.. Prior to addition of the LysoSensor stain the wells were washed to remove excess uninternalized nanoparticle.

Nanoparticle efficacy assays

Viability was determined through Trypan Blue exclusion hemocytometer cell counts and the Alamar Blue (ThermoFisher Scientific, Waltham, MA) viability assay. Amoeba cultures were suspended and centrifuged at 500 rcf for 5 minutes; the supernatant was removed and replaced with Nelson's medium supplemented with 5% FBS. The amoeba cell density was determined by hemocytometer and was adjusted to 5.0×10^5/mL, and 50 µl was pipetted into sterile 96 well tissue culture plates (TPP, Switzerland), separate plates were set up for each post-treatment time point of 24 hours,

72 hours, and 120 hours. Border wells of the plates were filled with sterile H_2O to buffer against evaporation of the treatment wells. The plates were placed in an incubator at 37°C and 5% CO_2 overnight.

The following day the plates were treated with soluble or nanoparticle treatments by the addition of 50 µl of medium containing the appropriate drug concentration for the treatment wells to achieve a dose range from 25 µg/mL (30.4 µM) to 1.56 µg/mL (1.9 µM) rifampicin as either conventional soluble drug or nanoparticles loaded with rifampicin. For azithromycin, the dose range was 30 µg/mL (40.1 µM), 20 µg/mL (26.7 µM), and 10µg/mL (13.4 µM). Fifty microliters of medium was also added to the untreated wells at this time to match the volume in the treatment groups. Approximate cell density of *N. fowleri* at time of treatment is 5.0 x 10^5 amoeba per mL. Each treatment group was performed in triplicate. At the appointed post-treatment time points 10 µL of Alamar Blue was added to each well; two hours later the plates were read by a fluorimeter (Fluostar Omega, BMG LABTECH, Cary, NC) at 544/590 and the wells were scraped to suspend the amoeba and mixed at a 1:1 ratio with Trypan blue for hemocytometer counts. An inverted light microscope was used to count the amoeba on the hemocytometer.

Pathogenesis of *N. fowleri* has previously been demonstrated *in vitro* using Vero cells to model cellular interaction with the amoeba (20). Vero cell monolayers were established in 96 well plates by seeding each well with 100 µL of Vero cell suspension at a cell density of 5.0 x 10^5 Vero cells per mL in DMEM with 10% FBS. The cells were allowed to replicate overnight in a 37ºC incubator at 5% CO_2. The following day the medium was removed and the Vero cells were stained with 5 µM Cell Tracker green

(ThermoFisher Scientific, Waltham, MA) in serum free DMEM for 30 minutes to allow for subsequent fluorescent microscopy of the disrupted monolayers by *N. fowleri*. Following staining the cells were washed with PBS to remove excess stain. Fifty microliters of a 2.0 x 10^6 amoeba per mL suspension in DMEM with 10% FBS was added to each treatment well. An hour after the addition of the amoeba the wells were treated with either soluble drug or nanoparticle encapsulated drug through the addition of 50 µL DMEM with 10% FBS containing an appropriate drug concentration to give 25 µg/mL rifampicin. Fifty microliters of media was also added to the untreated wells at this time to match the volume in the treatment groups. Confocal images were taken at identical XY coordinates every 24 hours for 72 hours using an IX71 DSU microscope (Olympus, Center Valley, PA) with Metamorph Advanced acquisition software. Images shown are representative of each treatment group. Post-acquisition processing was performed with ImageJ (https://fiji.sc/).

Results

Internalization of the nanoparticles by *Naegleria* was assessed at 2, 24, and 48 hours (Fig. 1A). The nanoparticles composed of the 20:80 CPH:SA chemistry was rapidly internalized, with 89% of surveyed amoeba having internalized nanoparticles after two hours of incubation; over the remaining time course this level of nanoparticles association was maintained with 90% and 85% of amoeba associated with nanoparticles at 24 and 48 hours. In the case of 20:80 CPTEG:CPH, approximately 50% of amoeba were associated with nanoparticles within two hours of exposure; by 24 and 48 hours, this number increased to 84% and 87%. Images taken appear to show the internalized nanoparticles localized within endosomal compartments due to the area of negative

staining surrounding the nanoparticles within the stained cytoplasm (Fig 1B). 50:50 CPTEG:CPH NPs were poorly internalized at all time points, with internalization of 37%, 62%, and 54% at 2 hours, 24 hours, and 48 hours post-treatment.

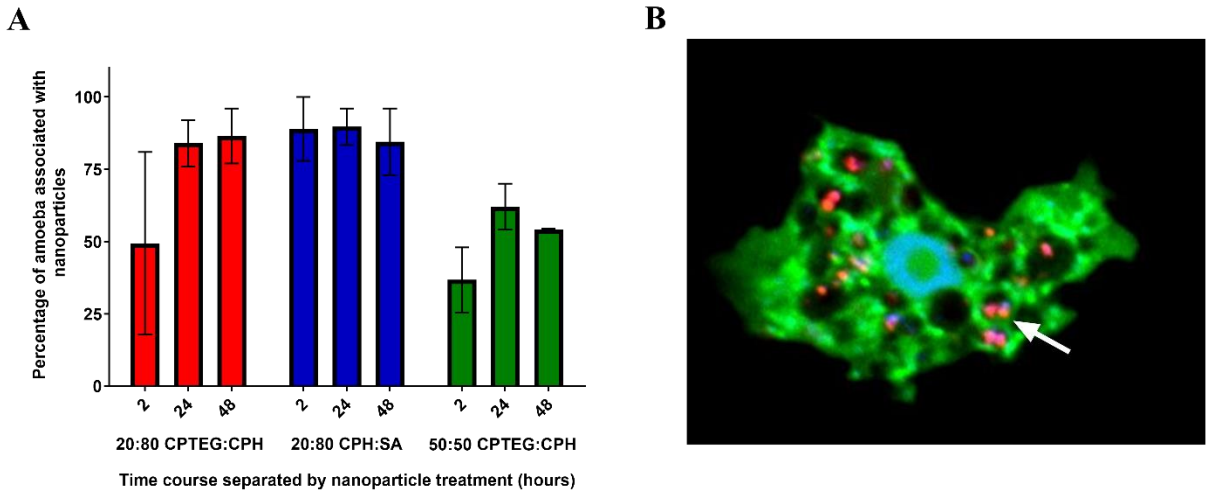

FIG 3-1. Association of polyanhydride nanoparticles with *Naegleria fowleri*. (A) Percentage of amoeba associated with polyanhydride nanoparticles. Values represent the means ± the SEM of two experiments with 200 amoeba scored per treatment group. (B) Laser scanning confocal image of 2% rhodamine-loaded 20:80 CPH:SA nanoparticles (red) internalized by *N. fowleri* at 48 hours post-treatment. Amoeba was stained with the cytosolic stain Cell Tracker Green and nucleus with DAPI (blue).

While amoeba treated with 20:80 CPTEG:CPH or 20:80 CPH:SA nanoparticles void of antimicrobials had similar numbers of amoeba with internalized nanoparticles following 24 hours of exposure; 20:80 CPTEG:CPH had no significant effect on replication or metabolic changes, while a decrease in amoeba counts and substantial reduction in metabolic activity was seen with 20:80 CPH:SA nanoparticles (Fig. 2).

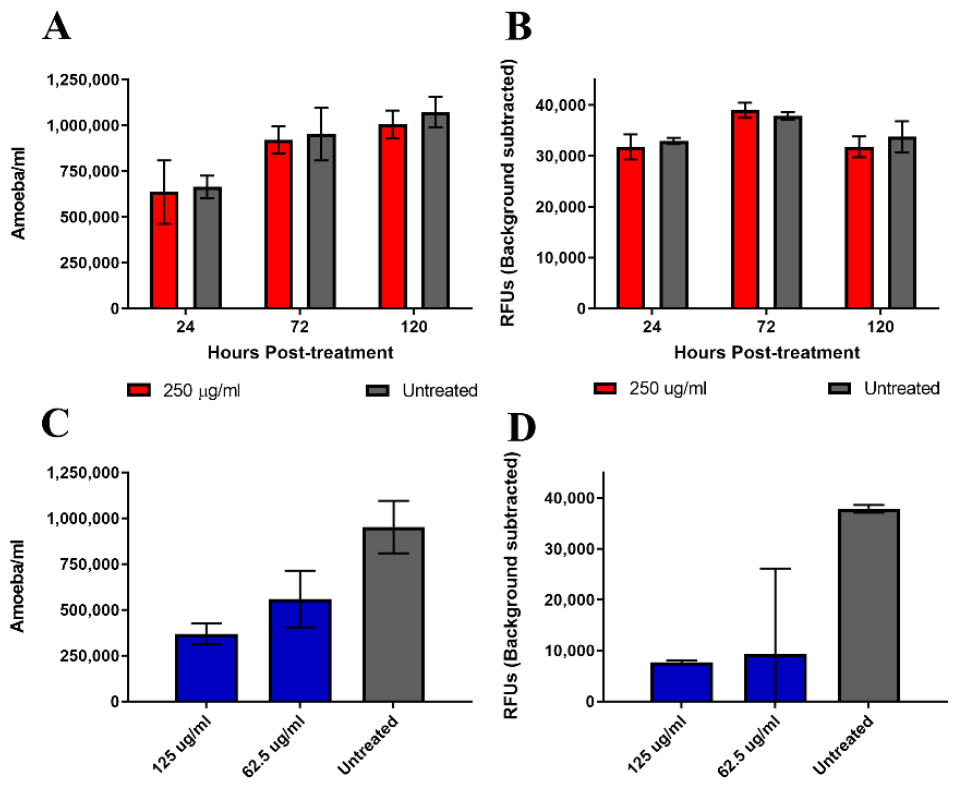

FIG 3-2. Polyanhydride nanoparticle effects on the replication & viability of *Naegleria fowleri*. (A) Effect of 20:80 CPTEG:CPH nanoparticles on the replication of *N. fowleri* over a 120-hour period. (B) Viability of *N. fowleri* following 120 hours of treatment with 20:80 CPTEG:CPH nanoparticles; as determined by resazurin reduction. (C) Effect of 20:80 CPH:SA nanoparticles on the replication of *N. fowleri* following 72 hours of treatment. (D) Viability of *N. fowleri* following 72 hours of treatment with 20:80 CPH:SA nanoparticles; as determined by resazurin reduction. Values represent the means ± a 95% confidence interval.

With 20:80 CPTEG:CPH no adverse effects on the amoeba was observed when treated with 250 µg/mL nanoparticles void of antimicrobials over a 5-day period (Fig. 2A & 2B). Conversely, with 20:80 CPH:SA a reduction in amoeba and metabolic activity was observed when treated with 62.5 µg/mL nanoparticles that were void of antimicrobials (Fig. 2C & 2D). Using the pH sensitive probe LysoSensor, a decrease in fluorescence was seen in vacuoles of amoeba treated with 20:80 CPH:SA nanoparticles compared to controls. This decrease in fluorescence intensity indicates that lysosomal pH

is higher in these nanoparticle treated amoeba (Fig. 3). The inclusion of 10 mM ammonium chloride resulted in a reduction in the fluorescent intensity in both the nanoparticle treated and control amoeba as expected (data not shown). As these images were taken with live amoeba, precise colocalization of nanoparticles with the LysoTracker stain is not possible due to movement of the amoeba between image acquisition; the reduction in fluorescence appears in vacuoles absent of nanoparticles. Morphological changes were also noted when the amoeba were treated with 20:80 CPH:SA nanoparticles, with these amoeba appearing to display more pseudopodia.

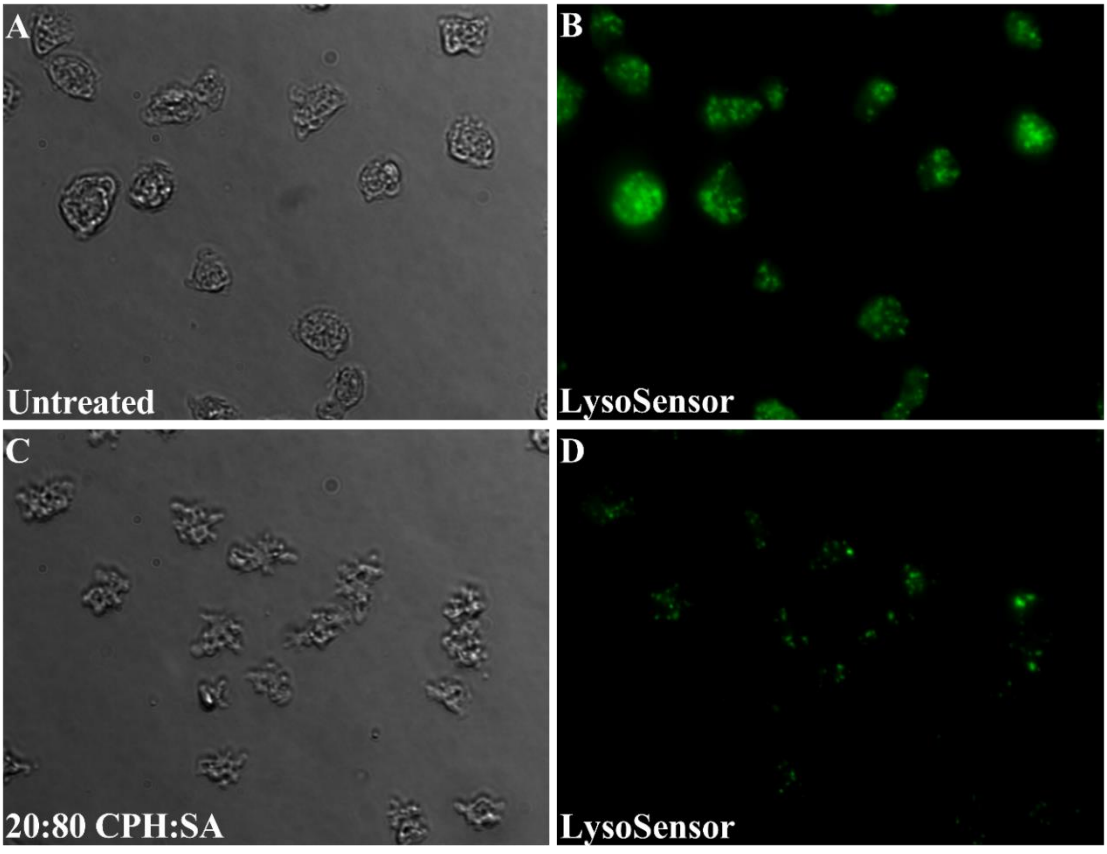

FIG 3-3. LysoSensor staining of nanoparticle treated *Naegleria fowleri*. (A) Brightfield image of untreated amoeba. (B) LysoSensor (green) stain of untreated amoeba. (C) Brightfield image of amoeba treated with 100 µg/mL 20:80 CPH:SA nanoparticles for 2 hours. (D) LysoSensor (green) stain of 20:80 CPH:SA treated amoeba. Representative images. 400x magnification.

When rifampicin was loaded in the nanoparticles, differences in replication and metabolic inhibition was seen between nanoparticle chemistries. Rifampicin is an antibiotic typically used to treated bacterial infections, and in bacteria it's mechanism of action is in the inhibition of RNA polymerase; it has a historical use in the treatment of PAM and is recommended by the CDC (21). When rifampicin was encapsulated in 20:80 CPTEG:CPH nanoparticles a significant inhibition of replication was seen compared to that of soluble rifampicin (Fig. 4) A significant reduction in proliferation of the amoeba was seen when 12.5 μg/mL rifampicin was delivered via nanoparticles; in contrast soluble rifampicin at 25 μg/mL had a negligible effect on the replication of the amoeba (Fig 4A). The use of nanoparticles to deliver rifampicin at 25 μg/mL had significant amoebastatic activity within 24 hours of treatment. 25 μg/mL rifampicin delivered by nanoparticle was able to inhibit the replication of the amoeba by 53% within the first 24 hours; in contrast an equivalent dose of soluble rifampicin inhibited the replication of the amoeba by only 18% (Fig. 4B). When the concentration of rifampicin was decreased to 12.5 μg/mL replication was inhibited by 24% for nanoparticle delivery and 7% for soluble delivery within the first 24 hours, which was not significantly different. Following 120 hours of treatment both 25.0 and 12.5 μg/mL rifampicin delivered by nanoparticle significantly inhibited the replication of the amoeba compared to soluble rifampicin. Twenty-five μg/mL rifampicin delivered by nanoparticle now had reduced the replication of the amoeba by 79% and 12.5 μg/mL rifampicin delivered by nanoparticle replication inhibition had increased to 55%. Equivalent concentrations of soluble rifampicin at 120 hours of treatment had reduced inhibition compared to inhibition observed at 24 hours treatment; inhibition with 25 μg/mL rifampicin was now

at 12%, which was at 18% inhibition earlier at 24 hours post-treatment. Inhibition with 12.5 µg/mL rifampicin was now at 3% inhibition which was half the level of inhibition seen at earlier timepoints. Viability of these amoeba as determined by resazurin reduction indicated that nanoparticle treated amoeba was further reduced compared to soluble rifampicin controls and correlates well to the reduction in amoeba counts (Figure 4C).

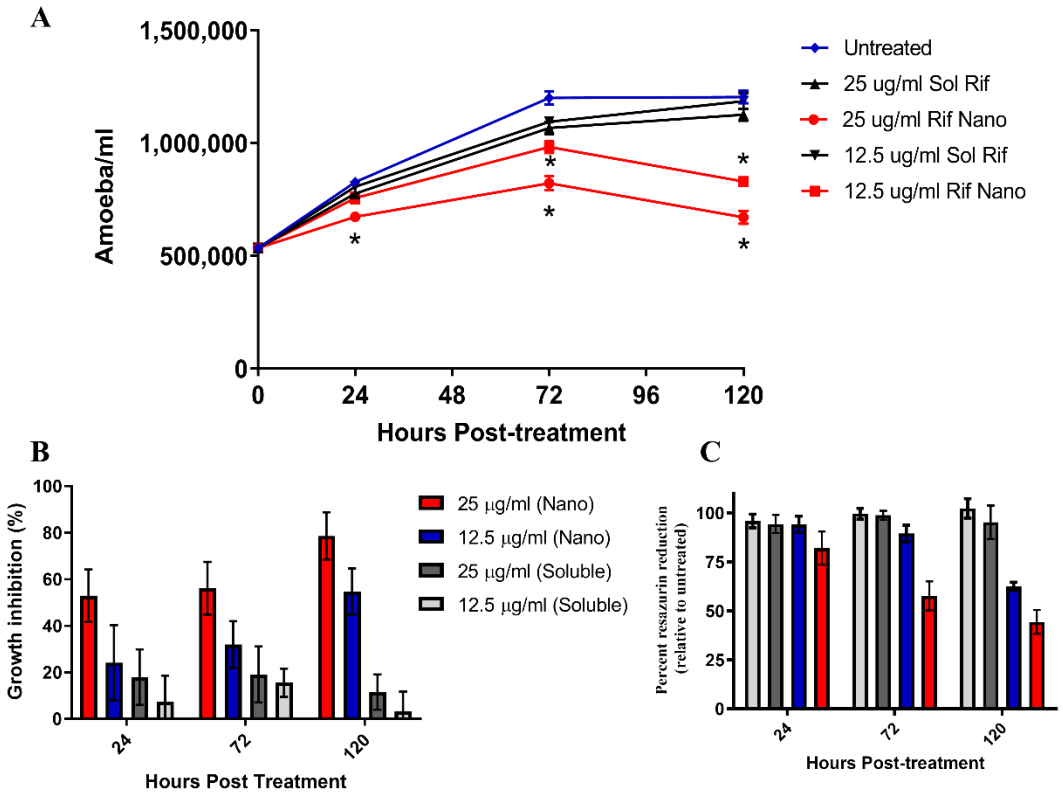

FIG 3-4. Replication and viability inhibition of *Naegleria fowleri* by 20:80 CPTEG:CPH rifampicin loaded nanoparticles. (A) Growth curve of rifampicin treated amoeba. Values represent the means ± the SEM of three experiments performed in triplicate. * indicates significant differences in growth inhibition between nanoparticle and soluble treatment (One-way ANOVA with Bonferroni's multiple comparison test); $p \leq 0.05$. (B). Percent replication inhibition of rifampicin treated amoeba. Values represent the means ± a 95% confidence interval. (C). Viability of rifampicin treated amoeba; determined through the reduction of resazurin. Values represent the means ± a 95% confidence interval.

Following 24 hours of treatment the viability of amoeba treated with 25 µg/mL rifampicin by nanoparticle delivery were reduced to that of 82% of controls, were as the

other treatments were comparable to controls. By 120 hours of treatment, both 25 and 12.5 µg/mL rifampicin delivered by nanoparticles had reduced viability of 44% and 62%. At the same time point, amoeba treated with soluble rifampicin at 25 and 12.5µg/mL had viabilities of 95% and 102%.

Altering the loading percentage of rifampicin in 20:80 CPTEG:CPH nanoparticles yielded no significant differences in replication inhibition of *Naegleria* (Fig. 5). It should be noted that in this experiment the starting number of amoeba per well was 5,000, not the 50,000 amoeba per well that was used in previous experiments.

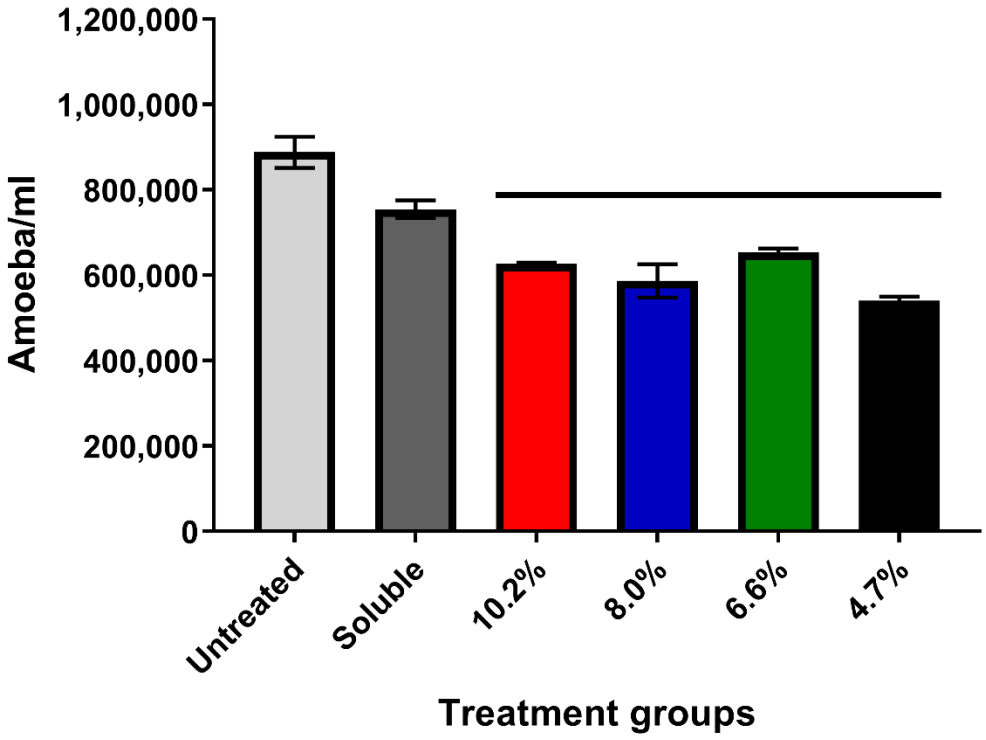

FIG 3-5. Effect of altering the rifampicin loading percentage in 20:80 CPTEG:CPH nanoparticles on the replication of *Naegleria fowleri* following 72 hours of treatment with 12.5 µg/mL rifampicin. Percentages shown on the x-axis indicate loading percentage of rifampicin in the nanoparticles. Values represent the means ± the SEM of an experiment performed in triplicate. Statistical analysis by one-way ANOVA with Tukey's multiple comparison (*$p \leq 0.05$).

Difference in CPTEG:CPH co-polymer ratios did have an effect on replication inhibition when treated with rifampicin loaded nanoparticles (Fig. 6); ratios of 10:90, 20:80, and 30:70 yielded similar reductions in metabolic activity of approximately a 75% reduction in metabolic activity. When a ratio of 50:50 CPTEG:CPH co-polymers was used a reduction of metabolic activity of 50% was observed.

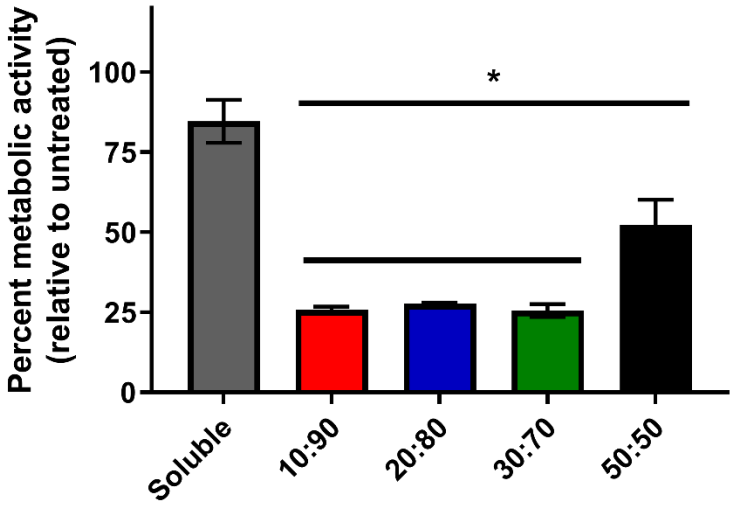

FIG 3-6. Effect of altering co-polymer ratios of CPTEG and CPH on the efficacy of reducing the viability of nanoparticle treated *Naegleria fowleri*. Nanoparticles were loaded with rifampicin and endpoint analysis was via resazurin reduction following a treatment of 120 hours with 25 µg/mL rifampicin. Ratios shown on the x-axis indicate co-polymer ratios tested. Values represent the means ± the SEM of an experiment performed in triplicate. Statistical analysis by one-way ANOVA with Tukey's multiple comparison (*$p \leq 0.05$).

When 20:80 CPH:SA co-polymer nanoparticles loaded with rifampicin were used a significant reduction in replication of the amoeba was seen (Fig. 7). Nanoparticles used at a rifampicin concentration of 6.25 µg/mL yielded an MIC_{100} following 72 hours of treatment, with a very abrupt decrease in replication after 24 hours of growth (Fig. 7A). Nanoparticle treatment resulted in a 60% inhibition of replication following 24 hours of treatment, while soluble resulted in a mere 3% inhibition of replication over the sane

treatment period. Resazurin reduction was also decreased over that of soluble treated amoeba, indicating a reduction in viability which corresponds with the decreased cell counts (Fig. 7B).

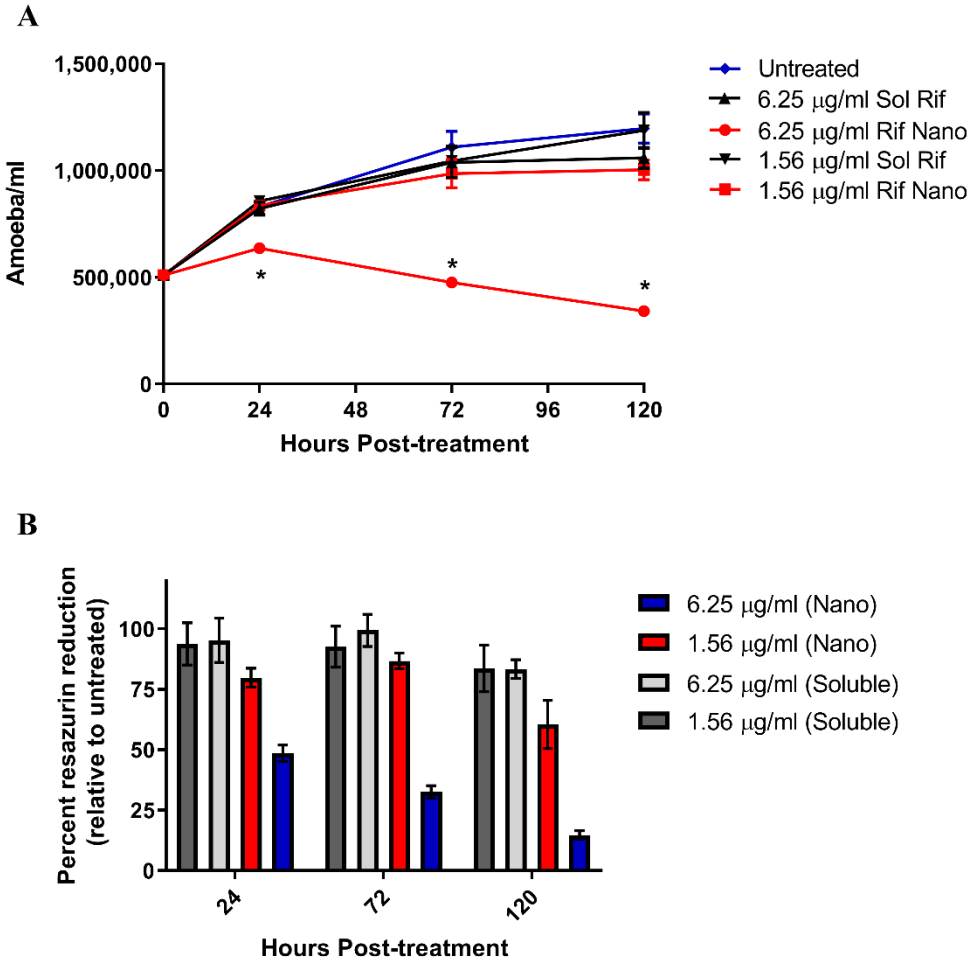

FIG 3-7. Replication and viability inhibition of *Naegleria fowleri* by 20:80 CPH:SA rifampicin loaded nanoparticles. (A) Growth curve of rifampicin treated amoeba. Values represent the means ± the SEM of two experiments performed in triplicate. Statistical analysis by one-way ANOVA with Bonferroni's multiple comparison (*$p \leq 0.05$). (B) Viability of rifampicin treated amoeba; determined through the reduction of resazurin. Values represent the means ± a 95% confidence interval.

Within 24 hours of treatment, viability was reduced by approximately 50% with nanoparticle treatment, but by only 5% with soluble treatment. By the last time point of 120 hours the viability of the nanoparticle treated amoeba dropped to 85% that of untreated amoeba, whereas soluble viability was only reduced by 17%. When the concentration of rifampicin loaded into the nanoparticles was dropped to 1.56 µg/mL no significant inhibition of replication was seen. While no alteration in replication was noted, there was significant differences in viability as measured by the reduction of resazurin. Within 24 hours of treatment with 1.56 µg/mL rifampicin via nanoparticle the viability of the amoeba was reduced by 20%, and by 120 hours post-treatment the viability was reduced by 40% compared to untreated controls. In contrast, soluble treated amoeba had an initial reduction in viability of 6% measured 24 hours post-treatment and by 120 hours the viability was reduced by 16% when compared to untreated controls.

Additional drugs were encapsulated into nanoparticles. Azithromycin, which is a macrolide antibiotic used to treat bacterial diseases and inhibits ribosomal synthesis of proteins. Amphotericin B, which is an antifungal drug that targets the sterol ergosterol in the cell membrane forming pores. Both these antimicrobials have a history in the treatment of PAM (22).

When azithromycin was encapsulated into 20:80 CPTEG:CPH nanoparticles an increase in *in vitro* efficacy was seen when treating the amoeba at 30 and 20 µg/mL azithromycin as determined by resazurin reduction (Fig. 8). At 10 µg/mL no significant difference was seen between nanoparticle and soluble treatments. The difference between nanoparticle and soluble was more pronounce following 96 hours of treatment vs 72 hours of treatment. Following 72 hours of treatment nanoparticle treatment at 30 µg/mL

showed relative viability of the amoeba at 51% that of untreated, while soluble treated amoeba were at 83% relative viability. By 96 hours post-treatment the relative viability of the nanoparticle treated amoeba was reduced to 25% and 49% for soluble azithromycin treated amoeba. When treated with 20 µg/mL azithromycin for 72 hours both nanoparticle and soluble treated amoeba had similar relative viabilities of 64% and 72%. At 96 hours post-treatment the viability of the nanoparticle treated amoeba was further reduced to 36% relative viability, while the soluble treated amoeba reduced to 49% relative viability.

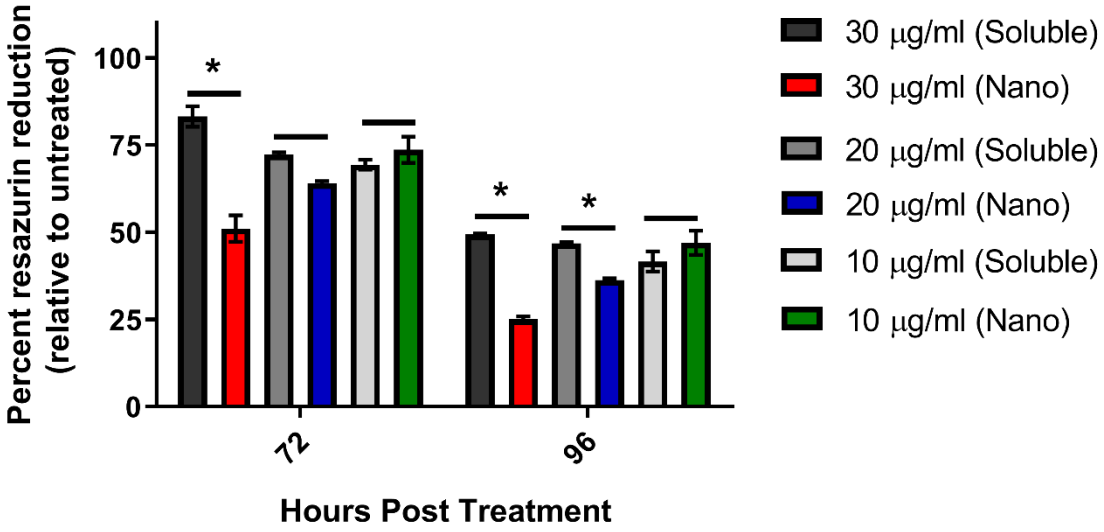

FIG 3-8. Viability of *Naegleria folweri* treated with azithromycin loaded 20:80 CPTEG:CPH polyanhydride nanoparticles. Viability of treated amoeba determined through the reduction of resazurin. Values represent the means ± the SEM of an experiment performed in triplicate. Statistical analysis by one-way ANOVA with Bonferroni's multiple comparison (*$p \leq 0.05$).

Lastly, amphotericin B when encapsulated into 20:80 CPH:SA nanoparticles showed a decrease in efficacy when compared to soluble drug (Fig. 9). When treated with 0.250 µg/mL amphotericin B encapsulated in these nanoparticles, while still

effective and having pronounced amoebicidal activity, there was a delay in activity when compared to soluble (Fig. 9A).

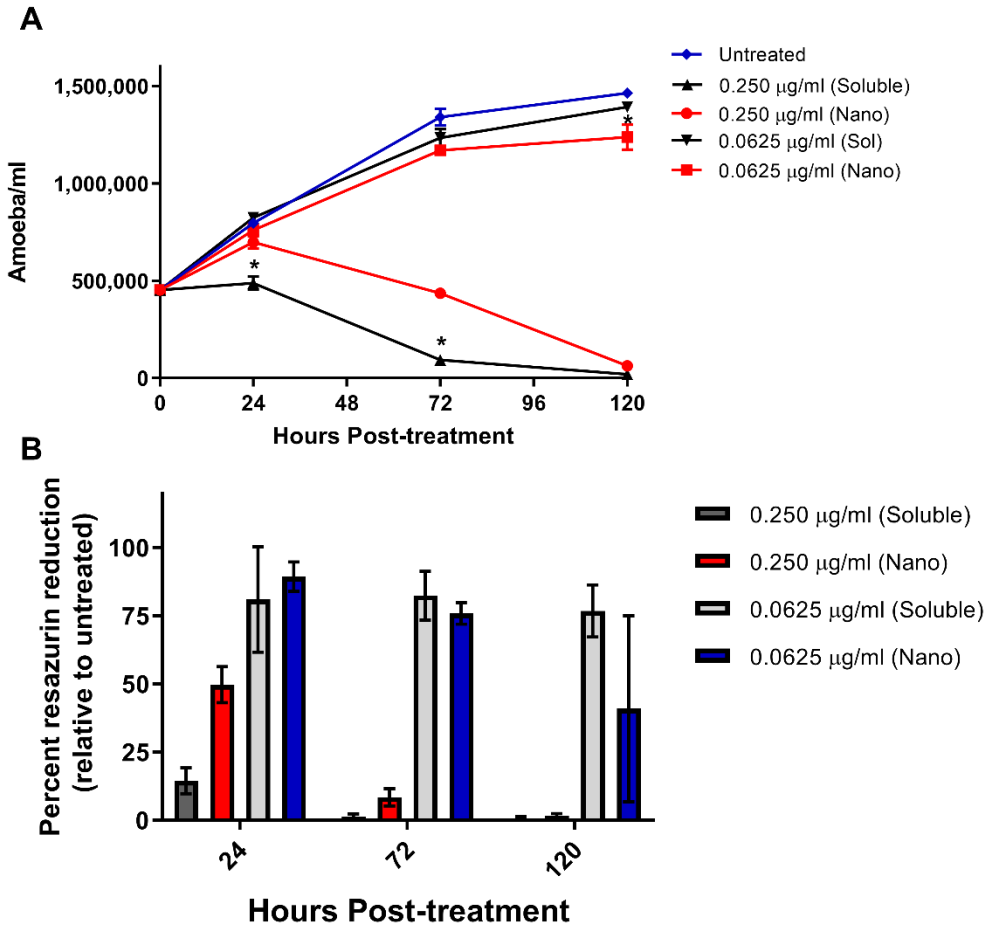

Figure 3-9. Growth and viability inhibition by 20:80 CPH:SA amphotericin B loaded nanoparticles on *Naegleria fowleri*. (A) Growth curve of rifampicin treated amoeba. Values represent the means ± the SEM of an experiment performed in triplicate. Statistical analysis by one-way ANOVA with Bonferroni's multiple comparison (*$p \leq$ 0.05). (B) Viability of rifampicin treated amoeba; determined through the reduction of resazurin. Values represent the means ± a 95% confidence interval.

By 24 hours the soluble drug had significant amoebastatic activity, with decreases in amoeba counts occurring over the next set of timepoints indicating amoebicidal activity. With nanoparticle delivered drug, significant growth inhibition was not noted until 72 hours and -cidal activity was evident by 120 hours. Metabolic inhibition as

indicated by the reduced reduction of resazurin mirrored the amoeba counts with the nanoparticle delivered amphotericin B trailing the soluble drug in efficacy; with the greatest difference seen at 24 hours post-treatment with nanoparticle treated showing a 50% reduction in metabolic activity and soluble treated showing an 85% reduction in metabolic activity (Fig. 9B). By 72 hours the difference between treatments had shrunk to nanoparticle giving a 92% reduction in metabolic activity and soluble giving a 99% reduction in metabolic activity; by the last time point at 120 hours the treatments gave a 98% and 99% reduction in metabolic activity respectively.

When combining therapies of co-administering 12.5 µg/mL rifampicin and 0.063 µg/mL amphotericin B in an all nano-encapsulated, all soluble, or soluble amphotericin B with nano-encapsulated rifampicin treatment differences in optimal performance were seen at varying timepoints between the three treatment (Fig. 10). Initially at 48 hours post-treatment both the all soluble and mixed nanoparticle/soluble treatments yielded similar metabolic inhibitions of 65% and 69% reductions in metabolic activity. At this time the all encapsulated yielded a mere 28% reduction in metabolic activity. Over the following timepoints at 72 and 96 hours the metabolic activity of the mixed nanoparticle/soluble group remained constant at 67% and 65% reduction in metabolic activity; showing a continued and static repression of metabolic activity throughout the experiment. In the case of the all soluble treatment the metabolic activity of the amoeba increased over the next intervening timepoints. At 72 hours post-treatment the metabolic activity showed a 47% reduction and by 96 hours a 14% reduction in metabolic activity. For the all encapsulated treatment there was a continuing decline in metabolic activity over the course of the experiment. By 72 hours the metabolic activity was reduced to

45% of that of untreated controls and by 96 hours the metabolic activity was further reduced to 62%.

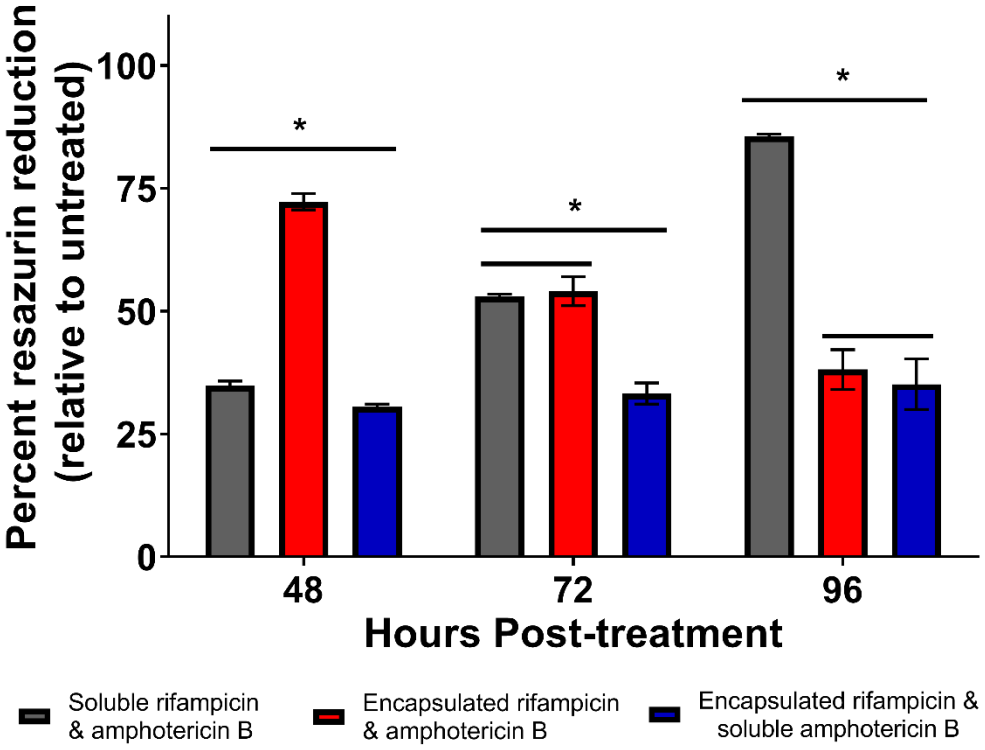

FIG 3-10. Viability of *Naegleria folweri* treated with the combination of amphotericin B (0.0625 µg/mL) and rifampicin (12.5 µg/mL) in either conventional soluble form, encapsulated in 20:80 CPTEG:CPH nanoparticles, or with amphotericin in soluble form and rifampicin encapsulated into 20:80 CPTEG:CPH nanoparticles. Viability of amoeba determined through the reduction of resazurin. Values represent the means ± the SEM of an experiment performed in triplicate. Statistical analysis by one-way ANOVA with Tukey's multiple comparison (*$p \leq 0.05$).

To further investigate if the treatment of these amoeba with nanoparticles could reduce the cytopathic effects (CPE) of the amoeba on tissue culture cells, the amoeba was cultured with Vero cells in the presence of soluble rifampicin or nanoparticle delivered rifampicin (Fig. 11). The dissolution of the Vero cell monolayer was an indication of amoeba derived CPE. Within 24 hours of co-incubation of the amoeba with the Vero

cells there was visual indications of CPE with gaps appearing within the Vero cell monolayer regardless on treatment. By 48 hours the Vero cell monolayer is completely absent in the soluble rifampicin treated group, which mirrors that of the amoeba left untreated. At this time the Vero cell monolayer is still somewhat intact with the nanoparticle delivered rifampicin treatment, with even many Vero cells remaining following 72 hours of co-incubation; it should be noted that the appearance on the Vero cells at these later timepoints does indicate a degree of CPE is occurring.

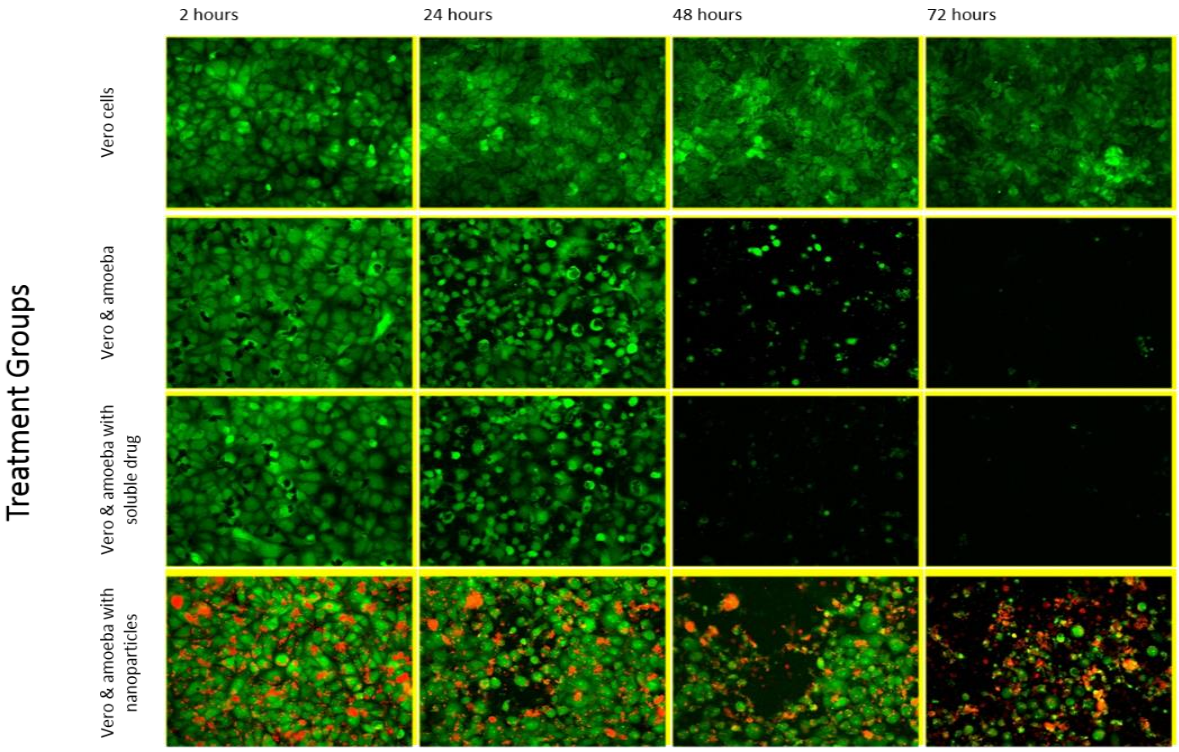

FIG 3-11. Inhibition of cytopathic effects of *Naegleria fowleri* on Vero cells by polyanhydride nanoparticles. Co-culture groups were treated with 25 µg/mL rifampicin, 25 µg/mL rifampicin loaded in 20:80 CPH:SA nanoparticles with rhodamine or left untreated. Vero cells stained with Cell Tracker Green. Nanoparticles are shown in red. Images were taken at identical XY coordinates for each treatment and are representative of all images taken.

Discussion

While disease caused by *N. fowleri* may be rare the outcome is usually fatal indicating that new avenues of treatment are needed (23). Here we show that the encapsulation of select antimicrobials commonly used to treat PAM are improved in their amoebastatic activity, which we attribute to the readily phagocytized nature of these nanoparticles. Both the 20:80 CPH:SA and 20:80 CPTEG:CPH nanoparticle chemistries were rapidly associated with the amoeba and remain associated with the amoeba over the course of 48 hours. Scanning laser confocal microscopy shows that the internalized nanoparticles come to reside in intracellular vacuoles suggesting that the nanoparticles are being internalized by phagocytic processes. It seems that the internalization of the 20:80 CPH:SA chemistry has an innate effect on the endosomal process which in itself is amoebastatic. Currently, the only understanding of this phenomenon resides in the LysoSensor staining and microscopy which showed alteration in the number and acidity of the endosomal vacuoles of the 20:80 CPH:SA treated amoeba along with morphological changes in the cell shape. This aspect of the 20:80 CPH:SA chemistry has made it difficult to determine which has a greater impact on these nanoparticles' efficacy, the encapsulated cargo or the innate amoebastatic properties of the particles. Having a particle that in itself is detrimental to the amoeba is beneficial and warrants further studies into nanoparticle polymer chemistry and interactions with cellular processes. In contrast the 20:80 CPTEG:CPH nanoparticles were inert when tested up 500 μg/mL; with no alteration in metabolic activity or replication of the amoeba.

In the case of both 20:80 CPTEG:CPH and 20:80 CPH:SA chemistries the encapsulation of rifampicin led to a substantial increase in efficacy. Rifampicin is

currently recommended by the CDC for the treatment of PAM even though *in vitro* data shows poor activity against this pathogen (11). What we have demonstrated with rifampicin is that we can take this antimicrobial with poor *in vitro* efficacy and now make it substantially better. In the assays, rifampicin loaded into the 20:80 CPTEG:CPH nanoparticles showed 6 times greater inhibition of replication. When loaded in the 20:80 CPH:SA nanoparticles not only was their an increase and rapid onset of inhibition of replication, there was also amoebicidal activity as indicated by the reduction in amoeba counts as the experiment progressed. In the case of the later we need to assume that some of the anti-amoeba activity is attributed to the nanoparticle chemistry itself. It should be noted that a similar co-polymer implantable product, the Gliadel wafer, is FDA approved for the treatment of brain tumors, and the toxicity of these nanoparticles has been studied in mice; this would suggest that the anti-amoeba properties of this chemistry would not carry over and harm the patient (15, 24).

Release kinetics associated with rifampicin loaded into either 20:80 CPH:SA or 20:80 CPTEG:CPH have shown a delayed release profile (25). What is perhaps notable about this is that with soluble treatment with rifampicin there appears to be a recover that is occurring with the amoeba following 72 hours of treatment; which is likely due to the breakdown of the rifampicin in the media. However, with nanoparticle delivered rifampicin we see continued and escalating amoebastatic and even amoebicidal activity out beyond 72 hours; these amoebae do not show the recovery that is occurring with the soluble rifampicin treated amoeba. This difference in longitudinal inhibition could be related to the delayed release profile of rifampicin when encapsulated in these nanoparticles. This finding suggests that fewer administrations of rifampicin could be

needed to treat susceptible diseases when these nanoparticles are employed, while exceeding the antimicrobial efficacy of conventionally delivered rifampicin.

The similar inhibition of replication seen between nanoparticles loaded with different percentage of rifampicin was unexpected as higher loading percentages give more rapid release profiles, and yet there was no significant difference in growth inhibition between nanoparticles loaded with 10% rifampicin vs 5% rifampicin. Differences in co-polymer ratios of the CPTEG and CPH monomers did yield striking differences in inhibition of these amoeba, which is likely due to differences in internalization. Earlier work showed that the 50:50 CPTEG:CPH nanoparticles were poorly internalized when compared to 20:80 CPTEG:CPH; the difference in inhibition seen between these two co-polymer ratios, with the 50:50 ratio achieving half the inhibition of the 20:80 ratio nanoparticles is likely due to the poorer internalization of these particles. This also underscores the importance that phagocytosis of these nanoparticles plays in their improved efficacy over soluble drug.

An interesting aside is that rifampicin targets prokaryotic RNA polymerases; hence its use in treating bacterial infections. *N. fowleri* is a eukaryotic organism, so its RNA polymerase should be minimally affected by rifampicin, which appears evident with the soluble treatment of these amoeba with rifampicin. Why is it that the inclusion of rifampicin in nanoparticles now makes it a viable weapon against *N. fowleri*; it is possible that rifampicin is acting upon the mitochondrial RNA polymerase within these amoebae which would resemble that of a prokaryotic organism and not the nuclear RNA polymerase. This hypothesis would need experimental data to support it, but it has been shown that rifampicin can adversely affect the mitochondrial RNA polymerase of

eukaryotic cells (26). If this is the case, these nanoparticles may be good vessels for the delivery of drugs specifically targeting the mitochondria of cells.

In the case of azithromycin, improvements in antimicrobial efficacy were not as great as that of rifampicin, but we did see an improvement over soluble which was most pronounced at higher azithromycin concentrations. This data relies solely on metabolic inhibition obtained through the reduction of resazurin; the work with rifampicin clearly showed correlation between reduced amoeba counts and resazurin reduction. The sensitivity of resazurin reduction over amoeba counts appears true, as significant changes in resazurin reduction were noted were there was no significant alteration in amoeba counts. This implies that resazurin is likely a better tool to assess the antimicrobial activities of drugs against *N. fowleri* and reduces the need for time consuming hemocytometer counts of amoeba. With that said, the encapsulation of azithromycin in the 20:80 CPTEG:CPH nanoparticles does improve its inhibitory effects on *N. fowleri*.

Amphotericin B is likely considered the most important drug in the treatment of PAM, due to the low concentration needed to kill the amoeba *in vitro*. Unlike rifampicin and azithromycin which saw benefit in encapsulation, the encapsulation of amphotericin B did not improve its efficacy over soluble. The opposite was seen it that the antimicrobial properties of amphotericin B when loaded into the nanoparticles was worse than that of soluble drug. Both the amoeba counts and resazurin reduction supported that the encapsulation of amphotericin B led to a decrease in efficacy. This leads us back to the central hypothesis that the encapsulation of anti-amoebic drugs into polyanhydride nanoparticles would increase their efficacy owing to a more direct targeting through phagocytosis. The results shown with rifampicin, azithromycin, and amphotericin B

support this hypothesis. This is easily observed with the rifampicin and azithromycin data as there is an increase in antimicrobial efficacy with their encapsulation. Both rifampicin and azithromycin have intracellular targets being RNA polymerase and ribosomes; an intracellular delivery via nanoparticle should and did improve efficacy of these drugs. Amphotericin B is different in that it targets ergosterol on the surface of the cell membrane, where it forms pores leading to membrane permeability and ion leakage. As amphotericin B does not need to gain access to the cytosol of the cell to function, therefore, there is no benefit to its encapsulation, and encapsulation could be detrimental to its use in sequestering the drug due to the release kinetics involved with nanoparticle encapsulation.

As PAM is not treated with a single drug, but a combination of drugs we tested amphotericin B together with rifampicin in a mixture of dose preparations: all soluble, all encapsulated, and encapsulated rifampicin with soluble amphotericin B. Here we saw that dose preparation and time led to very different results. While initially both the all soluble treatment and encapsulated rifampicin with soluble amphotericin B performed equally well, with subpar performance by the all encapsulated treatment. By the final time point the all encapsulated had improved in efficacy to match that of the encapsulated rifampicin with soluble amphotericin B, with a pronounced recover of the amoeba in the all soluble treated group by this later time point. In this experiment the mixture of encapsulated rifampicin with soluble amphotericin B yielded the best results in that the inhibition of the amoeba remained constant throughout the experimental time course, with both rapid and long-lasting inhibition. In contrast, the all soluble treatment started strong matching the encapsulated rifampicin with soluble amphotericin B, yet by 72

hours of treatment metabolic recovery of these amoeba was noted. By the final time point at 120 hours the recovery was now pronounced; in relation to untreated controls what began as a 65% reduction in viability was now only a 14% reduction in viability, indicating a substantial recovery of these amoeba. The inverse relationship between the all soluble and all encapsulated treatments is likely due to the low concentration of amphotericin B used and the poor stability of amphotericin B in culture media (27).

As *N. fowleri* infection is a very destructive process we attempted to see if nanoparticle treatment could protect Vero cells from the cytopathic onslaught of these amoeba. These amoebae can clear a monolayer of Vero cells within 48 hours through their lytic enzymes and trogocytic activities. With how rapidly PAM progresses rapid acting antimicrobial therapies are desired for the best patient outcome. For this we used the 20:80 CPH:SA chemistry loaded with rifampicin as this combination proved the most efficacious in single drug experiments with broth culture amoeba. The Vero cells were stained with Cell Tracker green to enable time-lapse imaging of the Vero cells to assess the integrity of the cell monolayer. While complete inhibition of cytopathic effects on the Vero cells was not achieved, and substantial CPE was observed in all treatments by the end of the experiment; the nanoparticle treated Vero cells had more remaining cells at 48 hours post-treatment.

While demonstrating these nanoparticles in an *in vivo* model of PAM using mice would settle many potential questions to include route of administration as these nanoparticles would need to reach the CNS and if indeed, they can improve patient outcome, this will need to be a addressed in a future study. The most likely route of administration used would be intrathecal as this route is already used in the treatment of

this disease to administer amphotericin B; this route would overcome any challenges in getting the nanoparticles across the blood brain barrier through intravenous administration. In these *in vitro* tests these nanoparticles have shown improved efficacy over soluble dosed drug in the event the drug has an intracellular target. If the drug targets the exterior cell membrane soluble dosing appears better than utilizing these nanoparticles. It is presented here that the phagocytosis of these nanoparticles by *N. fowleri* enables the drug to be more effectively delivered where it needs to work. By utilizing the drug delivery capabilities of these nanoparticles against PAM it is possible that improvements in patient outcomes could occur.

The use of nanoparticle delivered therapeutics could be beneficial in the treatment of other amoebic diseases. *Acanthamoeba* species cause diseases ranging from painful eye infections that can result in blindness to fatal encephalitis (28). Like PAM, diseases caused by *Acanthamoeba* are rare, but can be just as fatal. Treatment options for granulomatous encephalitis (GAE) caused by Acanthamoeba are just as lacking as they are for PAM. Initial work with our polyanhydride nanoparticles loaded with rifampicin shows similar degrees of enhancement seen with *N. fowleri* in two clinical isolates of *Acanthamoeba* (Fig. 12).

Future work substantiated with *in vivo* models could implicate nanoparticle delivered therapeutics in the treatment of amoebic diseases beyond *N. fowleri* and *Acanthamoeba*, but also to *Entamoeba histolytica* which causes amoebic dysentery with up to 50 million cases a year with 100,000 deaths (29).

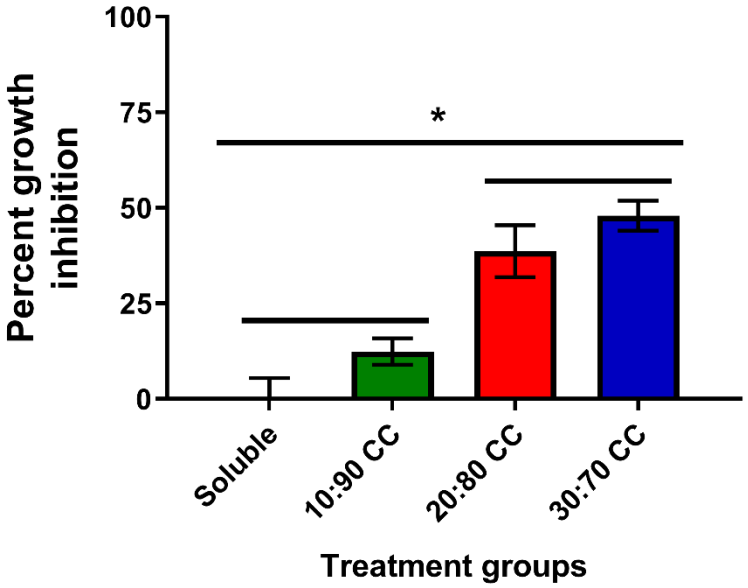

FIG 3-12. Growth inhibition of Acanthamoeba (CDC V062) by rifampicin loaded CPTEG:CPH polyanhydride nanoparticles. Amoeba were treated for 72 hours with various co-polymer ratios of CPTEG:CPH nanoparticles at 25 µg/mL rifampicin concentration. Values represent the means ± the SEM. Statistical analysis by one-way ANOVA with Tukey's multiple comparison (*$p \leq 0.05$).

References

1. Marciano-Cabral F. 1988. Biology of *Naegleria* spp. Microbiol Rev 52:114-33.

2. Fowler M, Carter RF. 1965. Acute pyogenic meningitis probably due to *Acanthamoeba* sp.: a preliminary report. Br Med J 2:740-2.

3. Yoder JS, Eddy BA, Visvesvara GS, Capewell L, Beach MJ. 2010. The epidemiology of primary amoebic meningoencephalitis in the USA, 1962-2008. Epidemiol Infect 138:968-75.

4. Marciano-Cabral F, Cabral GA. 2007. The immune response to *Naegleria fowleri* amebae and pathogenesis of infection. FEMS Immunol Med Microbiol 51:243-59.

5. Barnett ND, Kaplan AM, Hopkin RJ, Saubolle MA, Rudinsky MF. 1996. Primary amoebic meningoencephalitis with *Naegleria fowleri*: clinical review. Pediatr Neurol 15:230-4.

6. Jarolim KL, McCosh JK, Howard MJ, John DT. 2000. A light microscopy study of the migration of *Naegleria fowleri* from the nasal submucosa to the central

nervous system during the early stage of primary amebic meningoencephalitis in mice. J Parasitol 86:50-5.

7. Linam WM, Ahmed M, Cope JR, Chu C, Visvesvara GS, da Silva AJ, Qvarnstrom Y, Green J. 2015. Successful treatment of an adolescent with *Naegleria fowleri* primary amebic meningoencephalitis. Pediatrics 135:e744-8.

8. Lee KK, Karr SL, Wong MM, Hoeprich PD. 1979. In Vitro Susceptibilities of *Naegleria fowleri* Strain HB-1 to Selected Antimicrobial Agents, Singly and in Combination. Antimicrobial Agents and Chemotherapy 16:217-220.

9. CULBERTSON CG, ENSMINGER PW, OVERTON WM. 1968. Pathogenic *Naegleria* sp.—Study of a Strain Isolated from Human Cerebrospinal Fluid. The Journal of Protozoology 15:353-363.

10. Peroutka-Bigus N, Bellaire BH. 2018. Antiparasitic Activity of Auranofin against Pathogenic *Naegleria fowleri*. J Eukaryot Microbiol doi:10.1111/jeu.12706.

11. Ondarza RN, Iturbe A, Hernandez E. 2006. In vitro antiproliferative effects of neuroleptics, antimycotics and antibiotics on the human pathogens *Acanthamoeba polyphaga* and *Naegleria fowleri*. Arch Med Res 37:723-9.

12. Rajendran K, Anwar A, Khan NA, Siddiqui R. 2017. Brain-Eating Amoebae: Silver Nanoparticle Conjugation Enhanced Efficacy of Anti-Amoebic Drugs against *Naegleria fowleri*. ACS Chem Neurosci 8:2626-2630.

13. Anwar A, Siddiqui R, Hussain MA, Ahmed D, Shah MR, Khan NA. 2018. Silver nanoparticle conjugation affects antiacanthamoebic activities of amphotericin B, nystatin, and fluconazole. Parasitol Res 117:265-271.

14. Rajendran K, Anwar A, Khan NA, Shah MR, Siddiqui R. 2019. trans-Cinnamic Acid Conjugated Gold Nanoparticles as Potent Therapeutics against Brain-Eating Amoeba *Naegleria fowleri*. ACS Chem Neurosci 10:2692-2696.

15. Huntimer L, Ramer-Tait AE, Petersen LK, Ross KA, Walz KA, Wang C, Hostetter J, Narasimhan B, Wannemuehler MJ. 2013. Evaluation of biocompatibility and administration site reactogenicity of polyanhydride-particle-based platform for vaccine delivery. Adv Healthc Mater 2:369-78.

16. Kamaly N, Yameen B, Wu J, Farokhzad OC. 2016. Degradable Controlled-Release Polymers and Polymeric Nanoparticles: Mechanisms of Controlling Drug Release. Chem Rev 116:2602-63.

17. Shen E, Pizsczek R, Dziadul B, Narasimhan B. 2001. Microphase separation in bioerodible copolymers for drug delivery. Biomaterials 22:10.

18. Torres MP, Vogel BM, Narasimhan B, Mallapragada SK. 2006. Synthesis and characterization of novel polyanhydrides with tailored erosion mechanisms. Journal of Biomedical Materials Research Part A 76A:102-110.

19. Ulery BD, Petersen LK, Phanse Y, Kong CS, Broderick SR, Kumar D, Ramer-Tait AE, Carrillo-Conde B, Rajan K, Wannemuehler MJ, Bellaire BH, Metzger DW, Narasimhan B. 2011. Rational design of pathogen-mimicking amphiphilic materials as nanoadjuvants. Sci Rep 1:198.

20. Pringle HL, Bradley SG, Harris LS. 1979. Susceptibility of *Naegleria fowleri* to delta 9-tetrahydrocannabinol. Antimicrob Agents Chemother 16:674-9.

21. Martinez-Castillo M, Cardenas-Zuniga R, Coronado-Velazquez D, Debnath A, Serrano-Luna J, Shibayama M. 2016. *Naegleria fowleri* after 50 years: is it a neglected pathogen? J Med Microbiol 65:885-896.

22. Grace E, Asbill S, Virga K. 2015. *Naegleria fowleri*: pathogenesis, diagnosis, and treatment options. Antimicrob Agents Chemother 59:6677-81.

23. Siddiqui R, Khan NA. 2014. Primary amoebic meningoencephalitis caused by *Naegleria fowleri*: an old enemy presenting new challenges. PLoS Negl Trop Dis 8:e3017.

24. Attenello FJ, Mukherjee D, Datoo G, McGirt MJ, Bohan E, Weingart JD, Olivi A, Quinones-Hinojosa A, Brem H. 2008. Use of Gliadel (BCNU) wafer in the surgical treatment of malignant glioma: a 10-year institutional experience. Ann Surg Oncol 15:2887-93.

25. Mullis AS, Broderick SR, Binnebose AM, Peroutka-Bigus N, Bellaire BH, Rajan K, Narasimhan B. 2019. Data Analytics Approach for Rational Design of Nanomedicines with Programmable Drug Release. Mol Pharm 16:1917-1928.

26. Gadaleta MN, Greco M, Saccone C. 1970. The effect of rifampicin on mitochondrial RNA polymerase from rat liver. FEBS Letters 10:3.

27. Cheung SC, Medoff G, Schlessinger D, Kobayashi GS. 1975. Stability of amphotericin B in fungal culture media. Antimicrob Agents Chemother 8:3.

28. Marciano-Cabral F, Cabral G. 2003. *Acanthamoeba* spp. as agents of disease in humans. Clin Microbiol Rev 16:273-307.

29. Kantor M, Abrantes A, Estevez A, Schiller A, Torrent J, Gascon J, Hernandez R, Ochner C. 2018. *Entamoeba Histolytica*: Updates in Clinical Manifestation, Pathogenesis, and Vaccine Development. Can J Gastroenterol Hepatol 2018:4601420.

CHAPTER 4: ANTI-PARASITIC ACTIVITY OF AURANOFIN AGAINST PATHOGENIC *NAEGLERIA FOWLERI*

Modified from a manuscript published in the *Journal of Eukaryotic Microbiology*

Nathan Peroutka-Bigus[a,b] and Bryan H. Bellaire[a,b]

[a] Department of Veterinary Microbiology and Preventive Medicine

[b] Interdepartmental Microbiology

Iowa State University, Ames, Iowa 50011

Correspondence:

B. Bellaire, Dept. of Veterinary Microbiology and Preventive Medicine, Iowa State University, College of Veterinary Medicine, 1800 Christensen Drive, Rm 1136, Ames, Iowa, 50011-1134, USA

Telephone number +1 515-294-1006; e-mail: bbella@iastate.edu

Abstract

We report that the gold containing anti-rheumatoid drug auranofin is amoebicidal against human pathogenic *Naegleria fowleri*. Treatment of *N. fowleri* cultures at biologically relevant concentrations of 0.75 µg/mL to 3.0 µg/mL auranofin reduced amoeba counts, metabolic activity and increased cell permeability. These results suggest that the addition of auranofin may benefit the treatment of *N. fowleri* infected patients afflicted by the rapidly fatal disease primary amoebic meningoencephalitis.

Keywords

Primary Amoebic Meningoencephalitis; PAM; amoeba; antimicrobial; *in vitro*.

Introduction

The fatal disease primary amebic meningoencephalitis (PAM) is caused by the free-living amoeba *Naegleria fowleri*, colloquially referred to as the "brain eating amoeba"(1). Even though instances of PAM are rare, with typically fewer than 5 cases documented in the United States every year, this organism is ubiquitous in the environment and PAM has been documented in 16 countries (2, 3). Most cases of PAM in the U.S. are associated with recreational activities at lakes and involve children and young adults; PAM has also been acquired through nasal irrigation with contaminated tap water in the U.S. and also Pakistan were ritual ablution of the nose is common (3-5). While PAM has remained a rare disease, mortality with treatment is still near 100% demonstrating a need to improve therapeutic interventions. The rarity of PAM is likely due to the amoeba having to be introduced into the nasal cavity and then gain access to the olfactory neural epithelium before dissemination to the brain (6). Initial symptoms of PAM can resemble bacterial meningitis and can include fever, bifrontal headache, and emesis, with progression to seizures, comma, and death (7). The current recommended treatment for PAM issued by the Centers for Disease Control and Prevention (CDC) is based upon the few successful treatment outcomes and involves the simultaneous co-administration of amphotericin B, azithromycin, fluconazole, rifampicin, and miltefosine (8). Amphotericin B is recommended to be administered intrathecally by direct injection into the cerebral spinal fluid due to its poor ability to cross the blood brain barrier (BBB); oral or IV routes of administration are recommended for the other drugs used to treat PAM. Despite these extreme methods, surviving PAM is rare, with mortality greater than 95%, demonstrating a dire need for improved therapeutics. Auranofin is an FDA

approved drug for the treatment of rheumatoid arthritis and it has recently been shown to have anti-parasitic actions against *Giardia lamblia, Toxoplasma gondii, Trypanosoma* ssp, *Leishmania* spp, *Entamoeba histolytica* and others in both *in vitro* and *in vivo* assays (9, 10). With the limited success of the existing PAM therapy, we examined the antimicrobial activity of auranofin against pathogenic *N. fowleri* isolates. The mechanism of anti-parasitic action of auranofin is mediated through direct inhibition of the critical cellular enzyme thioredoxin reductase (TrxR) resulting in disruption of cellular redox state of the parasite. For instance, in *Schistosoma mansani* it was found that gold from auranofin binds to and inhibits thioredoxin-glutathione reductase (11). It was observed that auranofin inhibits TrxR through binding of a selenocysteine amino acid residue present in some TrxR proteins (12). It is of note that not all parasites that are sensitive to auranofin express TrxR with selenocysteine, suggesting either direct activity against TrxR is sufficient for antiparasitic activity or there are additional antiparasitic targets for auranofin. In *Entamoeba histolytica* the gold from auranofin was found not to bind to its TrxR (13). There is still some ambiguity when it comes to auranofins mechanism of action. The TrxR in the non-pathogenic, related amoeba *Naegleria gruberi* does contain a selenocysteine residue (14). It is possible that the mechanism of action of auranofin in *N. fowleri* is in the inhibition of TrxR. We observed that the gold containing drug auranofin is amoebicidal against *N. fowleri* at the biologically relevant concentration of 3.0 µg/mL.

Materials and Methods

Antimicrobial activity of auranofin was tested against clinical isolates of human pathogenic *N. fowleri* strains HB-1 (ATCC 30174) and LEE (ATCC 30894) received

from American Type Culture Collection (Manassas, VA). Cultures were maintained under axenic conditions in Nelson's media (ATCC medium 710) supplemented with 10% FBS at 37 °C and 5% CO_2 in 75 cm^2 tissue culture flasks in 12 mL of media. Amoeba in late logarithmic growth phase were harvested from 3-day old cultures and suspended in Nelson's media with 5% FBS at a cell density of 1.0 x 10^6 amoeba/mL; 5% FBS was used in the experiments as 10% serum concentrations interfered with fluorescence intensity measurements performed for the resazurin assay. A suspension of 50,000 amoeba was aliquoted in a volume of 50 µL into wells of a 96 well tissue culture plates; 50,000 amoeba per well was empirically chosen as it provided consistent resazurin reduction results with sufficient densities of amoeba culture for live/dead microscopic imaging. Auranofin was prepared at 2x strengths of 6, 3, and 1.5 µg/mL in culture media and 50 µL were added to each well with the amoeba to give auranofin concentrations of 3 µg/mL (4.4 µM), 1.5 µg/mL (2.2 µM), and 0.75 µg/mL (1.1 µM). Control experiments were conducted revealing that DMSO as a drug delivery vehicle did not change amoeba viability at all time points used in further experiments. The final concentration of 0.06% DMSO at 3 µg/mL auranofin was not inhibitory to the amoeba; inhibition was not detected at DMSO concentrations twice that at 0.12%. At 24 and 72 hours at 37ºC and 5% CO_2 the viability of the amoeba was assessed using the metabolic indicator resazurin (15) (Sigma, St. Louis, MO), direct observation hemocytometer counts, and Live/Dead™ BacLight™ staining (ThermoFisher Scientific, Waltham, MA). Resazurin assay was completed by adding 10 µL of 0.30 mg/mL solution to the treatment wells and incubating for 2 hours at 37°C at 5% CO_2. Using 540 nm excitation and 590 emission filter set of FLUOstar Omega plate reader (BMG Labtech, Offenburg, Germany), reduction of

resazurin was recorded for each well and the values of the treatment groups were converted to percentage resazurin reduction relative to untreated controls. A non-linear regression of the resazurin fluorescence data was used to calculate IC_{50} values (GraphPad Prism 7.03). IC_{50} is defined as the concentration of auranofin that resulted in a 50% reduction in metabolic activity at 3 days post-treatment relative to untreated controls. The extended dose ranges for IC_{50} testing for each strain as tested were 3.0 µg/mL, 1.5 µg/mL, 0.75 µg/mL, and 0.375 µg/mL auranofin for the HB-1 strain and 3.0 µg/mL, 2.25 µg/mL, 1.5 µg/mL, and 0.75 µg/mL auranofin for the LEE strain. Aliquots from treated wells were placed into a hemocytometer chamber for direct counting of amoeba trophozoites. A one-way ANOVA with Dunnett's multiple comparison was performed on the counts to determine significance. Following 72 hours of treatment the auranofin containing media was removed and replaced with fresh media to measure the recovery of the HB-1 strain following 3.0 and 6.0 µg/mL auranofin treatment. The reduction of resazurin was measured at 72 and 120 hours post-recovery. Live/Dead™ BacLight™ staining was performed according to manufacturer's instructions by incubating the amoeba in Nelson's media for 20 minutes supplemented with 5 µM SYTO 9 and 30 µM propidium iodide. Amoeba were subsequently imaged using an IX71 DSU microscope (Olympus, Center Valley, PA) with Metamorph Advanced acquisition software. Preparation of final images was performed with Fiji (https://fiji.sc/).

Results and Discussion

Treatment of human pathogenic *N. fowleri* with auranofin resulted in a significant, dose dependent reduction in metabolic activity and viability of amoeba *in vitro*. The HB-1 strain was significantly more sensitive to auranofin than the Lee strain

(Fig. 1 and S1). Growth of HB-1 cultures treated with 1.5 µg/mL and 3.0 µg/mL of auranofin was lower than untreated controls at 24 hours. Amoeba counts were lowered further at 72 hours to 45% and 82% for 1.5 µg/mL and 3.0 µg/mL in auranofin treated cultures. The decrease in amoeba counts coincides with decreased metabolic activity measured by resazurin reduction (Fig. 1B). The 0.75 µg/mL auranofin treated cultures were only reduced at 72 hours. This is interesting as it suggests that maintained low concentrations of auranofin are likely to be beneficial in treatment even as biological concentration decreases due to drug metabolism and excretion. Metabolic activity of auranofin treated HB-1 cultures at 24 hours was 28.4% and 8.7% with 1.5 and 3.0 µg/mL, respectively. It is notable that the metabolic activity of the 0.75 µg/mL auranofin culture reduced to 71.4% of untreated with a viable count equal to untreated. We interpret this result that the metabolic assay is sensitive to rapid changes in cell health due to the antimicrobial activity of the drug. By 72 hours, metabolic activity decreased further to 50.4%, 9.8%, and 0.4% with 0.75, 1.5, and 3.0 µg/mL of auranofin, respectively, providing an IC_{50} of 0.788 µg/mL. Qualitative assessment of membrane integrity is demonstrated by increased penetration of the membrane impermeable dye propidium iodide with auranofin treated *Naegleria*. These results corroborate the increase in membrane permeability with decreased metabolic activity and reduced direct amoeba counts, suggesting that auranofin exerts amoebicidal activity (Figs. 1C & 1D). In contrast, the LEE strain was unaffected by lower auranofin concentrations (S1). The IC_{50} for the Lee strain was calculated to be 2.18 µg/mL auranofin, which is 2.8x greater than that of the HB-1 strain. Phenotypic differences in relative sensitivity to antimicrobials have been observed among *Naegleria* strains (16, 17). Recovery of the HB-1 strain

following treatment with 3.0 µg/mL auranofin for 72 hours was gradual obtaining a metabolic rate of 6% of that of untreated controls after 5 days of recovery in auranofin free media; when treated with 6.0 µg/mL auranofin for 72 hours no increase in metabolic activity was noted, which suggest 100% killing of the amoeba (S2).

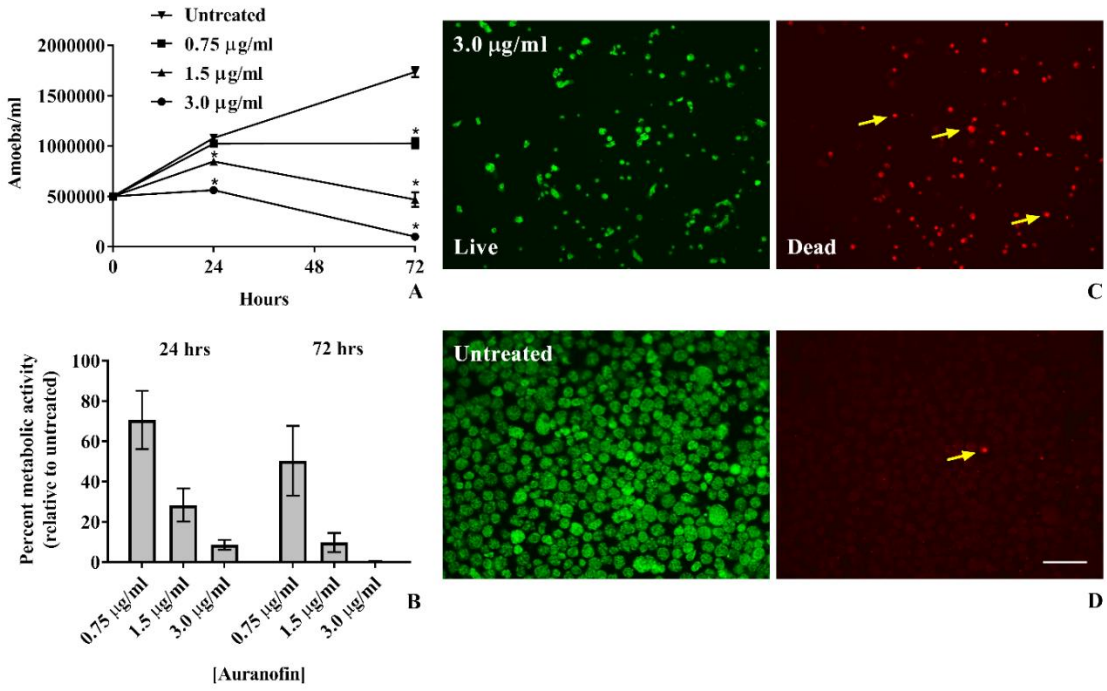

FIG 4-1. Effect of auranofin on growth and viability of *N. fowleri* HB-1. (A) Growth curves of *N. fowleri* following treatment with auranofin. Values represent the means ± the SEM of three experiments performed in triplicate. Statistical analysis by one-way ANOVA with Dunnett's multiple comparison (*$p < 0.01$). (B) Metabolic activity of auranofin treated *N. fowleri* relative to untreated controls. Metabolic activity was determined through the reduction of resazurin. Values represent the means ± a 95% confidence interval of three experiments performed in triplicate. (C) Representative live/dead images of *N. fowleri* treated with 3.0 µg/mL auranofin at 72 hours post-treatment, and (D) controls. Green Syto 9 staining of both live and dead cells. Red propidium iodide staining of dead cells (yellow arrows). Scale bar in D represents 40 µm.

We present data demonstrating that auranofin exerts an MIC of 1.5 µg/mL (2.2 µM) and IC_{50} of 0.788 µg/mL (1.16 µM) with the HB-1 strain and an MIC of 3.0 µg/mL (4.4 µM) and IC_{50} of 2.18 µg/mL (3.2 µM) with the Lee strain of *N. fowleri*. Staining of

these auranofin treated amoeba with membrane impermeable dye propidium iodide suggests that a proportion of the treated amoeba have been killed. Auranofin can cross the BBB with gold concentrations within the brain reaching 4.79 µM in mice through oral delivery of auranofin at 2 mg/kg once daily for seven days; it is unknown to what concentration auranofin would be found in the brains of humans (18). The dosing used in preceding experiment with mice represents an approximate 20 times greater concentration of auranofin than what is currently used in the treatment of rheumatoid arthritis in humans. In a recent phase I clinical trial aimed at evaluating auranofin as an antiparasitic agent (Clinicaltrials.gov NCT02089048) it was found that blood plasma levels of gold reached 0.52 µM and 1.58 µM at 1 and 7 days at 6 mg/day auranofin treatment; this trial did not look at CNS gold concentrations (12). In the case of PAM greater concentrations of auranofin may accumulate within the CNS as the BBB becomes compromised during meningitis along with there being reduced CSF outflow and decreased efflux pump activity (19). It is plausible that auranofin may obtain biologically relevant concentrations in the CNS to treat patients with PAM, however, a high loading dose or intrathecal delivery may be required to rapidly achieve therapeutic levels. Utilizing an animal model of PAM would provide more impactful results, than the *in vitro* results presented here. Little is known about the toxicity of auranofin in humans when administered at higher concentrations than what is currently used in the treatment of rheumatoid arthritis of 6 to 9 mg per day. Auranofin has been shown to upregulate expression of hemeoxygenase 1 (HOX-1) in astrocytes, which may prove beneficial in the treatment of PAM by reducing neuroinflammation and reactive oxygen species (ROS) dependent cell death induced by *N. fowleri* (20, 21). Based on these results, the

therapeutic regimen currently recommended for PAM may benefit from the addition of auranofin. While requiring further testing, auranofin may be useful in the treatment of infections caused by other free-living amoebae. Given the differences in susceptibility to auranofin between HB-1 and LEE isolates, clinical outcomes through the sole use of auranofin would be dependent on strain susceptibility and the concentration of auranofin to be present in human CNS following intrathecal administration. With these considerations, auranofin has the potential to be used as an adjunct therapy alongside conventional therapies. While disease caused by free-living amoeba are rare, they are frequently fatal and difficult to treat. The inclusion of new therapeutics in the treatment of these diseases could save lives.

Acknowlegements

The authors wish to acknowledge support for this research from Iowa State University College of Veterinary Medicine Office of Research, the Bill and Melinda Gates Foundation Grand Challenges Opportunity (1087610), and the technical assistance of Paul A. Lueth.

References

1. Carter RF. 1970. Description of a *Naegleria* sp. isolated from two cases of primary amoebic meningo-encephalitis, and of the experimental pathological changes induced by it. J Pathol 100:217-44.

2. Visvesvara GS, Stehr-Green JK. 1990. Epidemiology of Free-Living Ameba Infections. The Journal of Protozoology 37:25s-33s.

3. Yoder JS, Eddy BA, Visvesvara GS, Capewell L, Beach MJ. 2010. The epidemiology of primary amoebic meningoencephalitis in the USA, 1962-2008. Epidemiol Infect 138:968-75.

4. Siddiqui R, Khan NA. 2014. Primary amoebic meningoencephalitis caused by *Naegleria fowleri*: an old enemy presenting new challenges. PLoS Negl Trop Dis 8:e3017.

5. Yoder JS, Straif-Bourgeois S, Roy SL, Moore TA, Visvesvara GS, Ratard RC, Hill VR, Wilson JD, Linscott AJ, Crager R, Kozak NA, Sriram R, Narayanan J, Mull B, Kahler AM, Schneeberger C, da Silva AJ, Poudel M, Baumgarten KL, Xiao L, Beach MJ. 2012. Primary amebic meningoencephalitis deaths associated with sinus irrigation using contaminated tap water. Clin Infect Dis 55:e79-85.

6. Jarolim KL, McCosh JK, Howard MJ, John DT. 2000. A light microscopy study of the migration of *Naegleria fowleri* from the nasal submucosa to the central nervous system during the early stage of primary amebic meningoencephalitis in mice. J Parasitol 86:50-5.

7. Barnett ND, Kaplan AM, Hopkin RJ, Saubolle MA, Rudinsky MF. 1996. Primary amoebic meningoencephalitis with *Naegleria fowleri*: clinical review. Pediatr Neurol 15:230-4.

8. Linam WM, Ahmed M, Cope JR, Chu C, Visvesvara GS, da Silva AJ, Qvarnstrom Y, Green J. 2015. Successful treatment of an adolescent with *Naegleria fowleri* primary amebic meningoencephalitis. Pediatrics 135:e744-8.

9. Debnath A, Parsonage D, Andrade RM, He C, Cobo ER, Hirata K, Chen S, Garcia-Rivera G, Orozco E, Martinez MB, Gunatilleke SS, Barrios AM, Arkin MR, Poole LB, McKerrow JH, Reed SL. 2012. A high-throughput drug screen for *Entamoeba histolytica* identifies a new lead and target. Nat Med 18:956-60.

10. Roder C, Thomson MJ. 2015. Auranofin: repurposing an old drug for a golden new age. Drugs R D 15:13-20.

11. Angelucci F, Sayed AA, Williams DL, Boumis G, Brunori M, Dimastrogiovanni D, Miele AE, Pauly F, Bellelli A. 2009. Inhibition of *Schistosoma mansoni* thioredoxin-glutathione reductase by auranofin: structural and kinetic aspects. J Biol Chem 284:28977-85.

12. Capparelli EV, Bricker-Ford R, Rogers MJ, McKerrow JH, Reed SL. 2017. Phase I Clinical Trial Results of Auranofin, a Novel Antiparasitic Agent. Antimicrob Agents Chemother 61.

13. Parsonage D, Sheng F, Hirata K, Debnath A, McKerrow JH, Reed SL, Abagyan R, Poole LB, Podust LM. 2016. X-ray structures of thioredoxin and thioredoxin reductase from *Entamoeba histolytica* and prevailing hypothesis of the mechanism of Auranofin action. J Struct Biol 194:180-90.

14. da Silva MT, Caldas VE, Costa FC, Silvestre DA, Thiemann OH. 2013. Selenocysteine biosynthesis and insertion machinery in *Naegleria gruberi.* Mol Biochem Parasitol 188:87-90.

15. Rice CA, Colon BL, Alp M, Goker H, Boykin DW, Kyle DE. 2015. Bis-benzimidazole hits against *Naegleria fowleri* discovered with new high-throughput screens. Antimicrob Agents Chemother 59:2037-44.

16. Kim JH, Jung SY, Lee YJ, Song KJ, Kwon D, Kim K, Park S, Im KI, Shin HJ. 2008. Effect of therapeutic chemical agents in vitro and on experimental meningoencephalitis due to *Naegleria fowleri*. Antimicrob Agents Chemother 52:4010-6.

17. Ondarza RN, Iturbe A, Hernandez E. 2006. In vitro antiproliferative effects of neuroleptics, antimycotics and antibiotics on the human pathogens *Acanthamoeba polyphaga* and *Naegleria fowleri*. Arch Med Res 37:723-9.

18. Madeira JM, Renschler CJ, Mueller B, Hashioka S, Gibson DL, Klegeris A. 2013. Novel protective properties of auranofin: inhibition of human astrocyte cytotoxic secretions and direct neuroprotection. Life Sci 92:1072-80.

19. Nau R, Sorgel F, Eiffert H. 2010. Penetration of drugs through the blood-cerebrospinal fluid/blood-brain barrier for treatment of central nervous system infections. Clin Microbiol Rev 23:858-83.

20. Madeira JM, Schindler SM, Klegeris A. 2015. A new look at auranofin, dextromethorphan and rosiglitazone for reduction of glia-mediated inflammation in neurodegenerative diseases. Neural Regen Res 10:391-3.

21. Song KJ, Jang YS, Lee YA, Kim KA, Lee SK, Shin MH. 2011. Reactive oxygen species-dependent necroptosis in Jurkat T cells induced by pathogenic free-living *Naegleria fowleri*. Parasite Immunol 33:390-400.

Supporting Information

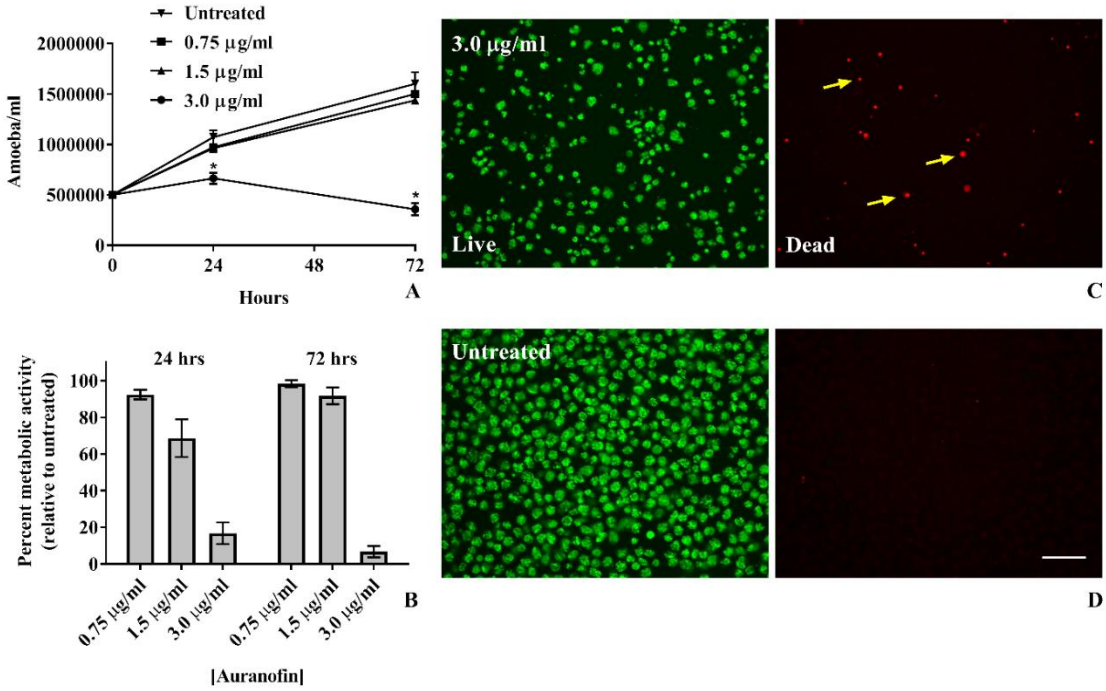

FIG 4-S1. Effect of auranofin on growth and viability of *N. fowleri* Lee. (A) Growth curves of *N. fowleri* following treatment with auranofin. Values represent the means ± the SEM of three experiments performed in triplicate. Statistical analysis by one-way ANOVA with Dunnett's multiple comparison (*$p < 0.01$). (B) Metabolic activity of auranofin treated *N. fowleri* relative to untreated controls. Metabolic activity was determined through the reduction of resazurin. Values represent the means ± a 95% confidence interval of three experiments performed in triplicate. (C) Representative live/dead images of *N. fowleri* treated with 3.0 µg/mL auranofin at 72 hours post-treatment, and (D) controls. Green Syto 9 staining of both live and dead cells. Red propidium iodide staining of dead cells (yellow arrows). Scale bar in D represents 40 µm.

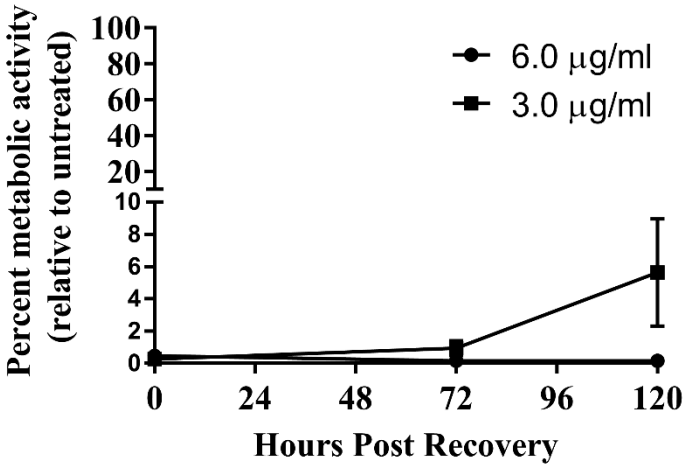

FIG 4-S2. Recovery of auranofin treated *N. fowleri* HB-1 in auranofin free media. Recovery of amoeba was assessed by measuring metabolic activity of amoeba post-treatment with either 3.0 µg/mL or 6.0 µg/mL auranofin. Post-treatment recovery was performed by incubating cells in auranofin free media for 120 hours. No metabolic recovery was detected in cells recovered from 6.0 µg/mL treatment. Values represent the means ± a 95% confidence interval.

CHAPTER 5: INFLUENCE OF CATECHOLAMINES ON BACTERIAL REPLICATION AND RESPONSE TO ANTIBIOTICS WITH *BACILLUS ANTHRACIS* AND *YERSINIA PESTIS*

Modified from a manuscript to be submitted to Infection and Immunity

Nathan Peroutka-Bigus,[a,b] Mark Lyte,[a,b] Bryan H Bellaire[a,b,c]

[a]Department of Veterinary Microbiology and Preventive Medicine, Iowa State University, Ames, IA, USA, [b]Interdepartmental Microbiology Program, Iowa State University, Ames, IA, USA, [c]Nanovaccine Institute, Iowa State University, Ames, IA, USA

Abstract

Recent advances in microbiology has shown that numerous pathogenic bacteria respond to the catecholamine hormones norepinephrine, and epinephrine. These responses can be alterations in replication rate, increased iron acquisition, resistance to antibiotics, and induction of virulence factors. This is the first examination of how these catecholamines affect the virulent bacteria, *Bacillus anthracis* and *Yersinia pestis*. The pathogenesis of both of these bacteria can result in fatal pulmonary infections, yet these two bacteria have differing responses to catecholamines. *In vitro* replication in the presence of catecholamines, along with susceptibility to antibiotics was examined. Norepinephrine accelerates the replication of *B. anthracis*, while with *Y. pestis* these catecholamines inhibited replication. The response of *Y. pestis* to catecholamines is divergent to that of the related bacteria *Yersinia enterocolitica* and *Yersinia pseudotuberculosis*. The β-adrenergic receptor antagonist propranolol was shown to restore normal growth phenotype in *Y. pestis* when norepinephrine was administered, suggesting the possibility of a receptor through which norepinephrine is signally through. With *B. anthracis*, norepinephrine was found to cause an increased resistance to the

antibiotic rifampicin, which could be attenuated through the administration of propranolol. These findings reveal the possibility for complex chemical interactions between host and these bacteria, with relevance in pathogenesis and treatment.

Introduction

The catecholamine hormones norepinephrine, epinephrine, and dopamine have previously been shown to accelerate the replication of pathogenic bacteria, induce greater resistance to antibiotics, and modulate virulence factors; some select examples include increasing the rate of replication and iron acquisition from transferrin in *Bordetella bronchiseptica*, *Pseudomonas aeruginosa*, and *Listeria monocytogenes* by norepinephrine (1-4). In *Vibrio parahaemolyticus* norepinephrine modulates its type III secretion system (5). The uptake of enterotoxigenic *Escherichia coli* into jejunal Peyer's patches is increased by norepinephrine (6). Pre-treatment of *Salmonella typhimurium* with norepinephrine was shown to increase replication in experimentally infected pigs (7). Epinephrine was shown to increase growth rate and resistance to oxidative stress in *Burkholderia psuedomallei* but had no effect on cell invasion (8). In *Yersinia enterocolitica* it was shown that dopamine and norepinephrine increase growth rate and increase iron acquisition from transferrin while epinephrine doesn't impact the replication of *Y. enterocolitica* and additionally acted as an antagonist towards the effects of dopamine and norepinephrine (9). While there has already been a vast exploration of this host derived hormone response on bacterial pathogens, the current species studied do not include many of the most fearsome bacterial pathogens out there. This chapter addresses how these menaces of humankind, *Yersinia pestis* and *Bacillus anthracis*, respond to these catecholamines. In addition, the closely related *Yersinia pseudotuberculosis* and

Yersinia enterocolitica will be compared to *Y. pestis*. *Bacillus cereus* is included as a comparison to *B. anthracis*.

The bacterium *Bacillus anthracis* is perhaps best known for its designation as a biowarfare agent. The spores produced by this bacterium when inhaled will cause the fatal disease pneumonic Anthrax (10). During the course of infection this bacterium will be exposed to host derived stress hormones. It should be noted that illness has been shown to increase norepinephrine expression (11, 12). Currently nothing is known how *B. anthracis* responds to these stress hormones, and how this interaction may affect pathogenesis and treatment. Here we show that vegetative *B. anthracis* bacilli exhibit an increased replication rate when exposed to the stress hormone norepinephrine, and that norepinephrine exposure leads to an increase in resistance to the antibiotic rifampicin. Through the addition of the β-adrenergic receptor antagonist propranolol, we could attenuate the rifampicin resistance brought on by norepinephrine, which possibly suggests that norepinephrine may be exerting its effect on *B. anthracis* through a receptor. A similar norepinephrine induced resistance to rifampicin was observed in the related species *Bacillus cereus*. Norepinephrine had no effect on the susceptibility to doxycycline or ciprofloxacin; doxycycline and ciprofloxacin being FDA approved first line drugs in the treatment of anthrax (13). However, when *B. anthracis* was treated with these antibiotics for 8 hours at concentrations sufficient to kill 99% of the bacteria, the addition of norepinephrine after the antimicrobial onslaught resulted in greater recovery of these antimicrobially damaged bacteria. Iron is an essential nutrient for bacterial growth and pathogenesis; within mammalian hosts free iron is very limited (14). The media used in these experiments mimics physiological conditions in that free iron is

restricted by the presence of transferrin. Norepinephrine has been shown to increase iron uptake in bacteria from the iron bound serum protein transferrin (15). *Bacillus anthracis* can meet its iron requirements *in vivo* through the production of siderophores which are able to scavenge iron that is bound to host proteins (16). When making this media iron replete the presence of norepinephrine is still required for resistance to rifampicin; indicating that iron scavenging by norepinephrine is not responsible for the resistant phenotype. The production of the toxins edema factor and lethal factor are essential for virulence, through a cell-based toxin assay norepinephrine was shown to have no effect on toxin production in *B. anthracis*, neither does norepinephrine influence spore germination.

Yersinia pestis is best known for its many plagues that have had devastating impacts on past civilizations; a large percent of Europe's population was killed by *Y. pestis* in the 14th century during the Black Death pandemic (17). Due to the organism's deadly nature and high infectivity it is considered a tier one select agent, as it would make a very efficient bio warfare agent (10).

Yersinia pestis is known to cause three distinct forms of disease. The bubonic form is causes through the bite from an infected arthropod or exposure to the organism through a break in the skin. In this form the organism travels from the site of infection to the regional draining lymph node via infected macrophages and dendritic cells. After replicating and overburdening the draining lymph node, spread to other lymph nodes is facilitated again by travel within infected phagocytic cell (18). Without treatment the disease usually progresses to a life-threatening septicemic form with hematogenous spread to other organs. Spread of the organism to the lungs will result in the pneumonic

form of the disease. The role of catecholamines in the pathogenesis of *Y. pestis* is unknown. Here we show that *Y. pestis* has a very different response to catecholamine when compared to other pathogenic bacteria and to the closely related *Y. enterocolitica* and *Y. pseudotuberculosis*. These data merely represent growth responses in relation to exposure to norepinephrine, epinephrine, and serotonin. What was seen was that these hormones greatly inhibit the replication of *Y. pestis*; this is opposite to what was seen in the other *Yersinia* species.

Materials & Methods

Cell culture

Bacillus anthracis, Anthrax Strain Collection (ASC) 386 (Ames), NR-36110, was obtained through BEI, *and Bacillus anthracis* Sterne strain (34F2) was obtained through the Colorado Serum company; with general cultivation on BHI agar at 37°C and 5% CO_2. *Bacillus cereus* was obtained from the lab of F. Chris Minion and maintained on BHI agar at 37°C and 5% CO_2. *Yersinia pestis*, strain CO92, NR-641, and *Yersinia pseudotuberculosis*, strain IP2775, NR-4375, were obtained through BEI with cultivation on TSA supplemented with 1% bovine hemoglobin at 3737°C and 5% CO_2. *Yersinia enterocolitica* was obtained from Robert Perry and maintained on TSA supplemented with 1% bovine hemoglobin at 37°C and 5% CO_2. Murine macrophages (RAW 246.7) were maintained in DMEM with 10% FBS at 37°C and 5% CO_2.

Generation of *B. anthracis* spores

Bacillus anthracis spores of the Sterne strain were prepared by cultivating the vegetative bacteria in modified G media for 72 hours at 30°C with shaking at 125 rpm.

The spores were harvested and subjugated to a 30-minute treatment at 60°C to kill any remaining vegetative cells followed by centrifugation and wash steps with sterile deionized water. The spores were stored at -80°C until needed for experiments. Modified G media was composed of 0.2% yeast extract, 0.17 mM $CaCl_2$, 2.87 mM K_2HPO_4, 0.81 mM $MgSO_4$, 0.24 mM $MnSO_4$, 17 µM $ZnCl_2$, 20 µM $CuSO_4$, 1.8 µM $FeCl_3$, and 15.5 mM $(NH_4)_2SO_4$ with the pH adjusted to 7.2.

Growth assays

Bacterial growth assays were performed in Serum-SAPI media (6.25 mM NH_4NO_3, 1.84 mM KH_2PO_4, 3.35 mM KCL, 1.01 mM $MgSO_4$, 2.77 mM glucose, pH 7.5, supplemented with 30% (v/v) adult bovine serum, and 25 mM HEPES) at 37°C and 5% CO_2. Initial bacterial concentrations of these cultures were ≤ 100 CFUs/mL. The bacteria were grown in the presence or absence of varying concentrations of the catecholamines norepinephrine, epinephrine, serotonin and/or the beta-adrenergic receptor antagonist propranolol for 20 hours for *Bacillus* species or 48 hours for *Yersinia* species, with replication quantification by CFU enumeration.

Antimicrobial susceptibility assays

Antimicrobial susceptibility testing of *Bacillus* species. Antibiotics with or without norepinephrine were prepared at a 2x concentration in Serum-SAPI media, and 50 µL were pipetted into the wells of a 96 well tissue culture plate. A bacteria suspension from a colony scrape was suspended in PBS and adjusted to an OD_{600} measurement of 0.5. Then a 1:100 dilution of the bacterial suspension was made in

Serum-SAPI media with 50 µL of this being added to each treatment well of a 96 plate. Norepinephrine was used at 100 µM, propranolol was used at 500 µM, and ferrous sulfate was used at 20 µM. After 20 hours at 37°C and 5% CO_2 CFU enumeration was done to assess antimicrobial susceptibility. It should be noted that antimicrobial susceptibility testing was only performed with *Bacillus* species as they facilitated robust growth in Serum-SAPI media in the absence of catecholamines. If bacterial cultures were pre-exposed to norepinephrine prior to antimicrobial challenge this was done in twenty-four hour 7 mL Serum-SAPI cultures at 37°C and 5% CO_2 which were then centrifuged at 1000 rcf for 10 minutes at room temperature to pellet the bacteria three times with PBS washes.

To test whether catecholates stimulate bacterial replication following antimicrobial damage, bacterial cultures in Serum-SAPI media were exposed to 1.0 µg/mL rifampicin 2.0 µg/mL ampicillin, or 1.6 µg/mL ciprofloxacin for 8 hours at 37°C and 5% CO_2, which was sufficient to kill 99% of the bacteria. These cultures were centrifuged at 1000 rcf at room temperature for 10 minutes to pellet the surviving bacteria three times with the supernatant removed and replaced with fresh media to remove most residual antibiotics. These antimicrobially damaged bacteria were then allowed to recovery in Serum-SAPI media in the presence or absence of 100 µM norepinephrine for 20 hours at 37°C and 5% CO_2, with CFU enumeration to determine growth recovery. For ampicillin and ciprofloxacin antimicrobially damaged cells were also allowed to recover in the presence of 20 µM ferrous sulfate. *B. anthracis* was the only species to be tested for recovery following antimicrobial insult.

Toxin production by *B. anthracis*

To test the impact norepinephrine has on toxin production in *B. anthracis*, Cultures of *B. anthracis* Sterne were grown for 24 hours in Serum-SAPI media in the presence or absence of 100 μM norepinephrine. These cultures were then centrifuged to pellet the bacteria at 1000 rcf at room temperature for 10 minutes. The supernatant was collected and passed through a sterile 0.2 μm syringe filter to ensure sterility of the supernatants. The supernatants were than processed through Centriprep centrifugal filter devices (10,000 MWCO) per the manufactures recommendations to remove excess catecholamines and to concentrate the toxins expressed into the supernatant. Murine macrophages (RAW 246.7) were utilized at a cell density of 1.0×10^6 cells/mL in a 100 μL volume in 96 well tissue culture plates. These cells are susceptible to the toxin produced by *B. anthracis* and will show a decrease in cell viability when exposed to the toxin. A titration of the processed bacterial supernatant was applied to the macrophages and the viability of the macrophages was assessed through the addition of MTT.

Results

Most bacterial species screened responded positively to the presence of norepinephrine, regarding increased replication rate; the only exception being *Yersinia pestis*. With *B. anthracis* (Sterne strain) we saw a 10-fold increase in replication in the presence of 100 μM norepinephrine (Fig. 1A). In the case of *B. anthracis* (ASC 386) we again saw a 10-fold increase in replication with 100 μM norepinephrine (Fig. 1B).

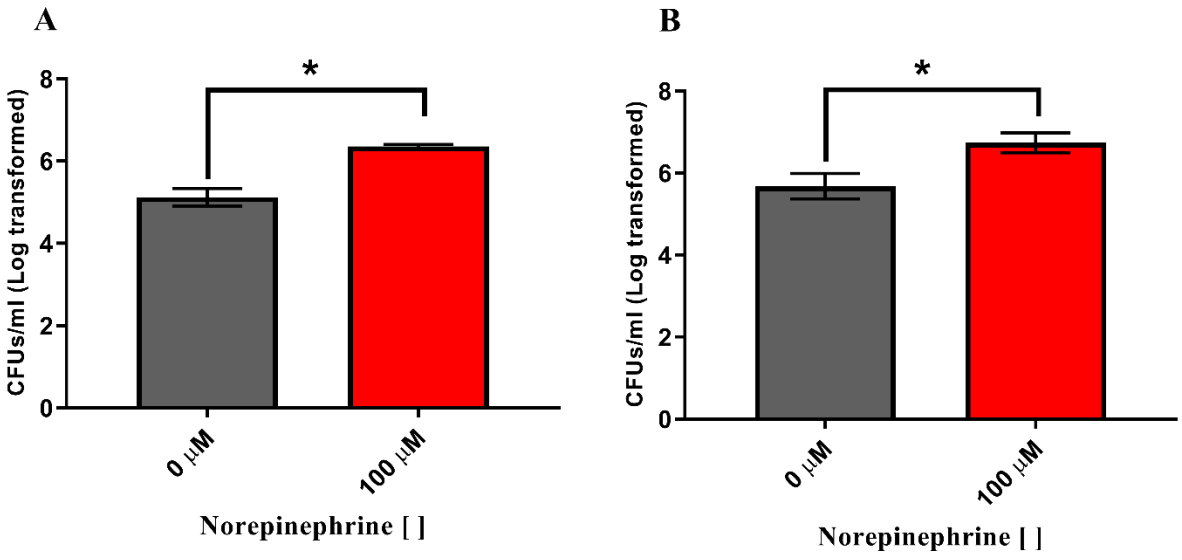

FIG 5-1. Enhanced replication of *Bacillus anthracis* in response to norepinephrine. Twenty-hour *in vitro* growth of *B. anthracis* in Serum-SAPI media in the presence or absence of 100 μM norepinephrine. (A) *Bacillus anthracis* (Sterne). (B) *Bacillus anthracis* (Ames). Values represent the means ± the SEM of two experiments performed in triplicate. Statistical analysis by Student's *t*-test (*$p \leq 0.05$).

Unexpectedly, the notorious pathogen *Y. pestis* showed an opposite response to norepinephrine than *B. anthracis* or even to its closely related bacteria *Y. enterocolitica* and *Y. pseudotuberculosis* (Fig. 2). When *Y. pestis* (CO92) was treated with norepinephrine at concentrations ranging from 50 μM to 200 μM for 48 hours there were no recoverable colonies; the control provided 7.9 x 10^4 CFUs/mL (Fig. 2A). In comparison, *Y. enterocolitica* provided similar numbers of CFUs/mL in its control (1.2 x 10^4 CFUs/mL), yet with norepinephrine treatment at 50, 100, and 200 μM replication was substantially stimulated with recovered CFUs of 1.5 x 10^8 CFUs/mL, 1.2 x 10^8 CFUs/mL, and 1.4 x 10^8 CFUs/mL respectively (Fig. 2B). To add further oddities to the *Yersinia* genus, *Y. pseudotuberculosis* grew very well in Serum-SAPI media without the addition of norepinephrine and was able to achieve a cell density of 1.2 x 10^8 CFUs/mL

(Fig. 2C). The supplementation of norepinephrine at 50, 100, and 200 µM led to no growth enhancement under these conditions with densities of 2.8 x 10^8, 2.0 x 10^8, and 1.0 x 10^8 CFUs/mL respectively.

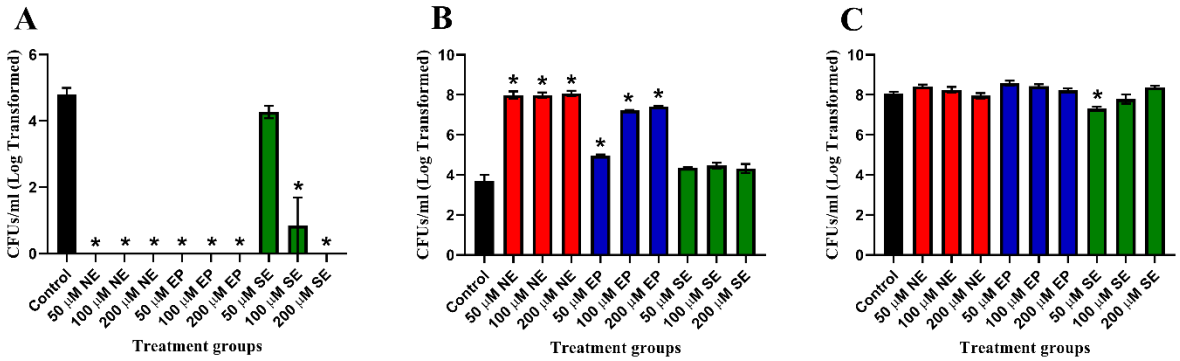

FIG 5-2. Alteration of growth of *Yersinia* species in response to norepinephrine (NE), epinephrine (EP) and serotonin (SE). Forty-eight-hour *in vitro* growth of *Yersinia* species in Serum-SAPI media in the presence or absence of norepinephrine, epinephrine, or serotonin. A). *Yersinia pestis* (CO92). B). *Yersinia enterocolitica*. C). *Yersinia pseudotuberculosis* (IP2775). Values represent the means ± the SEM of an experiment performed in triplicate. Statistical analysis by one-way ANOVA with Tukey's multiple comparison (*$p \leq 0.05$).

While norepinephrine was the only hormone tested against *Bacillus* species, in the case of *Yersinia*, epinephrine and serotonin were also screened. With epinephrine tested at 50, 100, and 200 µM, we again see an absence of recoverable colonies with *Y. pestis* (Fig. 2A). In the event of *Y. enterocolitica* we see a similar result as that of norepinephrine, with the only difference being that 50 µM epinephrine had less of an impact on replication resulting in 9.2 x 10^4 CFUs/mL (Fig. 2B). At 100 and 200 µM epinephrine we see approximately 3 logs greater replication compared to control cultures resulting in 1.7 x 10^7 CFUs/mL and 2.7 x 10^7 CFUs/mL; the control yielded 1.2 x 10^4 CFUs/mL. With *Y. pseudotuberculosis* we again see no enhancement of replication with either 50, 100, or 200 µM epinephrine under these test conditions (Fig. 2C). When

screening serotonin, we again see with *Y. pestis* an inhibition of replication (Fig. 2A). While 50 μM serotonin yielded no significant effect on the replication of *Y. pestis*, we do see a stark reduction in CFU counts with 100 μM serotonin, and an absence of recovered colonies with 200 μM serotonin. When *Y. enterocolitica* was exposed to serotonin at 50, 100, and 200 μM there was no significant inhibition or stimulation of replication (Fig. 2B). Lastly, exposing *Y. pseudotuberculosis* to serotonin at 50, 100, and 200 μM led to no significant differences in replication at 100 and 200 μM serotonin; there was a slight inhibition of replication seen at 50 μM serotonin (Fig. 2C).

Experiments carried out with a racemic mix of norepinephrine enantiomers showed decreased replication inhibition with *Y. pestis* when tested compared to that of the more biologically relevant L-norepinephrine enantiomer (Fig. 3). Here we see a pronounced dose response with norepinephrine exposure with treatment at 50, 100, and 200 μM yielding 4.0×10^4 CFUs/mL, 2.0×10^4 CFUs/mL, and 4.1×10^2 CFUs/mL: with the control yielding 2.2×10^5 CFUs/mL (Fi.g 3A). In a separate experiment is was shown that the beta androgenic receptor antagonist propranolol could attenuate the effects of norepinephrine and restore normal growth phenotype (Fig. 3B). The control yielded 5.8×10^5 CFUs/mL, while treatment with the racemic mix of norepinephrine at 100 μM reduced the replication of *Y. pestis* to 3.8×10^4 CFUs/mL. With the inclusion of propranolol at 500 μM in conjunction with 100 μM norepinephrine the number of recovered bacteria were 4.2×10^6 CFUs/mL. The presence of 500 μM propranolol alone yielded 3.2×10^6 CFUs/mL.

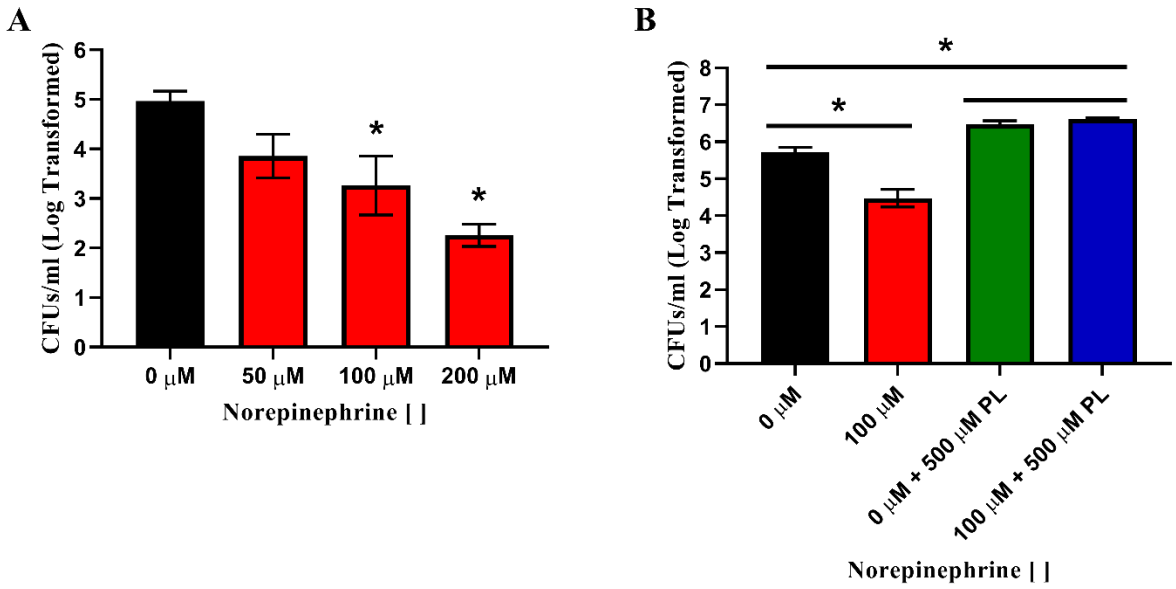

FIG 5-3. Alteration of growth of *Yersinia pestis* (CO92) in response to a racemic mix of norepinephrine and the beta-adrenergic receptor antagonist propranolol. Forty-eight-hour *in vitro* growth of *Y. pestis* in Serum-SAPI media in the presence or absence of norepinephrine and propranolol (PL). (A) Dose titration of a racemic mix of norepinephrine. Values represent the means ± the SEM of three experiments performed in triplicate. Statistical analysis by one-way ANOVA with Bonferroni's multiple comparison (*$p \leq 0.05$). (B) Antagonistic effects of propranolol on norepinephrine. Values represent the means ± the SEM of an experiment performed in triplicate. Statistical analysis by one-way ANOVA with Tukey's multiple comparison (*$p \leq 0.05$).

When investigating the reported phenomenon that norepinephrine exposure can increase resistance to the antibiotic rifampicin in *Staphylococcal* species, we saw a similar trend when we tested this with *Bacillus* species (19). In both *B. anthracis* Ames and Sterne strain we observed unfettered replication with the inclusion of 100 μM norepinephrine at rifampicin concentrations that inhibited all replication in the absence of norepinephrine (Fig. 4). In the case of the Ames strain an MIC of 0.15 μg/mL rifampicin was found; the inclusion of 100 μM norepinephrine shifted the MIC to 0.25 μg/mL rifampicin (Fig. 4A).

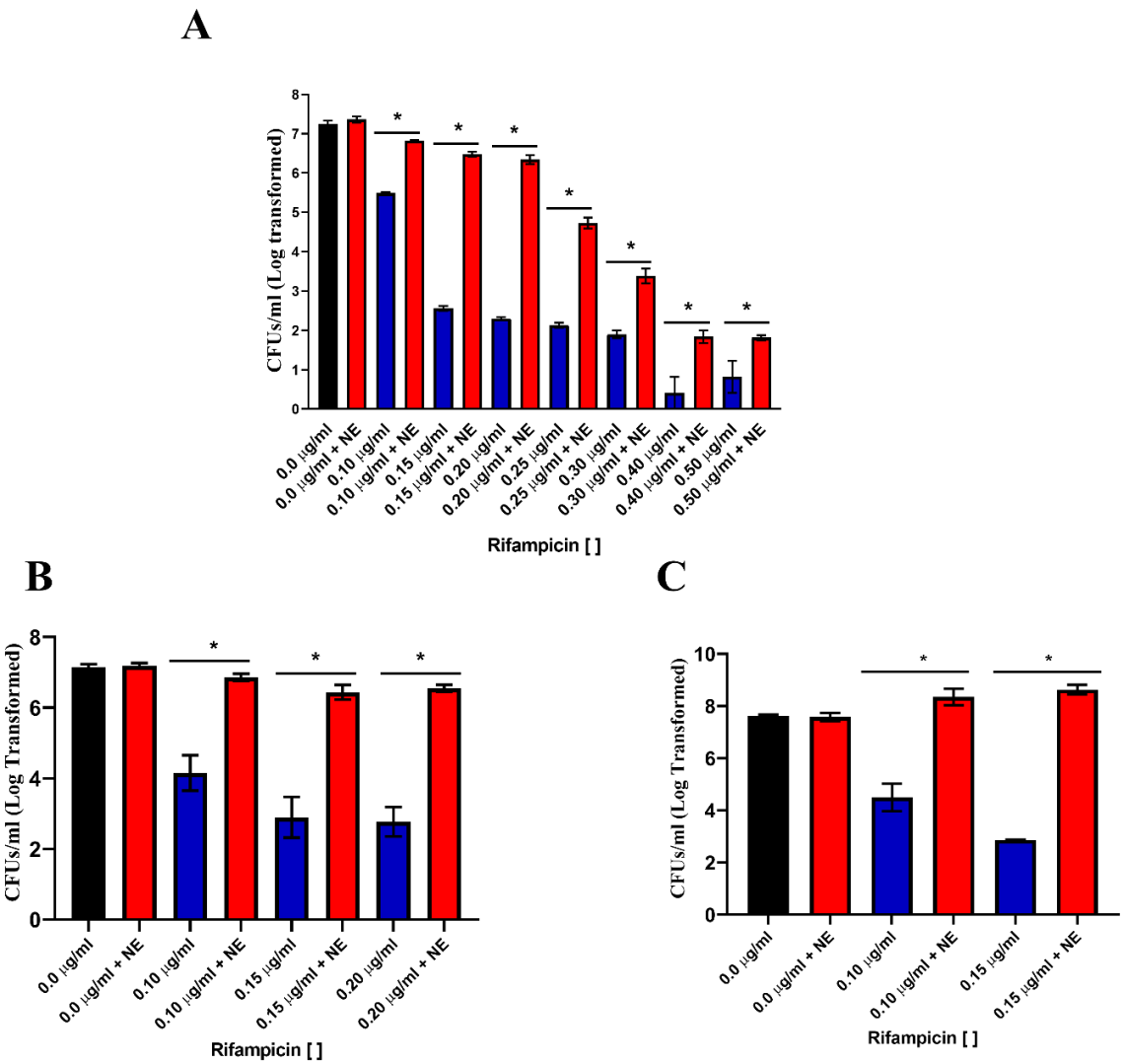

FIG 5-4. Norepinephrine induced resistance to rifampicin among *Bacillus* species. Twenty-hour *in vitro* growth of *Bacillus* species in Serum-SAPI media in the presence or absence of 100 µM norepinephrine (NE) with the antibiotic rifampicin. (A) *Bacillus anthracis* (Ames). Values represent the means ± the SEM of an experiment performed in triplicate. (B) *Bacillus anthracis* (Sterne). Values represent the means ± the SEM of three experiments performed in triplicate. (C) *Bacillus cereus*. Values represent the means ± the SEM of an experiment performed in triplicate. Statistical analysis by one-way ANOVA with Bonferroni's multiple comparison (*$p \leq 0.05$).

Significantly more bacteria were recovered from the norepinephrine treated cultures out to 0.50 µg/mL rifampicin. With Sterne strain replication consistent with untreated controls was sustained out to 0.20 µg/mL rifampicin when norepinephrine was

included; in the absence of norepinephrine the MIC was found to be 0.10 µg/mL (Fig. 4B). Concentration of rifampicin above 0.2 µg/mL rifampicin were not screened with the Sterne strain of *B. anthracis*. With *B. cereus* we saw results similar to that of *B. anthracis* (Fig. 4C). The MIC for *B. cereus* here was 0.10 µg/mL and with the inclusion of 100 µM NE we see replication reminiscent of the untreated controls out to 0.15 µg/mL rifampicin; like with the Sterne strain of *B. anthracis* a broader dose range of rifampicin was not tested. Interestingly, when we screened the antibiotics doxycycline, ampicillin, and ciprofloxacin against *B. anthracis* with the inclusion of 100 µM norepinephrine we did not see this same resistance phenotype that we saw with rifampicin (data not shown). It should be noted that in the experiments involving *Bacillus* species a racemic mix of norepinephrine was used in all experiments instead of using just the L-norepinephrine enantiomer, which would be more biologically relevant.

When the beta-adrenergic receptor antagonist propranolol was used a 5x the concentration of norepinephrine when the bacteria were challenged with rifampicin, we saw a significant reduction in the resistant phenotype elicited by norepinephrine (Fig. 5). It should be noted that treating these bacteria with propranolol in tandem with rifampicin also led to a significant reduction in bacteria compared to those treated with just rifampicin; this was most pronounced with the Sterne strain of *B. anthracis*. With the Ames strain of *B. anthracis,* the inclusion of propranolol with norepinephrine and rifampicin led to 3.4×10^5 bacteria recovered; when challenged with norepinephrine and rifampicin together 1.6×10^7 bacteria were recovered (Fig. 5A). The treatment with rifampicin alone yielded 5.7×10^2 recovered bacteria, and the inclusion of propranolol with rifampicin resulted in 1.0×10^2 recovered bacteria. Similar results were seen with

the Sterne strain of *B. anthracis* and with *B. cereus* (Figs. 5B and 5C). Of potential future interest in the treatment of anthrax, the alpha-adrenergic receptor antagonist phenoxybenzamine greatly inhibited the growth of *B. anthracis* Sterne strain, which was not seen with propranolol (Fig. 5D).

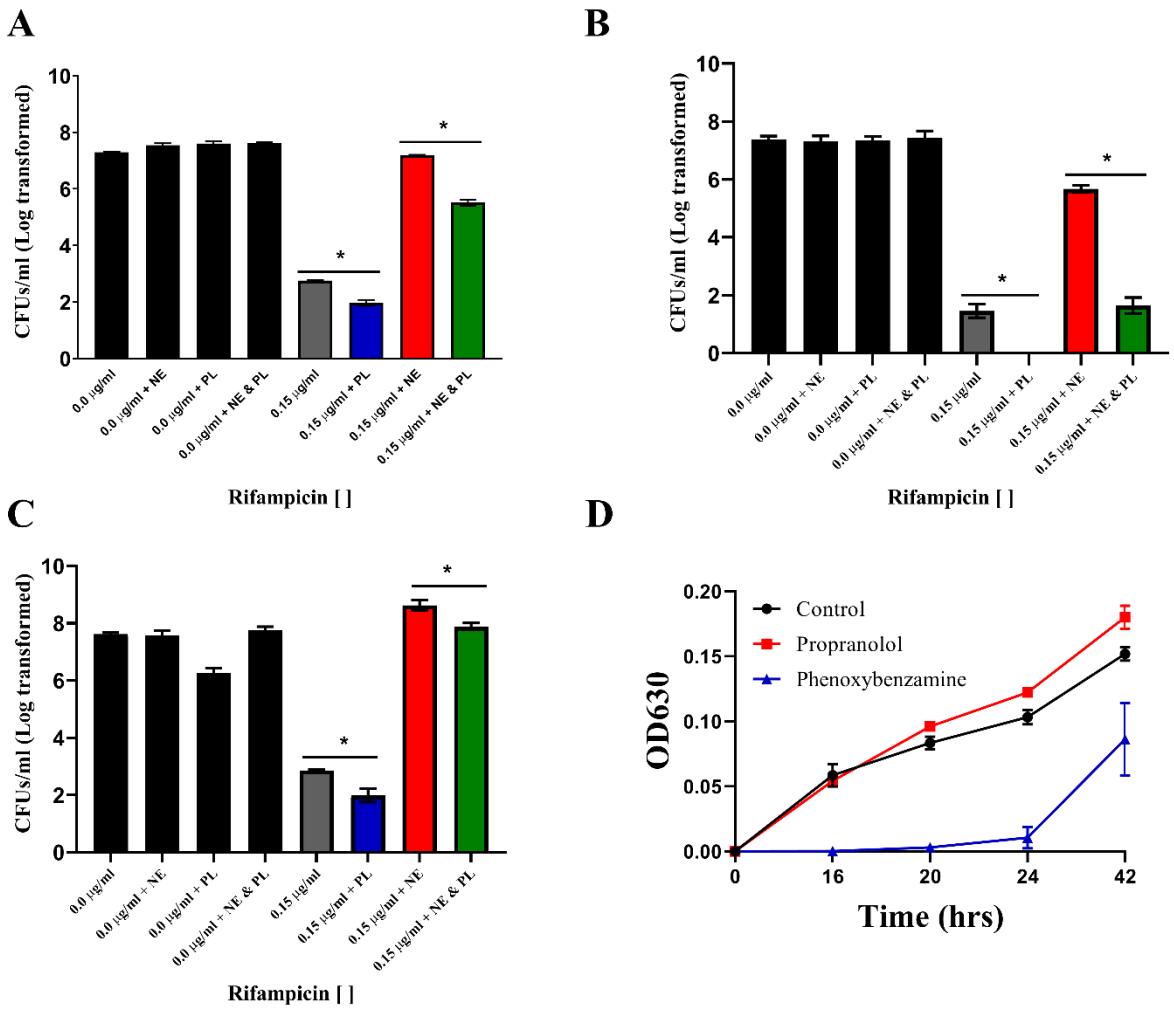

FIG 5-5. Adrenergic receptor antagonist impact on growth and norepinephrine induced resistance to rifampicin among *Bacillus* species. (A-C). Twenty-hour *in vitro* growth of *Bacillus* species in Serum-SAPI media in the presence or absence of 100 µM norepinephrine (NE) and 500 µM propranolol (PL) with the antibiotic rifampicin. (A) *Bacillus anthracis* (Ames). (B) *Bacillus anthracis* (Sterne). (C) *Bacillus cereus*. Values represent the means ± the SEM of an experiment performed in triplicate. Statistical analysis by one-way ANOVA with Tukey's multiple comparison (*$p \leq 0.05$). (D) Growth curve of *B. anthracis* (Sterne) in Serum-SAPI media in the presence or absence of 500 µM propranolol or 500 µM phenoxybenzamine.

It does seem that the concurrent exposure of norepinephrine with rifampicin is required for elicitation of this resistant phenotype (Fig. 6). Simply pre-exposing *B. anthracis* to norepinephrine and then removing most residual norepinephrine prior to rifampicin treatment did not elicit a resistant phenotype.

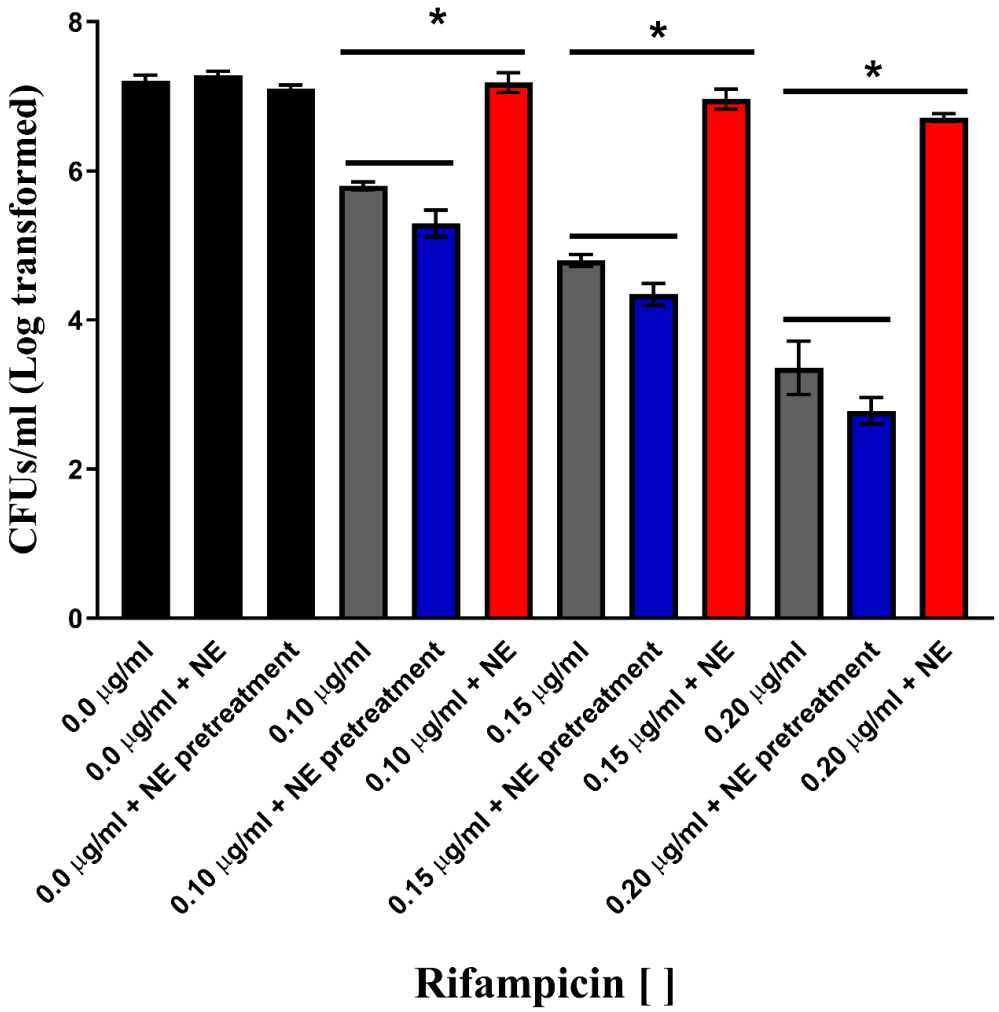

FIG 5-6. Continuous exposure to norepinephrine is required for resistance phenotype towards rifampicin. *Bacillus anthracis* Sterne was grown in the presence or absence of 100 μM norepinephrine (NE) in Serum-SAPI media for 24 hours prior to antimicrobial challenge with rifampicin; excess norepinephrine was removed prior to antimicrobial challenge. During rifampicin challenge a control included the addition of 100 μM norepinephrine. Values represent the means ± the SEM of an experiment performed in triplicate. Statistical analysis by one-way ANOVA with Tukey's multiple comparison (*$p \leq 0.05$).

Iron is an important growth factor for bacteria, and it has been shown that norepinephrine can increase iron uptake in iron limiting environments were iron is sequestered by transferrin (15). To explore this as a mechanism for the perceived rifampicin resistance the inclusion of ferrous sulfate at 20 μM was included in the assay. In both the Ames and Sterne strain of *B. anthracis* the inclusion of surplus iron did yield a slight increase in CFUs over that of rifampicin treated alone, yet it was not in line with the degree of resistance induced by the presence of norepinephrine (Fig. 7). In the case of the Ames strain when challenged with 0.10 μg/mL rifampicin we see the inclusion of excess iron improving the replication of *B. anthracis* to a similar degree as 100 μM norepinephrine with excess iron yielding 7.17 x 10^6 CFUs/mL and 100 μM norepinephrine yielding 7.4 x 10^6 CFUs/mL; in the absence of excess iron or norepinephrine we see 5.3 x 10^5 recovered CFUs/mL (Fig. 7A). When the concentration of rifampicin was increased to 0.20 μg/mL we see a stark difference between the number of recovered bacteria between the inclusion of excess iron and norepinephrine. Here, the inclusion of excess iron resulted in 3.2 x 10^3 CFUs/mL while the addition of 100 μM norepinephrine yielded 2.1 x 10^6 CFUs/mL; bacteria treated with rifampicin in the absence of either excess iron or norepinephrine resulted in 1.9 x 10^2 CFUs/mL. With the Stene strain we see similar results as that of the Ames strain of *B. anthracis* were at 0.10 μg/mL rifampicin there is no significant difference in recovered CFUs between the inclusion of excess iron or 100 μM norepinephrine. However, when the concentration of rifampicin was increased to 0.20 μg/mL there is a several log reduction in the number of recovered CFUs when excess iron was utilized compared to the inclusion of 100 μM

norepinephrine.

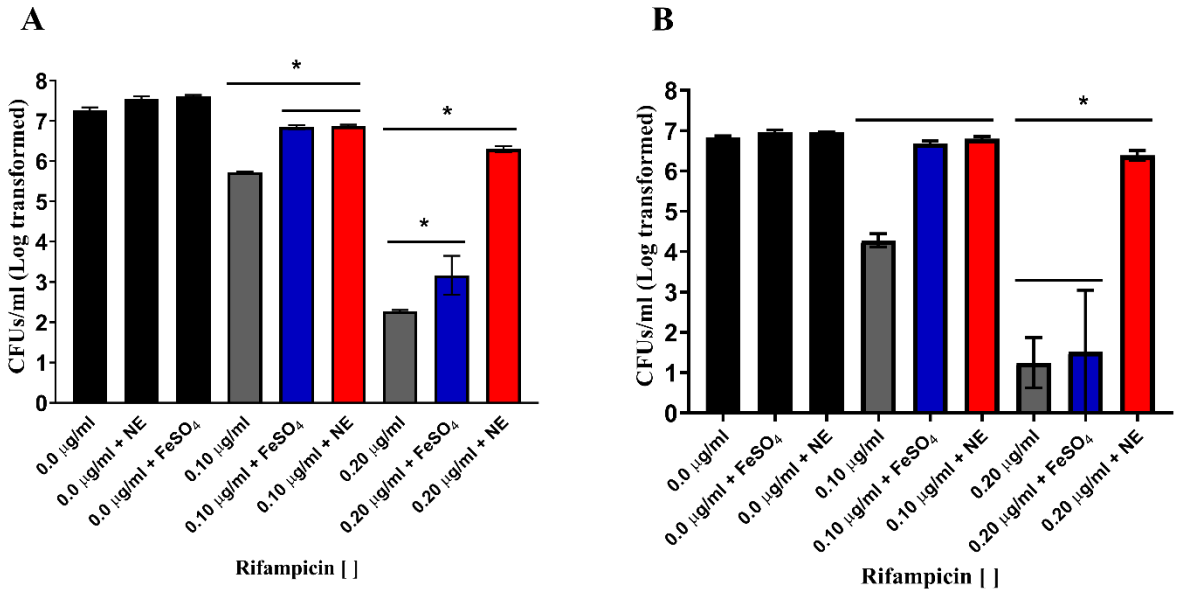

FIG 5-7. Impact of excess iron on the susceptibility of *Bacillus anthracis* to rifampicin with the comparison to the resistant phenotype derived from exposure to norepinephrine. *Bacillus anthracis* was grown in the presence or absence of 100 µM norepinephrine (NE) or 20 µM ferrous sulfate ($FeSO_4$) in Serum-SAPI media (A) *Bacillus anthracis* (Ames). (B) *Bacillus anthracis* (Sterne). Values represent the means ± the SEM of an experiment performed in triplicate. Statistical analysis by one-way ANOVA with Tukey's multiple comparison (*$p \leq 0.05$).

While norepinephrine did not elicit a resistant phenotype towards ciprofloxacin or ampicillin; exposing bacteria that were antimicrobially damaged by these two antibiotics to norepinephrine greatly increased the growth recovery. *B. anthracis* Sterne strain was exposed to 1.6 µg/mL ciprofloxacin, 2.0 µg/mL ampicillin, and 1.0 µg/mL rifampicin for 8 hours to effectively render 99% of the exposed bacteria non-viable by plate count. Following removal of residual antibiotics through multiple centrifugation steps, 100 µM norepinephrine was added (Fig. 8). What we found is that the presence of norepinephrine increased the replication rate of bacteria antimicrobially damaged by rifampicin by 63-fold, by ciprofloxacin by 12-fold, and by ampicillin by 20-fold. In the experiments

involving ciprofloxacin and ampicillin additional treatments included the inclusion of excess iron through the addition of 20 µM ferrous sulfate. In these groups treated with excess iron their recovery rate matched that of the groups treated with 100 µM norepinephrine.

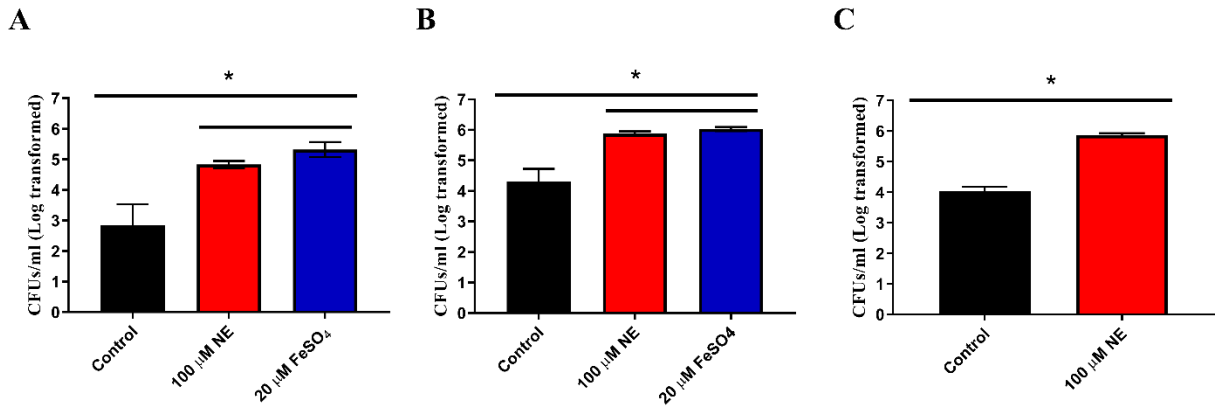

FIG 5-8. Impact of norepinephrine (NE) and iron ($FeSO_4$) on the ability of *Bacillus anthracis* Sterne to recovery from exposure to bactericidal concentrations of the antibiotic's ciprofloxacin (1.6 µg/mL), ampicillin (2.0 µg/mL), or rifampicin (1.0 µg/mL) for 8 hours. Excess antibiotics was removed prior to addition of norepinephrine or iron, and the bacteria were allowed to recover in Serum-SAPI media for 20 hours. A). Ciprofloxacin. B). Ampicillin. C). Rifampicin. A & B, values represent the means ± the SEM of an experiment performed in triplicate. Statistical analysis by one-way ANOVA with Tukey's multiple comparison (*$p \leq 0.05$). C, Values represent the means ± the SEM of an experiment performed in triplicate. Statistical analysis by Student's *t*-test (*$p \leq 0.05$).

The spore state in *B. anthracis* is important in its lifecycle. Norepinephrine alone was found to have no positive or negative impact on spore germination with the Sterne strain, and norepinephrine did not antagonize or enhance the known spore germinate alanine (20) (Fig. 9A). However, an interesting find was that germinated spores of the Sterne strain are more resistant to rifampicin than cultures maintained in a vegetative state (Fig. 9B). The endpoint of this assay was measured through the viability reagent resazurin, instead of CFU enumeration as the previous data has been shown.

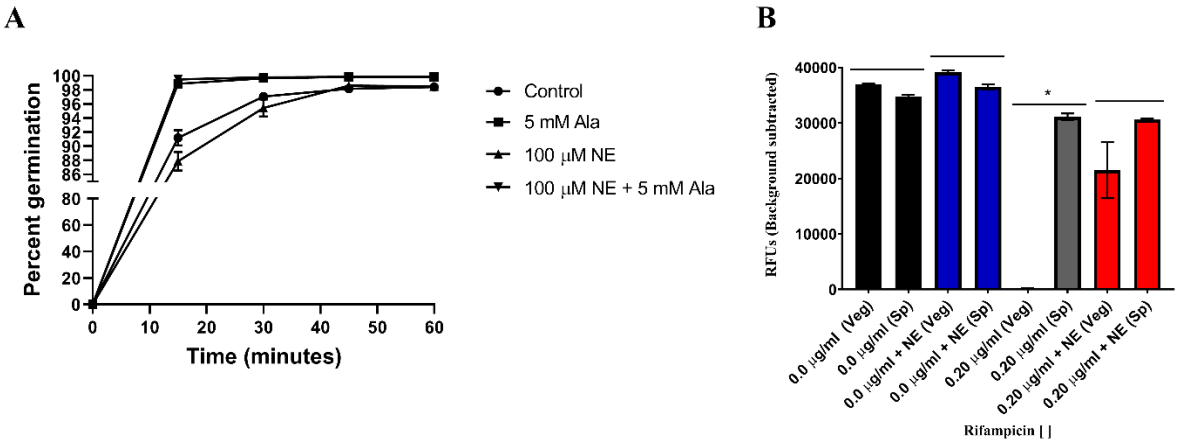

FIG 5-9. Impact of norepinephrine (NE) on the spore state of *Bacillus anthracis* (Sterne). (A). Germination of *B. anthracis* spores in Serum-SAPI media in the presence or absence of 100 μM norepinephrine; alanine was included as a positive control as it is known to accelerate germination. (B). Impact of the spore state of *B. anthracis* and 100 μM norepinephrine on the susceptibility to rifampicin in Serum-SAPI media; vegetative passaged cells (Veg), and spores (Sp). Note: 98% of spores germinate within 60 minutes of being in Serum-SAPI media. Values represent the means ± the SEM of an experiment performed in triplicate. Statistical analysis by one-way ANOVA with Tukey's multiple comparison (*$p \leq 0.05$).

The expression of toxins by *B. anthracis* is a critical part of its pathogenesis, and as norepinephrine has been shown to induce a positive growth phenotype it was deemed worthwhile to see if norepinephrine exposure would modulate toxin expression using the Sterne strain. Supernatants derived from broth cultures grown in the presence or absence of 100 μM norepinephrine and then purified and concentrated via Centriprep centrifugal filters were added to cultures of murine macrophages (RAW 246.7) and the presence of anthrax toxin was assayed via the decrease in viability of the macrophages using MTT (Fig. 10). The results indicate that norepinephrine at 100 μM resulted in a small but significant decrease in cytotoxicity, which would indicate reduced toxin expression.

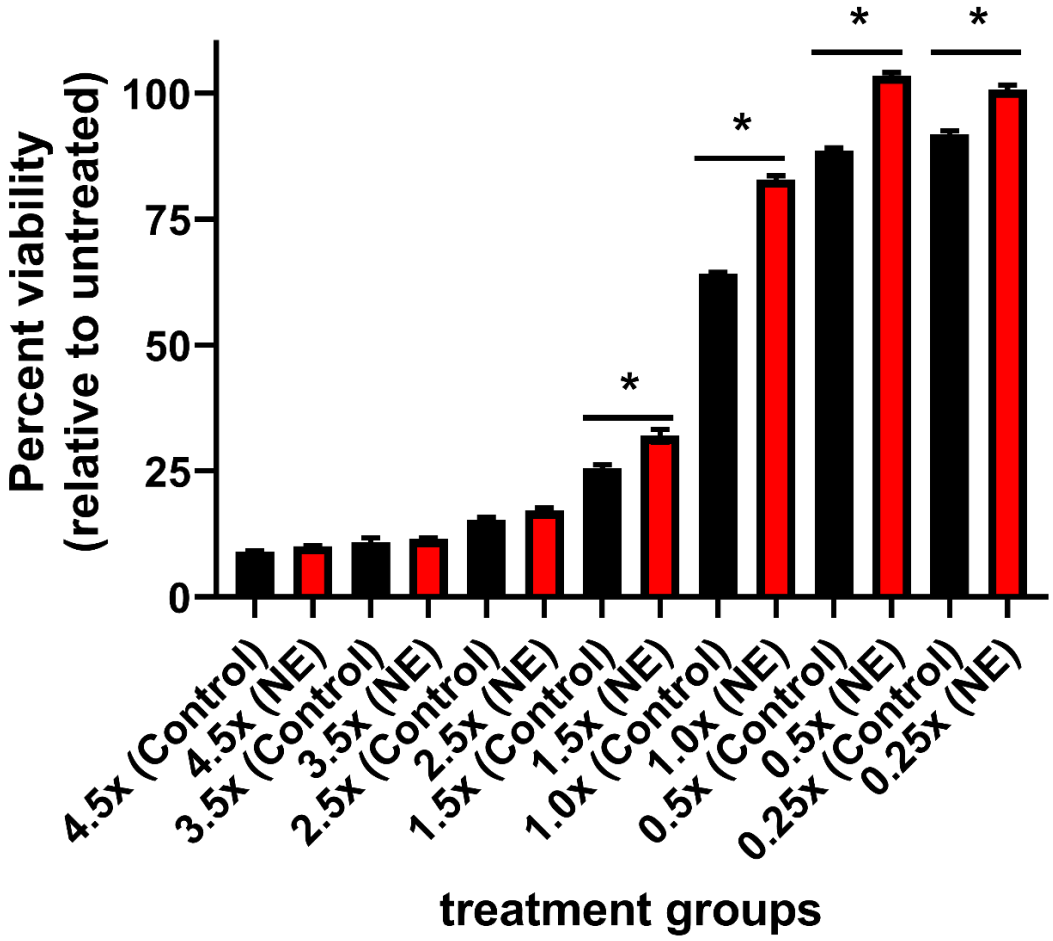

FIG 5-10. Impact of norepinephrine (NE) on the expression of toxins by *Bacillus anthracis* (Sterne). Vegetative cultures of *B. anthracis* were grown in the presence or absence of norepinephrine (100 µM) and the culture supernatant was purified and concentrated (Centriprep centrifugal filter device). A titration of the concentrate was applied to murine macrophages (RAW 246.7) and the loss of viability measured through the viability reagent MTT was indicative of the toxin production by the bacteria. Values represent the means ± the SEM of an experiment performed in triplicate. Statistical analysis by one-way ANOVA with Bonferroni's multiple comparison (*$p \leq 0.05$).

Discussion

Given the previous research involving microbial endocrinology, it is not surprising that norepinephrine was able to stimulate the replication of *B. anthracis*; what is a striking observation discovered is that norepinephrine and epinephrine do not stimulate the replication of *Y. pestis*. The list of bacteria that respond positively to the

presence of catecholamines is extensive. The fact that the related *Yersinia* species enterocolitica responds favorable to the presence of norepinephrine is well established in previous literature and again here, added a bit of a surprise in that *Y. pestis* appears to take the opposite approach to catecholamines and it's replication is in fact reduced by the presence of norepinephrine and epinephrine . In terms of evolutionary relatedness *Y. pestis* is more closely related to *Y. pseudotuberculosis*, which in these experiments was unfettered by the presence of norepinephrine or epinephrine, which like *Y. enterocolitica*, presented a much different phenotype to *Y. pestis*. The evolution of *Y. pestis* from *Y. pseudotuberculosis* involved the acquisition of plasmids conveying important virulence factors as well as gene loss; it is possible that through these processes of evolution *Y. pestis* emerged with an atypical response to catecholamines (21). Future studies will be needed to ascertain the genetic reason for this inversion of function and whether it was crucial in the emergence of *Y. pestis* from an enteric pathogen to one which causes systemic disease with a flea intermediate in its life cycle. The oddity in its response to norepinephrine is that in response to stress and illness norepinephrine would be expressed at higher levels in its host and in the case of pneumonic plague the lungs are enervated with norepinephrine expressing nerves; in the course of infection *Y. pestis* would undoubtedly be exposed to norepinephrine, so the observed growth inhibition is puzzling. In another respiratory tract pathogen, *Mycoplasma hyopneumoniae*, a profound reduction in replication brought on by exposure to norepinephrine was also observed; so, this observation is not unique to *Y. pestis* (22).

An additional oddity with *Y. pestis* is in how it responds to the hormone serotonin. Serotonin is often thought of as a neurotransmitter, but much of the serotonin produced in

the body is produced by enterochromaffin cells of the intestine and is found circulating in the blood stream (23). While the enteric *Yersinia* pathogens *enterocolitica* and *pseudotuberculosis* are unaffected or minimally affected by the presence of serotonin, in the case of *Y. pestis* there is a profound decrease in replication when exposed to serotonin. This response to serotonin is puzzling in that *Y. pestis* would be exposed to high levels of serotonin *in vivo* as platelet cells store serotonin and release it at sites of inflammation (24). Given the lethal nature of *Y. pestis* these inverted responses to catecholamines and serotonin must not be detrimental towards its pathogenicity. What may be observed here is a shift to a viable but non-culturable state: this would require further experimentation to determine.

An interesting observation with *Y. pestis* is that the inhibition of replication brought on through the exposure of norepinephrine can be ameliorated through the addition of the adrenergic receptor antagonist propranolol. In mammalian systems propranolol acts upon beta-adrenergic receptors were as norepinephrine signals preferentially through alpha-adrenergic receptors with signally through beta-adrenergic receptors happing at high norepinephrine concentrations; so, the association we are seeing here is unexpected (25). As of the writing of this dissertation a beta-adrenergic receptor antagonist has not been experimented with *Y. pestis*; the reason propranolol was chosen is that previous work with *Bacillus* species, which will be discussed later, found that propranolol attenuated the effects of norepinephrine. This finding could suggest that both norepinephrine and propranolol are acting through a receptor with some similarity to that found in mammalian systems. This would be an exciting discovery, and would require definitive mechanistic data to support, which is not presented here.

It should be noted that in these experiments *Y. enterocolitica* showed a positive growth response to the presence of epinephrine. This result is not consistent with previous results that showed an increase in replication in response to norepinephrine and dopamine, but not to epinephrine (9). Here we showed an increase in replication with both norepinephrine and epinephrine; dopamine was not tested. The published data included 14 strains of *Y. enterocolitica* that all responded similarly to epinephrine exposure. The different response seen here with the strain of *enterocolitica* used may warrant further study.

Research has previously shown that norepinephrine exposure can result in resistance to the antibiotic rifampicin in Staphylococcus species (19). The idea that norepinephrine or other catecholamines could elicit antimicrobial resistance is daunting given that antimicrobial resistance is already a priority issue and that norepinephrine is often administered to patients in septic shock (26). In the case of *B. anthracis* and *B. cereus* we do see an increase in the MIC to rifampicin when these bacteria are exposed to norepinephrine. It should be noted that even with this observed MIC shift the serum concentration of rifampicin achieved through normal therapeutic dosing should still be effective in treating diseases caused by these organisms; to add to this rifampicin isn't typically used to treat these diseases either. Cmax for rifampicin is approximately 8 to 12 µg/mL with a decrease over 12 hours to 2 µg/mL, which represents several fold higher concentrations than what we have shown to inhibit the replication of *B. anthracis* when norepinephrine is present (27). No resistant phenotype was found when *B. anthracis* was exposed to ciprofloxacin or doxycycline which would be drugs typically used to treat anthrax. The data here only shows a phenotypic shift in rifampicin resistance and

currently the mechanism for this norepinephrine induced resistance is not known. As was seen with *Y. pestis*, the addition of the beta-adrenergic receptor antagonist propranolol was able to attenuate the resistant phenotype to a small degree. This could suggest that norepinephrine is acting through a cell surface receptor to initiate this resistant phenotype, which is likely an unattended consequence of changes in gene expression brought on by exposure to norepinephrine. A continuous exposure to norepinephrine is required to drive this resistant phenotype in *B. anthracis*. It was observed that exposing these *Bacillus* species to propranolol did result in them being slightly more susceptible to rifampicin; this interaction could be further explored as a potential adjunct therapy. An interesting finding was that the alpha-adrenergic receptor antagonist phenoxybenzamine was shown to greatly inhibit the replication of *B. anthracis* and in itself may present a novel mechanism in developing a therapy against anthrax. To see if phenoxybenzamine universally inhibited the growth of bacteria, the gram-negative pathogen *Burkholderia pseudomallei*, was exposed to phenoxybenzamine and no inhibition was seen (data not shown).

Previous research has shown that norepinephrine will facilitate improved iron uptake from transferrin by bacteria. While the data presented does show that simply adding excess iron to the media does result in a slight increase in tolerance to rifampicin with *B. anthracis*, the excess iron could not match level of resistance generated through the addition of norepinephrine. This suggests that improved iron acquisition in iron limited environments does not fully explain this resistant phenotype. While excess iron did not drive the same level of resistance to rifampicin as norepinephrine did in these antimicrobial assays, we did see that in the case of ciprofloxacin and ampicillin, that

excess iron resulted in similar levels of growth recover as norepinephrine following exposing *B. anthracis* to bactericidal concentrations of these two antibiotics. Mechanistic data would add light to why this discrepancy between resistant phenotype and recovery exists.

While the spore state of *B. anthracis* is essential in its life cycle and infective nature, the presence of norepinephrine was found to have no impact on germination. An interesting result from these experiments is that bacillus derived from freshly germinated spores appear more resistant to the antibiotic rifampicin. It would be interesting to see if these newly vegetative cells are also resistant to other classes of antibiotics and for how long this phenotype persists as it could have implications in treatment.

While norepinephrine did increase the replication rate of *B. anthracis*, the presence of norepinephrine did not induce greater expression of toxins. This would suggest that norepinephrine does not influence the expression of the *atxA* gene in *B. anthracis* which regulates many virulence associated genes (28).

While the data presented here is based solely on phenotypic observations, there is compelling evidence that catecholamines produce a profound and varied response across these bacterial species. Across these two virulent bacteria, *Bacillus anthracis* and *Yersinia pestis*, we see a divergent response to the presence of norepinephrine. The common thread among bacteria seems to be a positive replication phenotype in the presence of norepinephrine and that is what we see with *B. anthracis*, but with *Y. pestis* there is a strong retardation of replication following exposure to norepinephrine, along with epinephrine and serotonin. These results are based upon CFU enumeration and it remains in the realm of possibilities that what was observed with *Y. pestis* was a shift to a

viable but non-culturable state brought on by exposure to these catecholamines as under many of the experimental conditions no colonies were recovered; a viable but non-culturable state has been described for *Y. pestis* (29). The *Yersinia* genus appears to be an ideal candidate for future studies examining the interplay between bacteria and catecholamines given the divergent responses to catecholamines within the genus.

References

1. Nakano M, Takahashi A, Sakai Y, Kawano M, Harada N, Mawatari K, Nakaya Y. 2007. Catecholamine-induced stimulation of growth in *Vibrio* species. Lett Appl Microbiol 44:649-53.

2. Anderson MT, Armstrong SK. 2008. Norepinephrine mediates acquisition of transferrin-iron in *Bordetella bronchiseptica*. J Bacteriol 190:3940-7.

3. Coulanges V, Andre P, Vidon D. 1998. Effect of siderophores, catecholamines, and catechol compounds on *Listeria* spp. Growth in iron-complexed medium. Biochemical and Biophysical Research Communications 249:5.

4. Hegde M, Wood TK, Jayaraman A. 2009. The neuroendocrine hormone norepinephrine increases *Pseudomonas aeruginosa* PA14 virulence through the las quorum-sensing pathway. Appl Microbiol Biotechnol 84:763-76.

5. Nakano M, Takahashi A, Sakai Y, Nakaya Y. 2007. Modulation of pathogenicity with norepinephrine related to the type III secretion system of *Vibrio parahaemolyticus*. J Infect Dis 195:1353-60.

6. Green BT, Lyte M, Kulkarni-Narla A, Brown DR. 2003. Neuromodulation of enteropathogen internalization in Peyer's patches from porcine jejunum. Journal of Neuroimmunology 141:74-82.

7. Toscano MJ, Stabel TJ, Bearson SMD, Bearson BL, Lay DC. 2007. Cultivation of *Salmonella enterica* serovar Typhimurium in a norepinephrine-containing medium alters in vivo tissue prevalence in swine. Journal of Experimental Animal Science 43:329-338.

8. Intarak N, Muangsombut V, Vattanaviboon P, Stevens MP, Korbsrisate S. 2014. Growth, motility and resistance to oxidative stress of the melioidosis pathogen *Burkholderia pseudomallei* are enhanced by epinephrine. Pathog Dis 72:24-31.

9. Freestone PP, Haigh RD, Lyte M. 2007. Specificity of catecholamine-induced growth in *Escherichia coli* O157:H7, *Salmonella enterica* and *Yersinia enterocolitica*. FEMS Microbiol Lett 269:221-8.

10. Withers MR. 2014. USAMRIID'S medical management of biological casualties handbook (8th ed.). Fort Detrick, MD: US Army Medical Research Institute of Infectious Diseases.

11. Benedict CR, Grahame-Smith DG. 1978. Plasma Noradrenaline and Adrenaline Concentrations and Dopamine-β-hydroxylase Activity in Patients With Shock Due to Septicaemia, Trauma and Haemorrhage. QJM: An International Journal of Medicine 47:1-20.

12. Boldt J, Menges T, Kuhn D, Diridis C, Hempelmann G. 1995. Alterations in circulating vasoactive substances in the critically ill —a comparison between survivors and non-survivors. Intensive Care Medicine 21:218-225.

13. Bower WA, Hendricks K, Pillai S, Guarnizo J, Meaney-Delman D. 2015. Clinical Framework and Medical Countermeasures Use During an Anthrax Mass-Casualty Incident. MMWR 64.

14. Ratledge C, Dover LG. 2000. Iron Metabolism in Pathogenic Bacteria. Annu Rev Microbiol 54:10.

15. Freestone PPE, Lyte M, Neal CP, Maggs AF, Haigh RD, Williams PH. 2000. The Mammalian Neuroendocrine Hormone Norepinephrine Supplies Iron for Bacterial Growth in the Presence of Transferrin or Lactoferrin. Journal of Bacteriology 182:8.

16. Hotta K, Kim CY, Fox DT, Koppisch AT. 2010. Siderophore-mediated iron acquisition in *Bacillus anthracis* and related strains. Microbiology 156:1918-1925.

17. Zietz BP, Dunkelberg H. 2004. The history of the plague and the research on the causative agent *Yersinia pestis*. Int J Hyg Environ Health 207:165-78.

18. St John AL, Ang WXG, Huang MN, Kunder CA, Chan EW, Gunn MD, Abraham SN. 2014. S1P-Dependent trafficking of intracellular *Yersinia pestis* through lymph nodes establishes Buboes and systemic infection. Immunity 41:440-450.

19. Freestone PP, Haigh RD, Lyte M. 2008. Catecholamine inotrope resuscitation of antibiotic-damaged staphylococci and its blockade by specific receptor antagonists. J Infect Dis 197:1044-52.

20. Titball RW, Manchee RJ. 1987. Factors affecting the germination of spores of *Bacillus anthracis*. Journal of Applied Bacteriology 62:269-273.

21. Chain PSG, Carniel E, Larimer FW, Lamerdin J, Stoutland PO, Regala WM, Georgescu AM, Vergez LM, Land ML, Motin VL, Brubaker RR, Fowler J, Hinnebusch J, Marceau M, Medigue C, Simonet M, Chenal-Francisque V, Souza B, Dacheux D, Elliott JM, Derbise A, Hauser LJ, Garcia E. 2004. Insights into the evolution of *Yersinia pestis* through whole-genome comparison with *Yersinia*

pseudotuberculosis. Proceedings of the National Academy of Sciences of the United States of America 101:13826-13831.

22. Oneal MJ, Schafer ER, Madsen ML, Minion FC. 2008. Global transcriptional analysis of *Mycoplasma hyopneumoniae* following exposure to norepinephrine. Microbiology 154:2581-2588.

23. Walther DJ, Peter JU, Bashammakh S, Hortnagl H, Voits M, Fink H, Bader M. 2003. Synthesis of serotonin by a second tryptophan hydroxylase isoform. Science 299:76.

24. Herr N, Bode C, Duerschmied D. 2017. The Effects of Serotonin in Immune Cells. Front Cardiovasc Med 4:48.

25. Arnsten AF, Wang MJ, Paspalas CD. 2012. Neuromodulation of thought: flexibilities and vulnerabilities in prefrontal cortical network synapses. Neuron 76:223-39.

26. Martin C, Viviand X, Leone M, Thirion X. 2000. Effect of norepinephrine on the outcome of septic shock. Critical Care Medicine 28:8.

27. Garnham JC, Taylor T, Turner P, Chasseaud LF. 1976. Serum Concentrations and Bioavailability of Rifampicin and Isoniazid in Combination. Br J clin Pharmac 3:6.

28. Fouet A. 2010. AtxA, a *Bacillus anthracis* global virulence regulator. Res Microbiol 161:735-42.

29. Pawlowski DR, Metzger DJ, Raslawsky A, Howlett A, Siebert G, Karalus RJ, Garrett S, Whitehouse CA. 2011. Entry of *Yersinia pestis* into the viable but nonculturable state in a low-temperature tap water microcosm. PLoS One 6:e17585.

CHAPTER 6: CONCLUSIONS

The bacteria and amoeba discussed in this research represent microbes that can have a profound negative impact on the health and wellbeing of those unfortunate enough to be infected by them, with death being a likely outcome. In the case of both *Burkholderia* species discussed and the "brain eating amoeba" *Naegleria fowleri* there exists a dire need for improved therapeutics to combat the diseases caused by them (1-3). In addition to the mortality associated with *Burkholderia* species, *B. pseudomallei* and *B. mallei* have potential for use as biowarfare or bioterrorism agents which would result in a mass casualty situation which could stretch local medical resources (4). There currently does not exist a therapy that is effective in treating primary amoebic meningoencephalitis caused by *N. fowleri*. In light of these obstacles this research demonstrates that polyanhydride nanoparticles are effective delivery vehicles for antimicrobials that are used to treat these diseases; in most instances the utilization of the nanoparticles as delivery vehicles increases the therapeutic efficacy of these drugs.

In addition to the utilization of nanoparticles as drug delivery vehicles this research also indicated that the antirheumatic drug auranofin is capable of killing *N. fowleri*. Lastly, that catecholamine hormones accelerate the replication and antimicrobial sensitivity of *Bacillus anthracis*, and that these catecholamines differentially alter the replication of different *Yersinia* species.

Chapter 2 details the research surrounding the use of polyanhydride nanoparticles as a means to delivery antibiotics targeting the potential biowarfare/bioterrorism agents *B. pseudomallei* and *B. mallei*. From this research it is evident that there are many confounding factors on whether an improvement in antimicrobial efficacy was achieved

through nanoparticle delivery; at this time many of these factors are not known. Nanoparticle co-polymer chemistry selection was vital in improving efficacy. While previous research with these polyanhydride nanoparticles has shown 20:80 CPTEG:CPH co-polymer chemistry to be effective in improving the antimicrobial efficacy against *Mycobacterium* species and *Brucella melitensis*, this co-polymer chemistry was ineffective in increasing the antimicrobial efficacy with *B. pseudomallei* (5, 6). In the event of *B. pseudomallei* the co-polymer chemistry that resulted in significant improvements in antimicrobial efficacy was 10:90 CPTEG:SA. With 10:90 CPTEG:SA nanoparticles a 5-fold increase in antimicrobial efficacy was seen with meropenem loading. The loading of ceftazidime and chloramphenicol into 10:90 CPTEG:SA nanoparticles resulted in a 2-fold increase in antimicrobial efficacy. Similar results were seen when targeting these antibiotics against *B. mallei*. Improvements in bacterial killing of *B. pseudomallei* and reduction of intracellular bacterial loads in THP-1 macrophages was improved with loading meropenem into 10:90 CPTEG:SA nanoparticles.

While the antibiotics meropenem, ceftazidime, and chloramphenicol showed improved efficacy when loaded into 10:90 CPTEG:SA nanoparticles, the same can't be said for the antibiotics doxycycline and rifampicin. In the event of rifampicin, a decrease in antimicrobial efficacy was seen with loading into 10:90 CPTEG:SA nanoparticles and doxycycline showed no improvement. The reason for these differences cannot be fully explained at this time. It is postulated that the reason that rifampicin performed so poorly is that the loading of rifampicin into these nanoparticles resulted in a release profile that was slower that what was seen with meropenem, ceftazidime, and chloramphenicol. The reason behind the failure to improve upon the efficacy of doxycycline through loading

into these nanoparticles is unknown at the moment as doxycycline has similar release profiles as that of meropenem, ceftazidime, and chloramphenicol. Both chloramphenicol and doxycycline target ribosomes so these differences in efficacy are likely not related to the antibiotics target. Future work will hopefully elucidate why these differences in efficacy are seen between antimicrobials and nanoparticle co-polymer chemistries. Studies utilizing the murine model of melioidosis are planned and will address the *in vivo* therapeutic nature of these polyanhydride nanoparticles.

A continuation of utilizing nanoparticle as antimicrobial delivery vehicles, Chapter 3 details the use of these nanoparticles to target antimicrobials against the pathogenic free-living amoeba *N. fowleri*. Given the lethal nature of primary amoebic meningoencephalitis any improvements in therapeutics could save lives; and previous research has shown that phagocytic cells internalize these polyanhydride nanoparticles very effectively and the hypothesis is that these amoeba, as phagocytic cells, would readily internalize these drug loaded nanoparticles (7). This research found that both 20:80 CPTEG:CPH and 20:80 CPH:SA nanoparticles are effective antimicrobial delivery vehicles, with nanoparticles being visualized in endosomal compartments. One striking difference between these two co-polymer chemistry is that 20:80 CPTEG:CPH nanoparticles appear inert in their native form, while 20:80 CPH:SA nanoparticles had anti-amoebic properties when devoid of any antimicrobial cargo. The anti-amoebic properties of the 20:80 CPH:SA nanoparticles appear to be due to a dysregulation of endosomal trafficking; the exact mechanism for this is unknown.

With the loading of rifampicin into 20:80 CPTEG:CPH nanoparticles an MIC_{50} of 12.5 μg/mL rifampicin was found, yet soluble rifampicin at 25 μg/mL yielded a mere

10% inhibition of replication. When rifampicin was loaded into 20:80 CPH:SA nanoparticles an MIC_{100} of 6.25 μg/mL rifampicin was found. Improvements in antimicrobial efficacy was also seen when the antibiotic azithromycin was loaded into 20:80 CPTEG:SA nanoparticles. Both rifampicin and azithromycin target intracellular processes, with rifampicin targeting RNA polymerase and azithromycin targeting ribosomes. When amphotericin B was loaded into 20:80 CPH:SA nanoparticles there was a reduction in the amoebicidal activity of this drug. This is likely due to the fact that amphotericin B targets ergosterol on the surface of the amoeba so an intercellular delivery is unneeded, and that when administered as a conventional soluble drug 100% of the drug is available to interact with its target, were as with nanoparticle delivery some of the drug would be sequestered within the nanoparticle for a given time depending on release kinetics.

In Chapter 4, research involving *N. fowleri* is continued, this time showing that the FDA approved anti-rheumatoid drug auranofin has amoebicidal properties. Previous research has shown that auranofin has anti-parasitic properties against the protozoan pathogens *toxoplasma gondii*, and *Entamoeba histolytica* (8, 9). Given the previously described anti-parasitic activity and the need for better therapeutics to treat primary amoebic meningoencephalitis it was deemed probably that auranofin would be effective in treating *N. fowleri*. Two pathogenic clinical isolates of *N. fowleri* were screened against auranofin, and differences in susceptibility were noted. The HB-1 strain, which was isolated from a patient from Orlando Florida in 1968 who succumbed from the infection, has an MIC of 1.5 μg/mL and an IC_{50} of 0.788 μg/mL auranofin. The Lee strain, which was isolated from a patient from Richmond Virginia in 1968 who

succumbed from the infection, has an MIC of 3.0 µg/mL and an IC_{50} of 2.18 µg/mL auranofin. Many of these auranofin treated amoeba stained with the cell membrane impermeable dye propidium iodide which suggests that auranofin had killed these cells.

These results are in line with those found with other protozoa, and a recent phase I clinical trial aimed at assessing the pharmacokinetics of auranofin as an anti-parasitic drug shows strong support for auranofin as a labeled anti-parasitic drug (10). Given the results presented here along with high level of interest in auranofin as an anti-parasitic drug, the use of auranofin as an adjunct therapy for primary amoebic meningoencephalitis seems plausible. Having *in vivo* data to support this statement would be ideal; future studies assessing auranofin in the mouse model of primary amoebic meningoencephalitis are planned.

Chapter 5 examines how elements of host neurophysiology affect bacterial replication and antimicrobial susceptibility. Previous research has shown that catecholamine hormones, such as norepinephrine, epinephrine, and dopamine, affect elements of bacterial replication, antimicrobial susceptibility, and virulence factors (11-14). This research represents the first time this phenomenon has been examined with the highly virulent bacteria *Bacillus anthracis* and *Yersinia pestis*. *B. anthracis* being the causative agent of anthrax and *Y. pestis* causing bubonic plague.

In the event of *B. anthracis*, a 10-fold increase in replication rate was noted when these bacteria were exposed to norepinephrine. The presence of norepinephrine also led to a decreased susceptibility to the antibiotic rifampicin, and bacteria that were damaged by the antibiotics ciprofloxacin, ampicillin, and rifampicin recovered at a far greater rate when exposed to norepinephrine post-exposure to these antibiotics. The mechanism

through which norepinephrine facilitated these growth phenotypes is unknown, but it seems that the accelerated recovery could be due to the increased iron uptake afforded by norepinephrine, but this doesn't seem to be the case with the increased resistance to rifampicin. A comprehensive antibiotic panel should be undertaken to see if norepinephrine elicits resistant phenotypes towards additional antibiotics. With *Y. pestis*, the inverse was seen with a pronounced reduction in replication when exposed to norepinephrine or epinephrine. Exposure to the hormone serotonin also resulted in a reduction in replication with *Y. pestis*. Interestingly, with the closely related pathogen *Yersinia enterocolitica* an increased replication rate was seen when exposed to norepinephrine or epinephrine. *Y. pestis* and Y. *enterocolitica* cause different pathologies, which could be the reason for the differences seen. Future work aimed at discerning the molecular basis for these differences could enlighten us on the role that these catecholamines may play in pathogenesis.

This dissertation presents data that supports the use of polyanhydride nanoparticles as effective antimicrobial delivery vehicles targeting both pathogenic bacteria and amoeba. The use of these nanoparticles could extend the usefulness of currently available antibiotics in our age of antimicrobial resistance. For the most efficacious use of these nanoparticles there is a degree of tailoring of the co-polymer chemistries needed. In addition, the anti-rheumatic drug auranofin was found to be an effective amoebicidal drug against the "brain eating amoeba" *N. fowleri*. Lastly, new insights into microbial endocrinology is included in the response of *B. anthracis* and *Y. pestis* to various catecholamine hormones.

References

1. Limmathurotsakul D, Golding N, Dance DAB, Messina JP, Pigott DM, Moyes CL, Rolim DB, Bertherat E, Day NPJ, Peacock SJ, Hay SI. 2016. Predicted global distribution of *Burkholderia pseudomallei* and burden of melioidosis. Nature Microbiology 1.

2. Estes DM, Dow SW, Schweizer HP, Torres AG. 2010. Present and future therapeutic strategies for melioidosis and glanders. Expert Rev Anti Infect Ther 8:325-38.

3. Capewell LG, Harris AM, Yoder JS, Cope JR, Eddy BA, Roy SL, Visvesvara GS, Fox LM, Beach MJ. 2015. Diagnosis, Clinical Course, and Treatment of Primary Amoebic Meningoencephalitis in the United States, 1937-2013. J Pediatric Infect Dis Soc 4:e68-75.

4. Withers MR. 2014. USAMRIID'S medical management of biological casualties handbook (8th ed.). Fort Detrick, MD: US Army Medical Research Institute of Infectious Diseases.

5. Binnebose AM. 2018. Development of a novel anti-infectivity platform for the treatment of neglected tropical and infectious diseases. Graduate Theses and Dissertations doi:https://doi.org/10.31274/etd-180810-5948.

6. Lueth P, Haughney SL, Binnebose AM, Mullis AS, Peroutka-Bigus N, Narasimhan B, Bellaire BH. 2019. Nanotherapeutic provides dose sparing and improved antimicrobial activity against *Brucella melitensis* infections. J Control Release 294:288-297.

7. Ulery BD, Phanse Y, Sinha A, Wannemuehler MJ, Narasimhan B, Bellaire BH. 2009. Polymer chemistry influences monocytic uptake of polyanhydride nanospheres. Pharm Res 26:683-90.

8. Andrade RM, Chaparro JD, Capparelli E, Reed SL. 2014. Auranofin is highly efficacious against *Toxoplasma gondii* in vitro and in an in vivo experimental model of acute toxoplasmosis. PLoS Negl Trop Dis 8:e2973.

9. Debnath A, Parsonage D, Andrade RM, He C, Cobo ER, Hirata K, Chen S, Garcia-Rivera G, Orozco E, Martinez MB, Gunatilleke SS, Barrios AM, Arkin MR, Poole LB, McKerrow JH, Reed SL. 2012. A high-throughput drug screen for *Entamoeba histolytica* identifies a new lead and target. Nat Med 18:956-60.

10. Capparelli EV, Bricker-Ford R, Rogers MJ, McKerrow JH, Reed SL. 2017. Phase I Clinical Trial Results of Auranofin, a Novel Antiparasitic Agent. Antimicrob Agents Chemother 61.

11. Freestone PP, Haigh RD, Lyte M. 2007. Specificity of catecholamine-induced growth in *Escherichia coli* O157:H7, *Salmonella enterica* and *Yersinia enterocolitica*. FEMS Microbiol Lett 269:221-8.

12. Halang P, Toulouse C, Geissel B, Michel B, Flauger B, Muller M, Voegele RT, Stefanski V, Steuber J. 2015. Response of *Vibrio cholerae* to the Catecholamine Hormones Epinephrine and Norepinephrine. J Bacteriol 197:3769-78.

13. Nakano M, Takahashi A, Sakai Y, Nakaya Y. 2007. Modulation of pathogenicity with norepinephrine related to the type III secretion system of *Vibrio parahaemolyticus*. J Infect Dis 195:1353-60.

14. Freestone PP, Haigh RD, Lyte M. 2008. Catecholamine inotrope resuscitation of antibiotic-damaged staphylococci and its blockade by specific receptor antagonists. J Infect Dis 197:1044-52.